

AD-A258 919



①

AFIT/GCE/ENG/92D-05

**DESIGN AND DEVELOPMENT
OF A HIGH-SPEED WINOGRAD
FAST FOURIER TRANSFORM
PROCESSOR BOARD**

THESIS

James F. Herron
CPT, USA

AFIT/GCE/ENG/92D-05

DTIC
SELECTE
S B D
JAN 07 1993


93-00106

Approved for Public Release; Distribution Unlimited

93 1 04 154

**DESIGN AND DEVELOPMENT
OF A HIGH-SPEED WINOGRAD
FAST FOURIER TRANSFORM
PROCESSOR BOARD**

THESIS

Presented to the Faculty of the School of Engineering
of the Air Force Institute of Technology
Air University
In Partial Fulfillment of the
Requirements for the Degree of
Master of Science (Computer Engineering)

James F. Herron, B.S.E.E.
CPT, USA

December 1992

Accession For	
NTIS GRA&I	<input checked="checked" type="checkbox"/>
DTIC TAB	<input type="checkbox"/>
Unannounced	<input type="checkbox"/>
Justification	
By	
Distribution/	
Availability Codes	
Dist	Avail and/or Special
A-1	

Approved for Public Release; Distribution Unlimited

DATA QUALITY INSPECTED 1

Acknowledgments

Before beginning this thesis, I would like to take the time to voice some of my own personal comments. Although, I might like to think of this thesis as a singular effort, the truth is that I received much needed help and support from a variety of sources. My thesis committee made up by MAJ Mark Mehalic, MAJ Kim Kanzaki and CPT Ken Scribner kept my nose to the grindstone with guidance and direction. My classmates (the VLSI crew) provided me with comradeship, giving me the assurance that I was not alone. My family and close friends supplied that special "long-distance" support that helps me get through every day to include those 13+ hour ones. Thanks also goes to the VLSI lab staff (Bruce Clay and Greg Richardson) for technical support and help on the systems. My sincere and heartfelt thanks go to you all.

After all is said and done, this thesis has been a demanding, yet rewarding experience. It has given me the opportunity to work on a completely new area of research in the computer engineering field and has given me an appreciation for "true" research. Maybe, one day, when the WFTA system is complete, I can look back and feel like I have helped in that arduous process. For all you future researchers in the WFTA project area, I wish you all good luck!

James F. Herron

Table of Contents

	Page
List of Figures	viii
List of Tables	xi
List of Abbreviations	xii
Abstract	xiii
I. Introduction	1
1.1 Background	2
1.2 Problem Statement	4
1.3 Objectives	4
1.4 Scope	5
1.5 Approach	6
1.5.1 Design of the VMEbus Interface.	6
1.5.2 Development of VHDL Code.	7
1.5.3 Construction of the WFTA System.	8
1.5.4 Development of Host Software.	8
1.6 Materials and Equipment	9
1.7 Sequence of Presentation	9
II. Literature Review	12
2.1 Introduction	12
2.2 AFIT Research	12
2.3 Other WFTA Efforts	16
2.4 Summary	17

	Page
III. Architecture of Prototype WFTA System	18
3.1 Introduction	18
3.2 The WFTA System	18
3.2.1 Functional Blocks.	19
3.2.2 Datapath and Address Lines.	22
3.2.3 Control Signals.	22
3.3 Design Decisions	23
3.4 Design Methodology	25
3.5 Summary	26
IV. Development of the VHDL code	27
4.1 Introduction	27
4.2 Synopsys Package	28
4.3 The WFTA System	28
4.3.1 Behavioral Descriptions.	30
4.3.2 Common Gates.	33
4.3.3 Bus Interface.	34
4.3.4 Input and Output Memory.	43
4.3.5 ACU.	51
4.3.6 APU – WFTA16 Processor.	57
4.3.7 MSPC.	58
4.4 Host	61
4.5 Test Plans	62
4.6 Evaluation of VHDL Development	64
4.6.1 Input Test Vector Selection.	64
4.6.2 Simulation of the WFTA System.	65
4.6.3 Results of WFTA System VHDL simulation.	67
4.7 Summary	67

	Page
V. Construction of the WFTA System	68
5.1 Introduction	68
5.2 Resources	69
5.2.1 Equipment and Tools.	69
5.2.2 Integrated Circuits.	70
5.2.3 Other Parts.	71
5.3 Partitioning of Functional Blocks	73
5.4 Construction Methodology and Testing	74
5.5 Specific Problems	76
5.5.1 Interface to Host.	76
5.5.2 Parts.	76
5.5.3 Testing.	77
5.6 Evaluation of Construction	77
5.7 Summary	77
VI. Development of the Host Driver Code	78
6.1 Introduction	78
6.2 Compilation, Download, and Run Procedures	79
6.3 Pseudocode for the Host Driver Program	79
6.4 Data Flow Diagram for Host Driver Code	81
6.5 Coding and Memory Map	82
6.6 Testing and Evaluation of Host Driver Program Development . .	84
6.7 Summary	84
VII. Conclusions and Recommendations	85
7.1 Introduction	85
7.2 Conclusions	85
7.2.1 Validation of WFTA System Design.	85

	Page
7.2.2 Continued Work in the WFTA System.	86
7.3 Recommendations	86
7.3.1 Further VLSI Work.	87
7.3.2 Asynchronous Signals.	87
7.3.3 Different Host.	88
7.3.4 Behavioral Descriptions of Chips.	88
7.3.5 Supply of Resources.	88
7.4 Lessons Learned	89
7.4.1 Scheduling of Construction.	89
7.4.2 Construction Methodology.	89
7.4.3 Ordering of Parts.	89
7.5 Summary	90
Appendix A. Schematics for Subcomponents	91
Appendix B. Timing Diagrams for Functional Blocks	106
Appendix C. Test Vectors for 1 Hz Sine Wave	118
Appendix D. Timing Diagrams for WFTA System	122
Appendix E. Major Distributors and Suppliers of Parts	130
Appendix F. Chip Layouts for the VMEbus Boards	132
Appendix G. Compilation, Download, and Run Procedures for Host Driver Code	138
G.1 Compilation Procedure	138
G.2 Download Procedure	139
G.3 Run Procedure	141
Appendix H. Changes to Pseudocode for Sustained Operations	143

	Page
Appendix I. Host Driver Code Listing	145
Appendix J. Operator's Manual for the 16-point WFTA System	147
J.1 Hardware	147
J.1.1 Setup.	147
J.1.2 WFTA Address Change.	147
J.2 Software	148
J.2.1 Host Driver Code and Data.	148
J.2.2 Running the Host Driver Program.	152
J.2.3 Reading the Output Data.	152
J.3 Problems in Operator's Manual	152
Appendix K. VHDL Code and Schematic Listing	153
References	154
Vita	157

List of Figures

Figure	Page
1. Simple Diagram of WFTA Architecture	3
2. Simple Diagram of WFTA Prototype Architecture	5
3. Initial 1985 WFTA Architecture	13
4. Reconfigurable WFTA Architecture	15
5. Prototype WFTA System Architecture	20
6. WFTA System Architecture	29
7. Memory Mapping for WFTA Prototype System	35
8. Bus Interface Schematic	37
9. Data Format for Control Word	39
10. Data Format for Output Word	40
11. Input Memory (MEM_IN Component)	45
12. Output Memory (MEM_OUT Component)	46
13. Arithmetic Control Unit	53
14. State Diagram for Minimal SPC	60
15. Host-WFTA Relationship	61
16. Partitioning and Interconnect Signals	74
17. Pseudocode for the Host Driver Program	80
18. Context Diagram for the Host Driver Program	82
19. Level 1 DFD for Host Driver Program	83
20. Memory Mapping for Host Driver Code and Data	83
21. Input Section Schematic-VMEbus Interface	92
22. Control Section Schematic-VMEbus Interface	93
23. Output Section Schematic-VMEbus Interface	94
24. DEMUX1 Block Schematic-Input Memory	95
25. DEMUX1a Block Schematic-Output Memory	96

Figure	Page
26. DEMUX2 Block Schematic-Input and Output Memory	97
27. DEMUX3 Block Schematic-Input and Output Memory	98
28. MEM_MCM6264 Block Schematic-Input and Output Memory	99
29. MUX2 Block Schematic-Input Memory	100
30. MUX2a Block Schematic-Input Memory	101
31. ACU_INIT Block Schematic-ACU	102
32. ACU_ADD Block Schematic-ACU	103
33. ACU_COUNTER Block Schematic-ACU	104
34. ACU_ADD1 Block Schematic-ACU	105
35. Timing Diagram-Input Section	107
36. Timing Diagram-Control Section(#1)	108
37. Timing Diagram-Control Section(#2)	109
38. Timing Diagram-Output Section(#1)	110
39. Timing Diagram-Output Section(#2)	111
40. Timing Diagram-Input Memory	112
41. Timing Diagram-Output Memory	113
42. Timing Diagram-ACU(#1)	114
43. Timing Diagram-ACU(#2)	115
44. Timing Diagram-MSPC	116
45. Timing Diagram-WFTA System(#1)	123
46. Timing Diagram-WFTA System(#2)	124
47. Timing Diagram-WFTA System(#3)	125
48. Timing Diagram-WFTA System(#4)	126
49. Timing Diagram-WFTA System(#5)	127
50. Timing Diagram-WFTA System(#6)	128
51. Timing Diagram-WFTA System(#7)	129
52. Layout of VME Board # 1	133

Figure	Page
53. Layout of VME Board # 2	135
54. Signal Mapping of 50-Pin Interconnect Cable	137
55. Pseudocode for a Sustainable Host Driver Program	144
56. Hardware Setup	148

List of Tables

Table	Page
1. Integrated Circuits and Behavioral Descriptions	31
2. Instantiated Propagation Delays for Common Gates	34
3. Decoding for WFTA Components	36
4. Common VMEbus Signals Interfaced to the WFTA	39
5. Test Benches	63
6. Integrated Circuit Requirements with Functional Blocks	71
7. MSPC Timing Table	117
8. Real Input Test Vectors for a 1 Hz Sine Wave	119
9. Expected and Actual Real Output Test Vectors for a 1 Hz Sine Wave . . .	120
10. Expected and Actual Imaginary Output Test Vectors for a 1 Hz Sine Wave	121
11. Integrated Circuits used on VME Board # 1	134
12. Integrated Circuits used on VME Board # 2	136

List of Abbreviations

Symbol	Page
digital signal processing (DSP)	1
Very large scale integration (VLSI)	1
Discrete Fourier Transform (DFT)	1
Air Force Institute of Technology (AFIT)	1
Winograd Fourier Transform Algorithm (WFTA)	1
Fast Fourier Transforms (FFT)	2
Prime Factoring Algorithm (PFA)	3
application-specific integrated circuits (ASIC)	3
Very High Speed Integrated Circuit (VHSIC) Hardware Description Language (VHDL)	4
computer-aided design (CAD)	7
Error-Correction Coding (ECC)	14
Arithmetic Processing Unit (APU)	16
Arithmetic Control Unit (ACU)	16
Small PFA Controller (SPC)	16
Minimal Small PFA Controller (MSPC)	19
signal-to-noise ratio (SNR)	24
Simulation Graphical Environment (SGE)	28
Multi-Valued Logic-7 levels (MVL7)	28
finite state machine (FSM)	59
Transistor-Transistor-Logic (TTL)	71
programmable gate array (PGA)	72
dual in-line package (DIP)	73
data flow diagram (DFD)	81

Abstract

Since 1985, the Air Force Institute of Technology has pursued a project to develop a 4080-point Discrete Fourier Transform processor using the Winograd Fourier Transform Algorithm (WFTA) and Good-Thomas Prime Factoring Algorithm (PFA). In the first attempt to build a working system, this research effort designed and constructed, in part, a modified single processor architecture in order to demonstrate the proof of concept of the WFTA system design. This prototype architecture is simpler in implementation but uses the same principles and procedures as those of the 4080-point WFTA design. The design developed in this thesis was validated using the Very High-Speed Integrated Circuit Hardware Description Language (VHDL) to simulate its operation. A partial construction of the design was built and tested verifying the VHDL results.

DESIGN AND DEVELOPMENT OF A HIGH-SPEED WINOGRAD FAST FOURIER TRANSFORM PROCESSOR BOARD

I. Introduction

In both commercial and military arenas, digital signal processing (DSP) has become a rapidly expanding area of interest. With this rising interest there continues to be a need for higher performance digital signal processors that are faster and able to handle larger amounts of data. Very large scale integration (VLSI) has provided the means by which faster calculations and higher throughput can be realizable with these DSP processors. Algorithms normally implemented through software can be made faster by directly implementing them on integrated circuits. This makes the integrated circuit specific in its use but generally faster than those used in general purpose machines.

One of the many DSP tools is the Discrete Fourier Transform (DFT) which is a mathematical tool that can be used to filter noise from a particular signal frequency [1]. This particular use of the DFT has direct applications in radar processing. One possible implementation is in the nose of "smart" ordnance where a fast DFT could be calculated to screen out the noise generated by the enemy or environment [2].

This thesis effort supported the ongoing project at the Air Force Institute of Technology (AFIT) to implement the Winograd Fourier Transform Algorithm (WFTA) in hardware. One of the processors which implements this algorithm is near completion but a system configuration to install that processor has not yet been implemented. This thesis effort demonstrates that chip in a system-level configuration and verifies that this fast means of DFT calculation is both realizable and practical.

1.1 Background

The Fourier transform has been used for decades as a mathematical tool by electrical engineers in the analysis of analog signals. The algorithm takes real physical processes described in the time domain and "transforms" them into the frequency domain [3]. However, the Fourier Transform only works on continuous signals and a different mathematical tool is necessary for digital (discrete) signals. The Discrete Fourier Transform (DFT) is an approximation of the Fourier transform where "samples of the continuous Fourier transform are evaluated numerically by using an approximation to the transformation integral." [4]. The DFT can be used on digital signals because of its discrete nature. Further, by increasing the numbers of samples, closer approximations to the Fourier transform can be realized.

However, the main problem with calculating DFT's using the straight summation definition is that their calculation is computationally intensive. In fact, the complexity of the Discrete Fourier Transform is an $O(N^2)$ process [3]. In answer to this problem of computational cost, many people have developed a class of algorithms called Fast Fourier Transforms (FFT). The FFT is a method for efficiently computing the DFT of a time series [5]. The Discrete Fourier Transform can, in fact, be computed in $O(N \log_2 N)$ operations using FFT algorithms [3]. These FFT algorithms represent a significant reduction in the computational complexity of the DFT, especially for larger N . There are many FFT approaches that can be found in the literature, like the Cooley-Tukey FFT algorithm and the base-4 FFT algorithm [3].

In his short paper, Schmucl Winograd develops a FFT algorithm which does not decrease the complexity of the DFT calculation but does, however, decrease the number of multiplications [6]. This reduction in the multiplications has important consequences in the world of VLSI and chip design, because fewer multiplications translates into increased speed and higher throughput. For this reason, the Winograd Fourier Transform Algorithm (WFTA) is the theoretical basis for the research effort here at the Air Force Institute of Technology. This effort has been to develop and build a specific co-processor which implements the Winograd Fast Fourier Transform algorithm in hardware on a single chip or suite of chips.

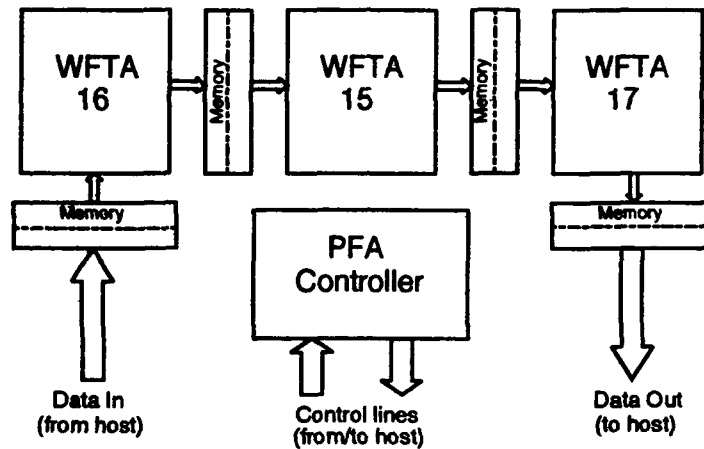


Figure 1. Simple Diagram of WFTA Architecture

Using the Winograd algorithm along with another algorithm called the Good-Thomas Prime Factoring Algorithm (PFA), a reconfigurable WFTA processing architecture has been developed [2]. This architecture, shown in Figure 1, is capable of calculating 15, 16, 17, 240, 255, 272 and 4080-point DFT's. The PFA uses the fact that transform sizes of the three processors in the system described are mutually prime to each other.

The reconfigurable WFTA system of Figure 1 consists of three separate FFT processors, bank-switchable memory, and a system controller. The three FFT processors (WFTA15, WFTA16, and WFTA17) are application-specific integrated circuits (ASIC) that are being currently developed here at AFIT. The number following the processor indicates the transform size that the processor is capable of calculating. The memory is bank-switchable for reasons of increased throughput. Bank switching keeps the pipeline of the WFTA system full. The PFA controller provides the control signals for all the components of the system and implements the Prime Factoring Algorithm. Using the PFA, the three processors can be combined with each other to provide the 240 (15 X 16), 255 (15 X 17), 272 (16 X 17), and 4080 (15 X 16 X 17) point DFT. In this reconfigurable system, the initial estimates for the sustained speed of the WFTA's operation is the calculation of a 4080-point DFT in approximately $119 \mu s$ [2].

1.2 Problem Statement

There is a lack of a platform or system environment, including an interface to a suitable host processor, for WFTA processor operation. This research was an effort to design and build a working 16-point WFTA system that interfaces to the VMEbus standard to demonstrate the proof of concept in the WFTA design developed at the Air Force Institute of Technology.

1.3 Objectives

This thesis effort had four main objectives: design of a VMEbus interface, development of Very High Speed Integrated Circuit (VHSIC) Hardware Description Language (VHDL) code describing the WFTA system, construction of a 16-point WFTA system, and development of the host software which can test the finished co-processor.

The first objective was to design an interface between the simplified WFTA system shown in Figure 2 and the VMEbus standard [7], a commercially available bus that is widely used in industry. This objective is tied into the next objective, the VHDL code objective, and was discussed in that chapter instead of being separate.

The second objective was to develop the VHDL code describing the WFTA system to be constructed down to the integrated circuit level. VHDL has been designed to be used in a top-down design method and can be used to simulate the behavior of a digital circuit at various levels of representation.

The third objective was to build the 16-point WFTA system, including the bus interface circuitry of the first objective, onto a VMEbus card using the wirewrap technique. This prototype could then be used to verify the WFTA system design simulated in the VHDL development.

The fourth and final objective was to develop a host program to drive the WFTA system. After the WFTA board has been constructed, there needs to be a means of driving it with data and control signals from a host processor, which for this thesis is the Motorola 68010 16-bit microprocessor.

An ancillary objective implied by these specific ones above was to generate an operator's manual for the constructed WFTA system which will guide the operator as to proper procedure and any particular considerations of the WFTA operation.

Documentation through these four objectives was stressed in order to provide follow-on work and researchers a basis for the smoothest transition possible.

1.4 Scope

The focus for previous theses in this line of research has been to design, fabricate, and test an application-specific integrated circuit using the techniques of VLSI and the VHSIC Hardware Description Language (VHDL). This thesis effort was the first attempt at integrating the WFTA ASIC chips developed previously and interfacing them into a commercially available standard. In order to scope this thesis within realizable goals, the final 4080-point WFTA architecture described in previous theses [2] was scaled down to a simpler architecture shown in Figure 2.

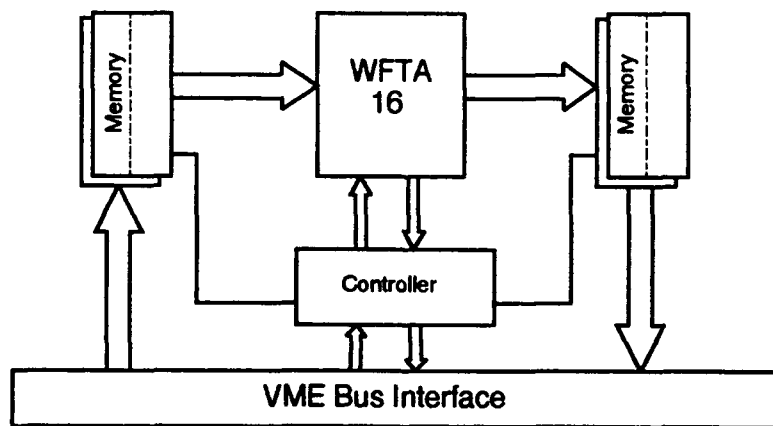


Figure 2. Simple Diagram of WFTA Prototype Architecture

Details of this modified WFTA architecture are discussed in Chapter III. The basic principles and general structures of this latest generation of the WFTA architecture remains intact, only scaled down to a realizable objective.

This test WFTA architecture has fewer components than the overall WFTA architecture described in Figure 1. There is only one FFT processor, the WFTA16, which is

capable of calculating a 16-point DFT. The two memories are bank-switchable like in the overall architecture and are similarly used to increase the throughput of the system. The system controller here is different than the one used in the overall WFTA design since it does not implement the Prime Factor Algorithm. This test architecture is limited to calculating only one DFT, the 16-point DFT.

Due to resource problems and time, the degree of completion on the construction of the WFTA system was also scoped to insure that whatever part of the system built could be demonstrated.

1.5 Approach

Each one of the objectives described above entails a different approach. In all these methodologies, there is a common thread of understanding. The future development of WFTA systems must be taken into account whenever possible in order to simplify the efforts of research that follow this thesis.

1.5.1 Design of the VMEbus Interface. The VMEbus standard [7] explicitly describes the requirements of the VMEbus, and by using fundamental digital design principles and heuristics, the interface between the WFTA system and the VMEbus can be built modularly. The WFTA system is essentially a co-processor or, in other words, a slave device waiting for the commands of the host processor. The WFTA system does not continuously operate and needs to be separated from the general operation of the VMEbus. This communication requires an interface between the VMEbus and the WFTA with a certain defined protocol. An example of one of the considerations for this interface is: How does the host processor tell the WFTA system to begin processing? These considerations along with others for this design are examined in detail in Chapter IV of this thesis.

There were no attempts to optimize the combinational logic of the design using currently available optimization tools. Future researchers should review this design and attempt to optimize the circuits whenever possible.

In short, the WFTA system cannot be directly connected to the VMEbus system. This interface provides the means of communication between the WFTA system and the

host processor. Without an adequate VMEbus interface, the WFTA cannot be loaded, told to operate, or have output read.

1.5.2 Development of VHDL Code. The use of VHDL is rapidly becoming commonplace in engineering circles. Using software to simulate a piece of hardware can save thousands of man-hours in the design process for large systems. The secret to its success is that the design can be built hierarchically from top to bottom (from a high block-level representation to a gate-level representation). At each level, the description can be simulated to demonstrate the correctness of the design. This thesis attempted to use VHDL in this fashion. Starting from a high-level depiction of the WFTA system, each of the modules was implemented in VHDL. Within each module the behavioral description of the module was replaced with the structural representation until the lowest-level behavioral descriptions of the components were taken from the actual specifications of the chips used in the construction of the WFTA system.

AFIT has recently acquired a software package produced by Synopsys, Incorporated which includes a VHDL simulation system. This computer-aided design (CAD) tool uses a graphical user interface which helps the designer to visualize the system through the use of schematics. A number of attractive features of this software package were used for this thesis. This Synopsys CAD tool was used heavily and extensively in the design and development of the VHDL code for the WFTA system tested.

VHDL also provides a means of self-documentation for the design. Following the hierarchical development of the design provides the reader with ample information on the actual construction of the digital system. The VHDL code for this thesis also has comments and headers in the code to help clarify the more difficult and possibly cryptic sections.

Again, development of the VHDL code was modular for ease of follow-on work in this area of research. These future researchers should be able to add new descriptions or augment the existing descriptions of components and simply "re-wire" the system for a different implementation. The only components that should change from different configurations would be the controllers, which would get more complex as additional functions are added with the larger point processors and larger configurations.

1.5.3 Construction of the WFTA System. As mentioned previously, the construction of the WFTA system described in Figure 2 is the main thrust of this thesis effort. Using commercially available chips whenever possible, the WFTA prototype system is built on two VME boards that slides into any VME backplane. Using the wire-wrap method of construction, all the components were connected on one side of the VME cards. The only ASIC chip used for this thesis was the WFTA16 FFT processor.

1.5.4 Development of Host Software. The host driver program is the program located in the host that "drives" the WFTA system. This program was written in the C programming language. Using a 68010 compiler, executable code is generated from the host driver program and downloaded through a specified procedure to the host.

This host program loads the input memory bank with 16 points of real data (real signals have no imaginary components) and tells the WFTA system controller to begin processing. When the memory switches to receive the input data into the WFTA16 processor, the host program continues to load as input the next set of points into the second memory bank. Once the WFTA system controller indicates to the host that it has completed a set of the data points, the host reads the output data (both real and imaginary parts) from the output memory bank. Meanwhile, the WFTA16 has read in the new data and continues calculating the DFT of the new data. The host driver program can then load a new set of points into the input memory bank. This process continues until an end of the set of data points is reached.

The host driver program was developed using sound and fundamental software engineering principles, paying particular attention to the concept of modularity. Development of the host driver program is discussed in Chapter VI. Subsequent thesis efforts in this area of research will continue the step-wise progress toward the overall WFTA architecture envisioned in Figure 1. The host driver program must be flexible enough to adapt to these modifications without undue difficulty. The C language, with its ability to manipulate bits at the machine level, was specifically chosen for this needed flexibility in the future development of host driver software. Furthermore, the C language is a high-level programming

language, which makes it easier to maintain programs written in C rather than in assembly language.

1.6 Materials and Equipment

The following list describes the major pieces of equipment and other resources that were used to support this thesis effort.

1. AFIT VLSI/VHSIC Laboratory Sparc2 workstations
2. VME backplane
3. 68010 host processor card with a means of user interface
4. Synopsys VHDL simulation environment (Version 2.2)
5. Tools and equipment in the Digital Design Lab
6. 68010 Compiler

1.7 Sequence of Presentation

The following paragraphs of this section outline the order of presentation in this thesis.

Chapter II documents the past efforts at AFIT in WFTA design and looks at other implementations of FFT processors using the Winograd Fast Fourier Transform Algorithm in the industrial and academic communities.

Chapter III presents the modified architecture of the WFTA system used in this thesis. This is the first time this scaled-down architecture has been used, so a detailed examination of its structure is given before beginning the discussion of each of the objectives.

The next three chapters discuss each one of the objectives outlined in this chapter. Chapter IV discusses the VHDL code development for the WFTA system. The chapter begins with the development of the behavioral descriptions created and continues through the final structural description of the WFTA system used.

Chapter V describes the modular construction of the WFTA design along with testing procedures used to ensure proper operation. Specific problems and resources are addressed.

Chapter VI describes the development of the host processor code that was used in the testing process.

Chapter VII discusses the conclusions of this research and recommendations for future thesis cycles.

Appendix A contains the schematics created during the VHDL development for sub-components of the WFTA system.

Appendix B contains timing diagrams generated from VHDL test benches showing the interrelationships of significant signals in each of the major functional blocks.

Appendix C contains the test vectors (both input and output) used in the system-level VHDL simulation to verify system design.

Appendix D contains the timing diagrams generated from the VHDL test bench simulation for the entire WFTA system. These timing diagrams in conjunction with the test vectors in Appendix C were used to verify the WFTA system design.

Appendix E is a listing of nationwide distributors with phone numbers that provided supplies for the construction phase of this thesis.

Appendix F is a layout of the two VMEbus boards on which the WFTA system was constructed with chip reference numbers and chip identifications.

Appendix G is the description of the procedures developed during this thesis to compile, download, and run the host driver program.

Appendix H contains the necessary additions to change the pseudocode of the host driver program from single FFT operation to multiple FFT operation.

Appendix I is a listing of the host driver program developed for driving the WFTA system.

Appendix J is a short operator's manual that can be used to guide the user in the use and peculiarities of the WFTA prototype system. It provides all the necessary instructions

to operate the WFTA system. This appendix was meant to be detached from the thesis and used as a handy guide with the WFTA system developed.

Appendix K is the listing of all the VHDL code, to include testbenches, and the Synopsys generated schematics discussed in the thesis.

II. Literature Review

2.1 Introduction

Research on the WFTA at the Air Force Institute of Technology has been on-going since 1985. This is the latest thesis in a long line of research conducted in the WFTA project area by master's candidates in the Electrical and Computer Engineering Department. Consequently, the bulk of literature available and the bulk of this search is from the work of past theses at AFIT.

The focus of this literature search was on the architecture of the WFTA system and how it has changed from the original design of 1985. Outside of the research at AFIT, there has been little work in implementing the Winograd Fast Fourier Transform Algorithm in hardware, but there have been some attempts. These outside efforts are included for completeness.

2.2 AFIT Research

The WFTA project at AFIT began back in 1985 when Linderman, director of AFIT VLSI Research Group, introduced the idea of a hardware implementation of the Winograd Fast Fourier Transform Algorithm [8]. That year, four AFIT students started the process of WFTA development with their thesis efforts. Each one worked in a specific area; Taylor in WFTA system development; Coutee in VLSI arithmetic circuitry; Rossbach in VLSI control circuitry; and Collins in VLSI circuit simulation.

Coutee developed the arithmetic circuitry necessary for the processing of data going through one of the FFT processors, the WFTA16 architecture. Using the techniques of VLSI design, Coutee designed a chip that performed the arithmetic calculations of the DFT using the Winograd Fast Fourier Transform algorithm [9].

Rossbach designed the control circuitry for the initial WFTA effort. He designed two circuits to control the arithmetic and address generation circuitry for the WFTA processor. A notable byproduct of Rossbach's thesis was that he developed a XROM compiler, which automatically generated a layout of the XROM Address Generator circuit discussed in his thesis [10].

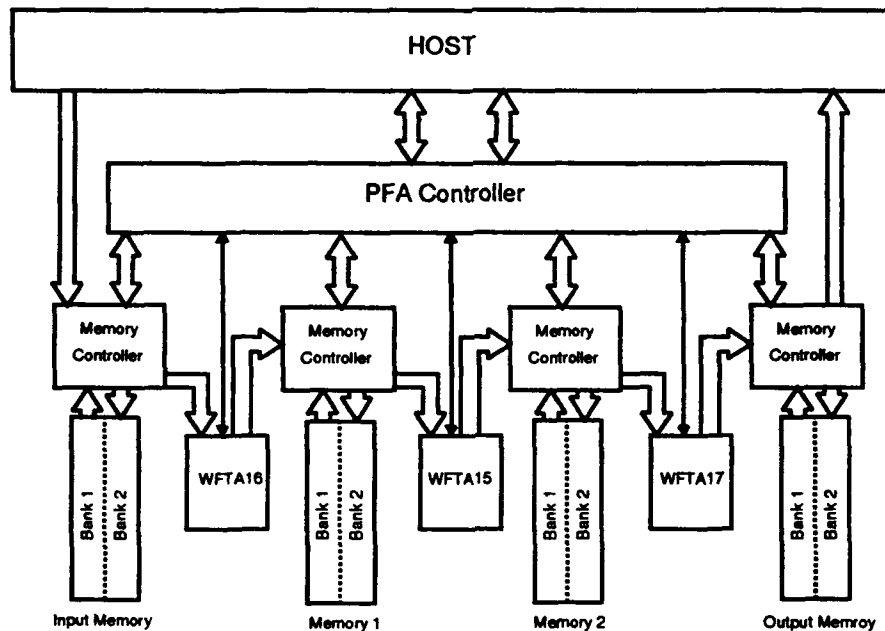


Figure 3. Initial 1985 WFTA Architecture

The third AFIT student from that 1985 group was Collins, who developed a simulation of the data flow in the WFTA-16 processor using the C programming language. He also started the VHDL descriptions of certain sections of the WFTA-16 [11].

The last of those four students was Taylor, who developed a detailed description of the WFTA algorithm as it applies to the system-level design. The layout or architecture for the first WFTA system is found in his thesis, and Figure 3 is a re-creation of that layout for the 4080-point processor. Taylor also provided the link between theory and hardware by verifying the algorithm's accuracy with computer simulations. The design required three WFTA processors (WFTA-15, WFTA-16, and WFTA-17), a PFA controller, and intermediate memories. The points of data are pipelined through the three processors according to the Prime Factor Algorithm to increase throughput of the system [8].

The memory was dual-ported (takes both a read and write address) with two separate banks of memory. The memory controller controlled the data flow of the pipeline depending on control signals from the interface processor or PFA controller. Write enable signals and addresses were generated by the WFTA processor control circuitry. Fault detection

was built into this system with Error-Correction Coding (ECC) circuitry and watchdog processors. The ECC was built into the memory, and along with parity checks, the WFTA processors would provide continuous checking of (corrected) data. The design called for two additional watchdog processors which were redundant, inactive processors that calculate the FFT at the same time and compare results to the active processor. If a difference is detected, the system recovered by alerting the PFA controller that a possible error has occurred. The PFA controller decided which output is allowed to continue to the next stage of the pipeline through voting circuitry between the three processors.

In the following year, 1986, hardware implementation began with the three AFIT students assigned to the WFTA project. These theses dealt with operational issues, but made no significant changes to the system architecture. Shepard continued work on the first implementation of the WFTA16 processor in silicon [12].

Hedrick was the second student from the 1986 group and worked in the design of the PFA controller as well as custom memory chips and memory controllers to be used in the WFTA system [13].

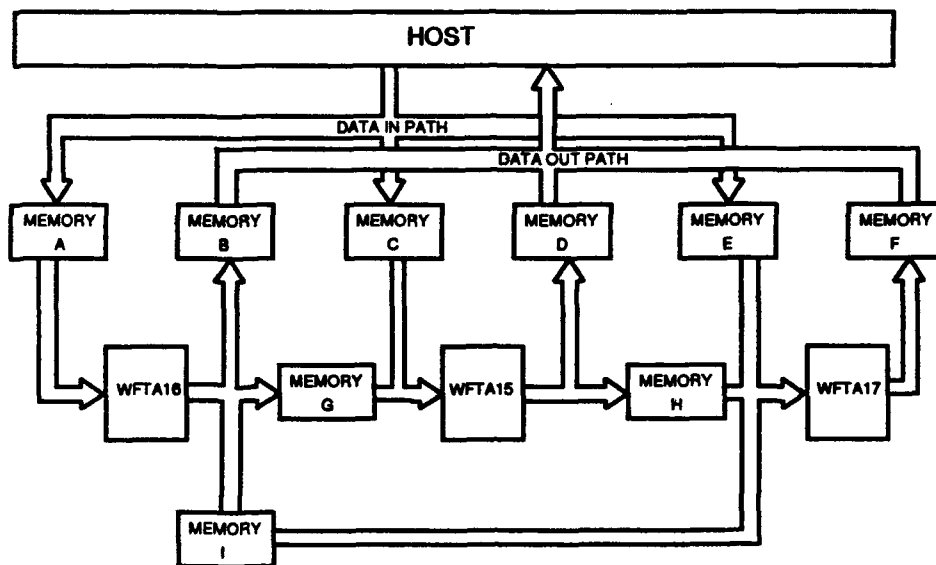
The third thesis student of the 1986 group was Cooper, who up-dated the VHDL description of the WFTA16 processor, incorporating the changes from the 1985 design [14].

In 1987, Hauser continued work in the design and implementation of the interconnecting memory modules and the PFA controller [15]. Hauser designed the ECC circuitry discussed earlier. Again there were no significant changes in this thesis to the architecture of the WFTA system.

In 1988, Tillie and Comtois designed the WFTA17 processor as a class project [16]. They modified existing macrocells used for the 16-point processor and designed new macrocells unique to the WFTA17 processor.

The next thesis was Pavick's, who in 1989 performed testing of the WFTA16 processors built earlier and re-designed cells in the processor [16]. The system architecture remained unaffected.

Baker used VHDL to validate the 4080-point WFTA processor design in 1990 [17]. He succeeded in developing behavioral descriptions of the three WFTA processors and



provided the nucleus for future VHDL work in the WFTA processors. The 4080-point design used here is essentially the same architecture developed in 1985.

Also in 1990, Sommer focused on the development of the WFTA cell library and the design of the WFTA15 processor [18]. Again, there were no major changes to the architecture of the WFTA system.

From the auspicious start of the WFTA project in 1985, there has been steady progress toward the realization of a 4080-point WFTA processor every year. However, up to last year, the basic architecture has remained faithful to the original design.

Last year, Scribner encapsulated the efforts of previous years and redesigned the WFTA system into a reconfigurable, non-redundant, 4080-point WFTA processor [2]. His work introduced the first architectural changes in the WFTA system since its conception. This architecture is depicted in Figure 4 which has been re-created from Scribner's thesis.

The earlier architecture for the WFTA was not reconfigurable. It was basically designed for calculating a 4080-point FFT. The system was limited to that specific transform size alone. Scribner introduced the reconfigurability option by adding additional memories to the system. This new architecture is capable of calculating either a 15, 16, 17, 240, 255,

272 or an 4080-point FFT. The additional memories are selectable, and by re-defining the datapath through the system, user-selectable FFT point sizes can be realized. For example, to calculate a 16-point FFT, the two memories in Figure 4 would be enabled (Memory A and Memory B), thereby bypassing the WFTA15 and WFTA17 processor. This reconfiguration feature does, however, make the PFA controller (not pictured in Figure 4) more complicated than the original design since it must now control the datapath through the latches throughout the system.

Scribner also introduced some functional decompositions in the architecture by separating the WFTA FFT arithmetic circuitry and its addressing components, creating two entities called the Arithmetic Processing Unit (APU) which calculates the FFT and the Arithmetic Control Unit (ACU) which generates the addresses and write enable for the memory.

Scribner also developed the Small PFA Controller (SPC) in place of the PFA Controller to be used to support WFTA system testing. Many of the capabilities of the PFA are not implemented in order to simplify the circuitry and provide a platform by providing control signals to test existing processor designs.

Furthermore, Scribner simulated the entire system in VHDL and verified the design through sample cases of data. Most of the application-specific integrated circuits (ASIC) for the 4080-point WFTA processor were also fabricated.

2.3 Other WFTA Efforts

The earliest design of a non-AFIT, FFT-specific processor was at the University of Maryland in 1986 [19]. The design uses the Winograd Fast Fourier Transform Algorithm along with the Prime Factor Algorithm. The architecture consists of three modules (the summation component, the scaling component, and the transpose component) that are interconnected. The researchers at the University of Maryland anticipated the computation of DFT of 840 complex numbers in 100 ms, with a throughput of 30,000 such Fourier transforms per second using fabricated chips.

Another design effort developing a FFT processor using the Winograd Fast Fourier Transform has been started at the Department of National Defense, Ottawa, Canada [20] this year. The processor has been developed to satisfy the DSP requirements of future electronic warfare systems. The design has been optimized for short (20–60 points) transforms using a $0.7\ \mu$ CMOS process.

2.4 Summary

This chapter has covered the available literature on the hardware implementation of the Winograd Fast Fourier Transform Algorithm. The bulk of this chapter has been based on previous theses here at AFIT where the work has been on-going since 1985. The focus through these theses was on the architecture of the WFTA system and its changes to the present. There has been little research outside of AFIT using the Winograd Fast Fourier Transform Algorithm. The efforts described here are included for completeness. The next chapter examines the single processor WFTA architecture that was prototyped for this thesis.

III. Architecture of Prototype WFTA System

3.1 Introduction

The entire intent of this thesis was to develop a system into which one of the WFTA processors could be placed to demonstrate proof of concept with the WFTA design. This system, coined the WFTA system by the author, is different than the earlier versions of the WFTA architecture. It is a simple architecture consisting of a single processor and the minimum amount of circuitry and components to insure proper operation.

This was the first effort at AFIT to incorporate the WFTA processor into a system connected to a standard bus. With the experience garnered from this thesis, future WFTA system design thesis efforts can continue to strive toward development of the reconfigurable 4080-point FFT processor.

This chapter starts with a discussion of the architecture of the prototype WFTA system in Figure 2. The design decisions particular to this design are then examined, followed by a short discussion of the design methodology that guided the design of the WFTA system.

3.2 The WFTA System

The WFTA system depicted in Figure 2 was rudimentary and not complete. It is, however, indicative of the general structure of the WFTA system that was constructed and was simple enough to be included in the introduction of this thesis. For example, none of the control signals used in the architecture were discussed and the datapaths was not illustrated. This section details the modified architecture of the system that was developed and constructed.

In short, the prototype WFTA system provided the platform necessary for the WFTA16 processor to calculate a 16-point FFT of a real signal. The WFTA16 APU is the only chip that actually calculates the FFT. The rest of the system only provides an adequate environment suitable for the operation of the WFTA16 processor.

This single processor architecture design could be used with any of the other WFTA processors with a re-design of the arithmetic control unit (ACU). The ACU for this thesis is tailored for the WFTA16 processor latency time and the WFTA16 addressing requirements. However, the rest of the design is compatible with either the WFTA15 or WFTA17 processors.

The WFTA system described by Figure 5 is more complete, showing all the functional blocks, the datapaths, and the important control signals designed in this thesis. Figure 5 is a simpler system and many of the signals discussed by Scribner [2] are not supported. Simplicity in design was an important objective in order to develop a complete platform during this thesis cycle. Signals related to more advanced features of the WFTA are left for future researchers to implement in a system configuration. Only the major control signals that were actually used for this design are depicted in Figure 5.

The rest of this section is a general discussion of the architecture used for this thesis. The major functional blocks are described in general detail. The datapath through the system is highlighted. Finally, the important control signals used are identified and described.

3.2.1 Functional Blocks. There are six major logical functional blocks used in this design: the VMEbus interface, the input memory, the Arithmetic Processing Unit (APU), the Arithmetic Control Unit (ACU), the Minimal Small PFA Controller (MSPC), and the output memory. Each of these blocks are discussed below with a general description of the function. Specific design details are left for Chapter IV on VHDL development.

The VMEbus is an asynchronous bus directly suited for the Motorola 68010 micro-processor. The VMEbus interface provides the WFTA system with the necessary interface between the VMEbus and the WFTA system. The host processor accesses logic within this block for all communications with the WFTA system. This communication includes writing data to the input memory, reading data from the output memory, instructing the MSPC to begin operation, and receiving notification when the MSPC is completed with a FFT calculation.

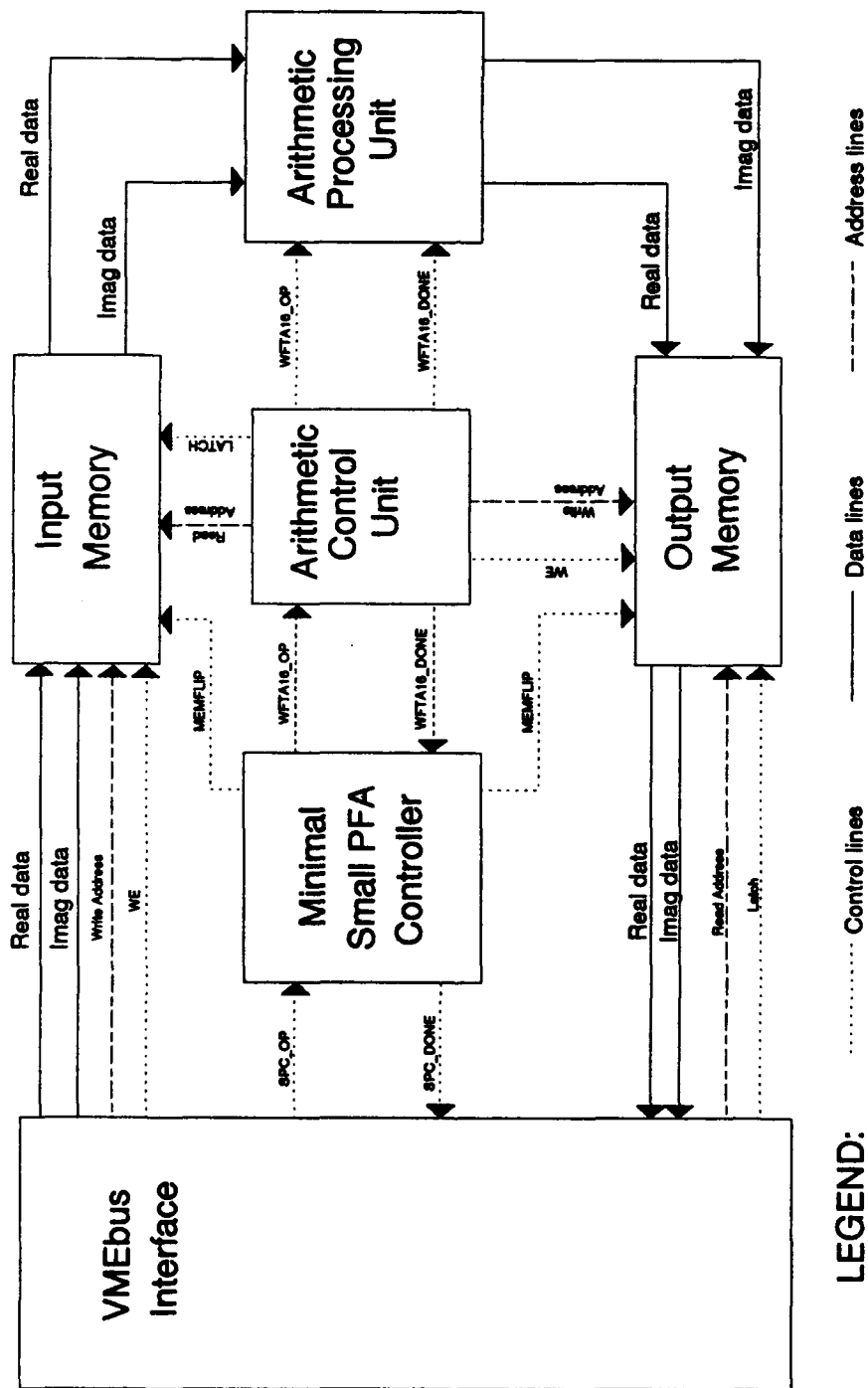


Figure 5. Prototype WFTA System Architecture

The input memory actually consists of two memories (real and imaginary), each containing two switchable banks of memory. This bank-switched architecture is used in order to increase the throughput of the device. The host writes to the one bank of memory while the APU reads from the other bank of memory. The two address ports on this memory allow simultaneous access to both banks of memory, which is necessary in order to keep the WFTA system pipeline full. Additionally, the input memory is even-byte addressable from the VMEbus. The host can only write to the input memory, it cannot read back any of the data.

The Arithmetic Processing Unit (APU) is an application-specific integrated circuit designed at AFIT that reads in data from the input memory, calculates the FFT, and outputs the transformed data to the output memory.

The Arithmetic Control Unit (ACU) works in conjunction with the APU in order to read and write data to and from the input and output memories. The ACU generates the addresses for the input memory and output memory as well as a write enable pulse for the output memory at the correct time. The timing between the ACU and APU are critical and must be synchronized for the input and output of data to and from the APU.

The Minimal Small PFA Controller (MSPC) is the main controller for the entire WFTA system, providing control signals to the system to ensure smooth and proper flow of data through the system. Depending on the input signals, this controller transitions through its states with changes in the corresponding output. This controller was developed specifically for this thesis and minimizes the number of control signals necessary for complete system implementation. The detailed design of the MSPC is discussed in Chapter IV.

The output memory, like the input memory, consists of two memories (real and imaginary) each containing two banks of memory. However, the host reads from one bank of memory while the APU writes to the other. Like the input memory, the output memory is also even-byte addressable from the VMEbus. Additionally, the host can only read from the output memory and cannot write to the output data addresses.

3.2.2 Datapath and Address Lines. The datapath for the real and imaginary data flows in a clockwise direction in Figure 5, as indicated by the arrows on the data lines. The host writes to the input memory, at which point the ACU and APU reads this data into the APU and calculates the FFT. The output of the APU is written to the output memory with addresses and a write enable generated by the ACU. After alerting the host that data is available in the output memory, the host can then read the calculated FFT from the output memory.

There are two addresses which are fed into the memory blocks shown in Figure 5 with directions indicated. There are two addresses because the two banks of memory can be simultaneously accessed. In the input memory, the VMEbus interface provides the write address and the ACU provides the read address. Thus, the host can write data to one of the banks of input memory, while the ACU can read data from the other bank of memory. Similarly, in the output memory, the ACU provides the write address and the read address is given by the VMEbus interface. The ACU can write data to one of the banks of memory, while the host can read the other bank.

The address lines coming from and going to the VMEbus interface are simply the lower eight address line bits on the VMEbus. In this design only sixteen data points are addressed, which requires only four addressing bits. The four additional bits allows for future expansion to other incremental architectures.

3.2.3 Control Signals. The major control signals used in this architecture are highlighted in Figure 5 with the direction indicated by the arrow. Each of these major control lines is covered in a short discussion below. The other control signals mentioned in the reconfigurable system of [2] not covered in this section are not supported in the design and are left for the future development of this system.

The following control signals are signals that already exist in the architecture discussed by Scribner [2]. The *SPCOP* signal going from the VMEbus interface to the MSPC tells the MSPC to begin operations on the set of data in the appropriate bank of input memory. The *SPCDONE* signal, which originates in the MSPC, goes to the VMEbus interface to tell the host the FFT has been completed and the output memory is ready

to be read by the host. The *MEMFLIP* signal going to both the input and output memory from the MSPC controls which bank of memory is oriented towards the host or the APU. The *WFTA16.OP* signal coming from the MSPC goes to both the ACU and the APU to begin calculation of the FFT using the set of data in the input memory, while the *WFTA16.DONE* signal generated by the ACU tells the MSPC when the data from the WFTA system has been written to the output memory. This *WFTA16.DONE* signal also tells the APU to reset some of its internal counters to prepare for the next FFT calculation.

The remaining control signals discussed in this section are peculiar to the WFTA architecture of this thesis. The two *LATCH* signals are present because of the design of the two memories. The *LATCH* signal coming from the ACU to the input memory controls a multiplexer in the memory used to latch data from the bank of memory indicated by the *MEMFLIP* control signal, and to output that data to the APU. Similarly, the *LATCH* signal coming from the VMEbus interface to the output memory controls another multiplexer used to latch data going to the VMEbus interface. Both these *LATCH* signals are asserted after approximately 100 ns. This delay in assertion accounts for propagation delays of integrated circuits in the memory associated with establishing the datapath, in addition to the memory access times.

One control signal not pictured in Figure 5 is the *CONTROL.CLEAR* signal, which clears the control register in the VMEbus interface that feeds into the MSPC. This signal is used to terminate the *SPCOP* signal after six clock cycles before the MSPC transitions to its next state. Without this signal, there is no input signal to the MSPC to hold it in the proper FFT-completion state.

3.3 Design Decisions

Several design decisions were made prior to and during the development of the WFTA system design. Since this system was to be prototyped in AFIT's digital logic lab, there was a desire to minimize the total chip count and to reduce the system to the fewest number of VME cards possible. There was also a consideration to keep the design complexity at a minimum to try to assure a working prototype by the end of this thesis. These two factors,

minimization of chip count and minimization of design complexity, were the general basis for the design decisions made during this thesis.

One design decision was to select the type of host processor to be used in the prototyping of this design. Since the datapath of the WFTA system is 24-bits, a 32-bit microprocessor, like the Motorola 68020 or Intel 486, seems to be the logical choice. However, there was a problem with resources, and the only microprocessor available for the chassis used was the 16-bit Motorola 68010.

Another design decision was to reduce the width of the datapath from 24 bits to 16 bits. The original WFTA design called for a 24-bit wide datapath to insure the designers of the required signal-to-noise ratio (SNR) for the original design specifications. This created a design problem. Even though the platform for this system is the VMEbus backplane, which can at a maximum be configured for 32 bit operations, the host planned for use is the 16-bit Motorola 68010. The additional eight bits would have made the bus interface more complicated, as a single write or read from the memory would take two bus accesses instead of one. There is also an increase in the number of chips for the WFTA system to handle a 24-bit datapath (approximately 32 chips in the memories alone). With these two disadvantages, the WFTA system was decreased to a 16-bit datapath, with the WFTA system providing the parity bit that is needed for the APU. To be sure a 16-bit FFT would have adequate accuracy and SNR, tests were conducted by Mehalic [21] to determine whether the reduction of data would have an adverse effect on the FFT calculated by the APU. The tests between 24 bits and 16 bits indicated that the difference between outputs were insignificant for the accuracy of the WFTA.

Another design decision was to eliminate the imaginary input memory for the WFTA system. There was a problem acquiring the memory chips, which only allowed enough chips for seven of the eight banks of memory required by the system. This factor, coupled with the desire to decrease the total number of chips for the design, made elimination of the imaginary input memory viable. This decision is reasonable since the WFTA is currently expected to calculate the FFT of real signals only, which means the imaginary component of the signal is non-existent, or zero.

Another design decision involved the polling mode of operation used to determine when the WFTA has completed calculating a FFT. The fastest mode of operation, especially with an asynchronous bus such as the VMEbus, would be an interrupt driven system with the WFTA interrupting the host processor immediately when the WFTA was completed. In this system, using the Motorola 68010 host microprocessor, the difference between polling and interrupt operations is negligible because the host does nothing while the WFTA is calculating the FFT. In another system where the host is busy with other tasks, this difference is much more noticable. However, the addition of a interrupt handler module to request and respond to the interrupt lines of the VMEbus would have added many more chips to the design of the bus interface, and decreased available space on the VME cards. Therefore, polling was used for this prototype.

Another design decision was designing this prototype platform for use with only one of the WFTA processors, specifically the WFTA16 processor. The only difference between a system with a WFTA15 or WFTA17 processor is the design of the ACU. There are different FFT processing cycle times associated with these processors versus the WFTA16, as well as a different number of addresses to be generated. Again, however, to completely design a reconfigurable WFTA, the ACU that would be required to generate the correct signals for either the WFTA15, WFTA16 or the WFTA17 processor. This design would have again increased the total number of chips. Furthermore, AFIT is now directing research efforts towards the WFTA16, as the total transistor count for the WFTA16 is less than the WFTA15 or WFTA17. This makes a prototype designed for the WFTA16 alone feasible, and even desirable.

3.4 Design Methodology

The methodology used in design of this system was to functionally decompose the design using a top-down design philosophy. This first level decomposition is essentially completed with the architecture illustrated in Figure 5. The bus interface provides the necessary interaction between the WFTA system and the VMEbus. The input memory stores the 16 points of real data from the host and feeds it to the APU. The ACU provides the addresses and write enable signal to the respective memories at the correct time. The

APU calculates the FFT and outputs this information to the output memory. The output memory stores the FFT from the APU and waits for the host to access the transformed data. Finally, the MSPC orchestrates this interchange, controlling all the components of the WFTA system. The schematics, as well as structural VHDL, in Appendix K generated during the VHDL development of Chapter IV of this thesis provide the necessary detail for further levels of design decompositions.

3.5 Summary

This chapter has covered the modified WFTA system of this thesis. This simplified single processor architecture has not been developed in previous theses and was discussed in this chapter. The architecture for this system was discussed in detail including the major functional blocks, the data path and address lines, and the significant control signals. The major design decisions made prior to construction were also included to provide a historical background to the system design. Finally, the top-down design methodology used in this thesis was briefly covered. The next chapter deals with the development of the VHDL code that simulates the WFTA system.

IV. Development of the VHDL code

4.1 Introduction

One of the objectives of this thesis was to develop the VHDL code to accompany and document the design of the WFTA system to the component level. This chapter discusses the VHDL development for the simplified WFTA system shown in Figure 5. Along with this VHDL development comes the natural discussion of the hardware design of this prototype WFTA system. The only behavioral VHDL descriptions of this system are at the chip level with the more abstract functional blocks, such as the input memory or the ACU, composed of structural VHDL descriptions using the behavioral chip descriptions.

VHDL is a powerful language available to the VLSI design engineer that can be used to simulate hardware systems prior to implementation or construction for verification of design. VHDL is a standard hardware description language developed under the auspices of the Department of Defense in order to manage the documentation of digital designs. There are many advantages to VHDL, including its public availability and technological independence [22]. One of the major benefits of VHDL is that the language takes timing into account. VHDL was adopted as an IEEE standard in December of 1987 [23]. In fact, the reason that VHDL is used in this thesis is to provide verification for the WFTA system design of Figure 5. Before prototyping one chip to a VME board, the designer can be reasonably assured that the design is correct with results from VHDL simulation.

This chapter starts with a short discussion of the Synopsys CAD tool used to design the WFTA system, followed by an examination of the WFTA system concentrating on each one of the major functional blocks. The design described in this chapter represents the final design after all design iterations. The explanation of the test plans used for individual testing and evaluation follows the comprehensive discussion of each of the functional decompositions. The next section of this chapter concerns the host (described in VHDL) used for the testing the entire system, followed with a discussion of the test plans for the VHDL entities. Finally, the last section looks at an evaluation of the actual results compared with the stated objective in Chapter I.

4.2 Synopsys Package

The VHDL analyzer and simulator used for this thesis was the Synopsys VHDL System Simulator Core Programs, which include the Analyzer, Design Library, and Simulator [24]. The Analyzer compiles VHDL source files and produces an object file the Simulator uses to simulate the system. A VHDL debugger program was also especially useful in tracing down logical errors in the VHDL source code.

The Simulation Graphical Environment (SGE) is an environment used for creating and verifying designs [25]. This package is extremely powerful, as it takes schematics with block structures and signals and extracting the structural VHDL, to include the configuration file. This tool was used extensively for this thesis. It was used to create all the structural VHDL files for this WFTA system design, as well the basic structure for the test benches.

The VHDL code development is based on the use of the multi-level logic type, called Multi-Valued Logic-7 levels (MVL7), that is part of the Synopsys package. MVL7 is an enumerated data type of seven distinct levels that a signal can possess; '1' (high), '0' (low), 'X' (unknown), 'W' (weak unknown), 'L' (weak low), 'H' (weak high), and 'Z' (high impedance). Other signals from the Synopsys standard types package were used exclusively. A bit vector or bus, of MVL7 is defined of type MVL7_VECTOR was used for logically adjacent signals. In conjunction with the MVL7 and MVL7_VECTOR type, this thesis also uses the resolved signal types DOTX and BUSX. Resolved signal types use a resolution function to determine the value of a node when more than one module in the VHDL code drives the signal.

4.3 The WFTA System

The modified architecture of the WFTA system of this thesis was briefly discussed in Chapter III. This section covers the detailed design of the WFTA system. The architecture described by Figure 2 was translated into the Synopsys SGE environment resulting in the schematic shown in Figure 6. This figure includes all the signals and ports that were required to be implemented in the final design of the single processor architecture.

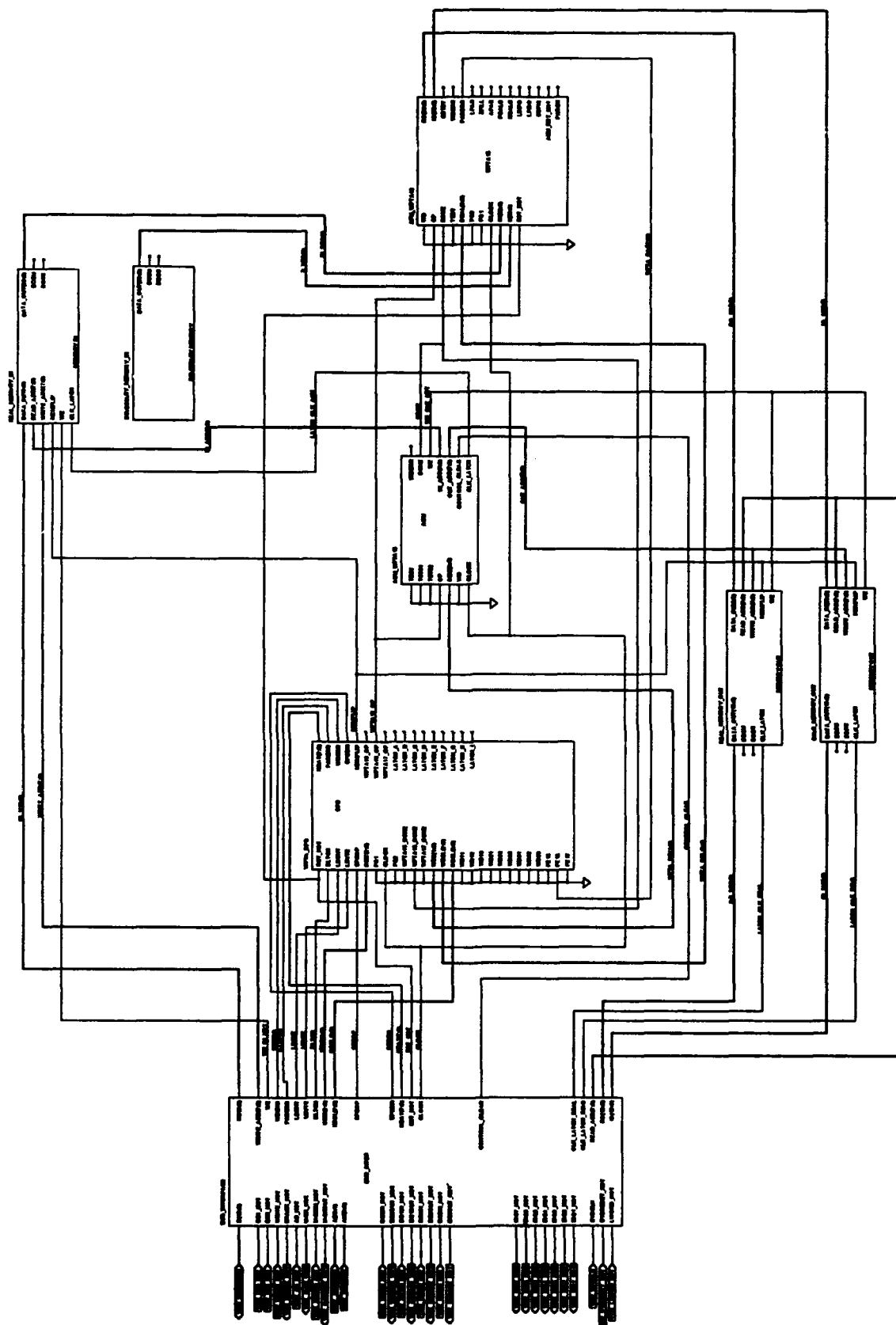


Figure 6. WFTA System Architecture

The first level functional decomposition discussed in Chapter III essentially forms the structure for the rest of this chapter. Each first level component or major functional block is discussed in the pages that follow. The complete set of schematics developed and used for this thesis are located in Appendix K of this thesis. A few of these same schematics are also included in this chapter and Appendix A to provide the reader with illustrations of the written design. The major functional block timing diagrams showing the interrelationships of signals are also provided in Appendix B. Additionally, the complete listing of VHDL descriptions (both behavioral and structural) to include entity, architecture, and configuration data is also located in Appendix K of this thesis.

Following a section on the behavioral description of the integrated circuits and other modules used in the WFTA design, the specific and detailed descriptions of the structural VHDL code of each of functional blocks are discussed.

4.3.1 Behavioral Descriptions. The intent of this VHDL development was to model, as closely as possible, the actual design and construction of the proposed WFTA system. The basic building blocks for this design are behavioral VHDL descriptions of integrated circuits, modules which allow for future expansion, or modules used to model hardware considerations. Starting with an high-level, abstract conception of the WFTA system, the design can be functionally decomposed into hierarchically functional blocks using a top-down design methodology. At the lowest level of the structural VHDL descriptions are the behavioral VHDL descriptions discussed below.

4.3.1.1 Integrated Circuits. At the bottom of this hierarchically structural WFTA system design are the actual chips used in the construction of the system. Taking the specifications and datasheets of the integrated circuits [26, 27, 28], which describe the function and timing of each of the chips used in the design, behavioral descriptions in VHDL were written. Due to the great number of integrated circuits, a detailed discussion of the behavioral VHDL descriptions is not possible, however, the behavioral VHDL can be found in Appendix K. Table 1 provides a listing of the chips along with the filename of its associated behavioral description. For the common chips, the behavioral descriptions used are from the Synopsys library and are annotated SYNOPSYS in Table 1. In the MSPC, a

Table 1. Integrated Circuits and Behavioral Descriptions

<i>Type</i>	<i>Name</i>	<i>Source or Filename</i>
MCM6264	8K X 8 SRAM	mcm6264.vhd
SN74LS00	Quadruple 2-Input Positive NAND gate	DESIGN
SN74LS02	Quadruple 2-Input Positive NOR gate	DESIGN
SN74LS04	Hex Inverter	SYNOPSYS
SN74LS08	Quadruple 2-Input Positive AND gate	SYNOPSYS
SN74LS10	Triple 3-Input Positive NAND gate	DESIGN
SN74LS31	Delay Element	sn31.vhd
SN74LS32	Quadruple 2-Input Positive OR gate	SYNOPSYS
SN74LS73	Dual JK Flip Flop with Clear	DESIGN
SN74LS74	Dual D-type Flip Flops	sn74.vhd
SN74LS135	2-Input Exclusive OR gate	SYNOPSYS
SN74LS109	Dual JK Flip Flop	sn109.vhd
SN74116	Dual 4-bit Latches	sn116.vhd
SN74121	Monostable Multivibrator	sn121.vhd
SN74161	Synchronous 4-bit Counter	sn161.vhd
SN74180	9-bit Odd/Even Parity Generator/Checker	sn180.vhd
SN74LS373	Octal D-type Latch and Flip Flops	sn373.vhd
SN74LS374	Octal D-type Latch and Flip Flops	sn374.vhd
SN74ALS520	8-bit Identity Comparator	sn522.vhd
SN74ALS604	Octal 2-input Multiplexed Latches	sn604.vhd
SN74ALS747	Octal Buffers and Line Drivers	sn747.vhd
SN74ALS757	Octal Buffers and Line Drivers	sn757.vhd

different behavioral description was used in conjunction with the Design Compiler and is discussed in detail in the MSPC section of this chapter. These entries are marked DESIGN.

It should be noted that these descriptions are not complete in the sense that they perfectly model the functional behavior of the chips. Due to time constraints, detailed behavioral VHDL descriptions of these integrated circuits could not be developed. The descriptions are, however, reasonably complete, in an overall functional sense, to provide evidence that the design for this thesis is functionally correct and feasible.

During the following discussions of the design of the WFTA system, the integrated circuits are mentioned only by type, i.e., SN74LS373. For a description of the function associated with that type, cross reference using Table 1.

4.3.1.2 Modules for Future Enhancement or Hardware Consideration. There were other modules of the design that were left in the behavioral VHDL format to either simulate hardware considerations or provide room for future enhancements and modifications. A hardware consideration is a physical fact concerning construction, like grounding or direct connections. These hardware considerations must be simulated in the VHDL code. An example of a module simulating hardware considerations would be the a module that grounds the imaginary input data lines to the APU. For those modules that are left for future enhancements, the signals associated are discussed in [2] but were not implemented in this initial system design. These files are enumerated below with a short explanation for each concerning their functionality.

1. *acu_not_used.vhd* This file has been left for future enhancements of the VHDL code and system design. This module includes signals which are not implemented in the ACU design and makes no contribution to the VHDL simulation. This module was included for completeness. Future researchers will be able to augment the system design by coding functionality into the module.
2. *grounded.vhd* This file models a hardware consideration. These signals model the physical property of wiring these signals to ground.
3. *imag_in.vhd* This file models a hardware consideration. As previously discussed, due to lack of available memory chips, the imaginary input memory was not implemented. In order to maintain logical continuity, this module models the grounded pins on the WFTA processor.
4. *interrupt.vhd* This file has been left for future enhancements. For the maximum throughput and speed the WFTA system needs to notify the host processor when it has completed a FFT using an interrupt system instead of the host polling the WFTA for completion.
5. *mem_check.vhd* This file has been left for future enhancements. In the original design of the WFTA, the memory was to have a memory error detection and correction ability. This feature was not implemented with this thesis.

6. *reset.vhd* This file models a hardware consideration. Whenever the VMEbus resets, this system reset would reset the WFTA board.
7. *spc_not_used.vhd* This file has been left for future enhancements. This module is similar to the *acu_not_used.vhd* file above. This module includes signals which are not implemented in this MSPC design and was included for completeness.

4.3.1.3 Modules for Ease of Use in the Synopsys SGE Environment. The Synopsys SGE environment does have certain operational limitations. These files provided a bypass for the schematic graphical environment's safeguards. One of the problems encountered in this thesis was the inability to connect two named nets directly in the schematic. A named net is a specific node of a circuit and the SGE tool does not allow a node to have more than one name. The two files *straight.vhd* & *straight1.vhd* were used make this connection possible. The VHDL code simply assigns the incoming signal to the outgoing signal. Another problem is that GND and VCC are not associated with the MVL7 values '0' and '1', respectively. This problem was dealt with using a package called *wfta_types.vhd* which makes a default assignment with GND assigned '0' and VCC assigned '1'. Also included in this file are a few type conversion functions which are necessary for the use of previously created VHDL behavioral code for the WFTA processor or APU. Each structural description generated from the schematic includes this file in order to eliminate this problem.

4.3.2 Common Gates. Throughout the design, there are several instantiations of standard logic gates, such as AND gates, inverter gates, and the like. The behavioral descriptions used for these gates are the ones found in the Synopsys standard library. The propagation delays for these gates defaults to 0 nanoseconds for both THL (propagation delay from input high to output low) and TLH (propagation delay from input low to output high). This instantaneous result is not indicative of actual timing delays, and in order to simulate the constructed system, reasonable values for timing were mapped to the generic map of these behavioral descriptions. In the VHDL code developed for this thesis the times annotated in Table 2 are used in all the VHDL simulations. The times that are used in

Table 2. Instantiated Propagation Delays for Common Gates

<i>Type of Gate</i>	<i>TLH</i>	<i>THL</i>
Inverter	6.0 NS	6.5 NS
OR gate	5.0 NS	5.0 NS
AND gate	6.0 NS	7.5 NS
NAND gate	4.5 NS	5.0 NS
NOR gate	5.0 NS	5.0 NS

Table 2 were taken from the TTL Databook from Texas Instruments [26] and represent real time delays in the corresponding gates.

4.3.3 Bus Interface. This functional block of the design provides an interface between the WFTA system and the selected bus standard, the VMEbus. It contains all the decoding circuitry and separates the WFTA from the VMEbus until the host has decided to address the system. All communication with the host takes place through the bus interface.

The VMEbus is a popular bus standard with industry and its specifications are located in IEEE standard 1014 [7]. For this thesis, the configuration of the VMEbus is for a 16-bit machine in a 96-line bus with 23 address lines and 16 data lines. One of the features of this bus is that it is asynchronous and directly suited for the host processor that is used with this thesis, a Motorola 68010. The VHDL code for this thesis uses most of the signals associated with the IEEE standard, but does not model them all because all the signals are not necessary to model the system. For example, the VMEbus standard includes pins for +5 volts DC and ground which are not included in the VHDL simulations because they are unnecessary. This thesis focuses on those signals associated with data transfer functions and those particular signals used for the host that is driving the WFTA system.

A block of 32K bytes of the VMEbus address space has been allocated for the WFTA system. Although this large block is not used in its entirety, this address space allows for an easier decoding scheme for the bus interface. This decoding scheme allows for future

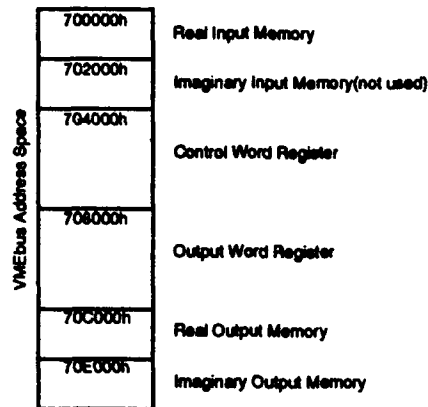


Figure 7. Memory Mapping for WFTA Prototype System

expansion to any of the two WFTA processor architectures. However, for the 4080-point WFTA system (all three processors included), this decoding scheme is inadequate and would have to be revised. In the 4080-point WFTA system, the memory requires an 8K byte memory space (4K words of 2 bytes each). For this thesis, the assumption was that each one of the memories for the WFTA system has an 4K byte memory space. Since there are "logically" four memories (the imaginary input memory was eliminated) this adds up to 16K bytes of VMEbus address space. The two registers in the control section of the bus interface use the remaining 16K bytes of address space. The memory mapping used for the WFTA is depicted in Figure 7.

With this decoding scheme in mind, the top eight bits of the address lines (A23 - A16) are common to all the WFTA system components and have been arbitrarily set at "01110000" in binary notation or "70" in hexadecimal notation. The next three bits are decoded for the particular section of the WFTA that the host is addressing. The scheme for decoding is shown in Table 3. The 'X' values in the table represent "don't cares" (either '1' or '0').

The bus interface is logically separated into three distinct and abstract functional blocks; the input section, output section, and the control section. The input section provides the datapath from the VMEbus to the input memory, the control section provides the control functions necessary for the WFTA system, and the output section provides the

Table 3. Decoding for WFTA Components

<i>A15</i>	<i>A14</i>	<i>A13</i>	<i>Component</i>
'0'	'0'	'0'	Real Data Input Memory
'0'	'1'	'X'	Control Word Register
'1'	'0'	'X'	Output Word Register
'1'	'1'	'0'	Real Data Output Memory
'1'	'1'	'1'	Imaginary Data Output Memory

datapath from the VMEbus to the output memory. Figure 8 is the schematic created in the SGE environment.

There is one functional block in the schematic not discussed below, which is marked as STRAIGHT in Figure 8. This has no function in the operation of the WFTA and is only meant to be a reminder to the user that bus grants are daisy-chained under the VMEbus standard. If there are more than two devices on the VMEbus which can become bus master, then the bus grant from the bus controller is transmitted via the bus grant lines. The WFTA system described in this thesis is merely a slave device and does not use these signals. These lines must be jumpered in the slot for the WFTA processor on the VMEbus.

4.3.3.1 INPUT_SECTION block. This functional block decodes the appropriate bits for a memory write from the host processor to the real input memory of the WFTA system and passes the corresponding data and address lines. It also generates a positive write enable pulse at the correct time to write data to the memory. The schematic for the input section is shown in Figure 21 of Appendix A.

The single SN74LS520 monitors the VMEbus until the condition for a write to the input memory occurs. The comparator decodes the three address bits discussed above and enables the data and address lines through three SN74LS374 to the real input memory. The output of the identity comparator is asserted low and requires an inverter to latch the positive edge-triggered SN74LS374 latches.

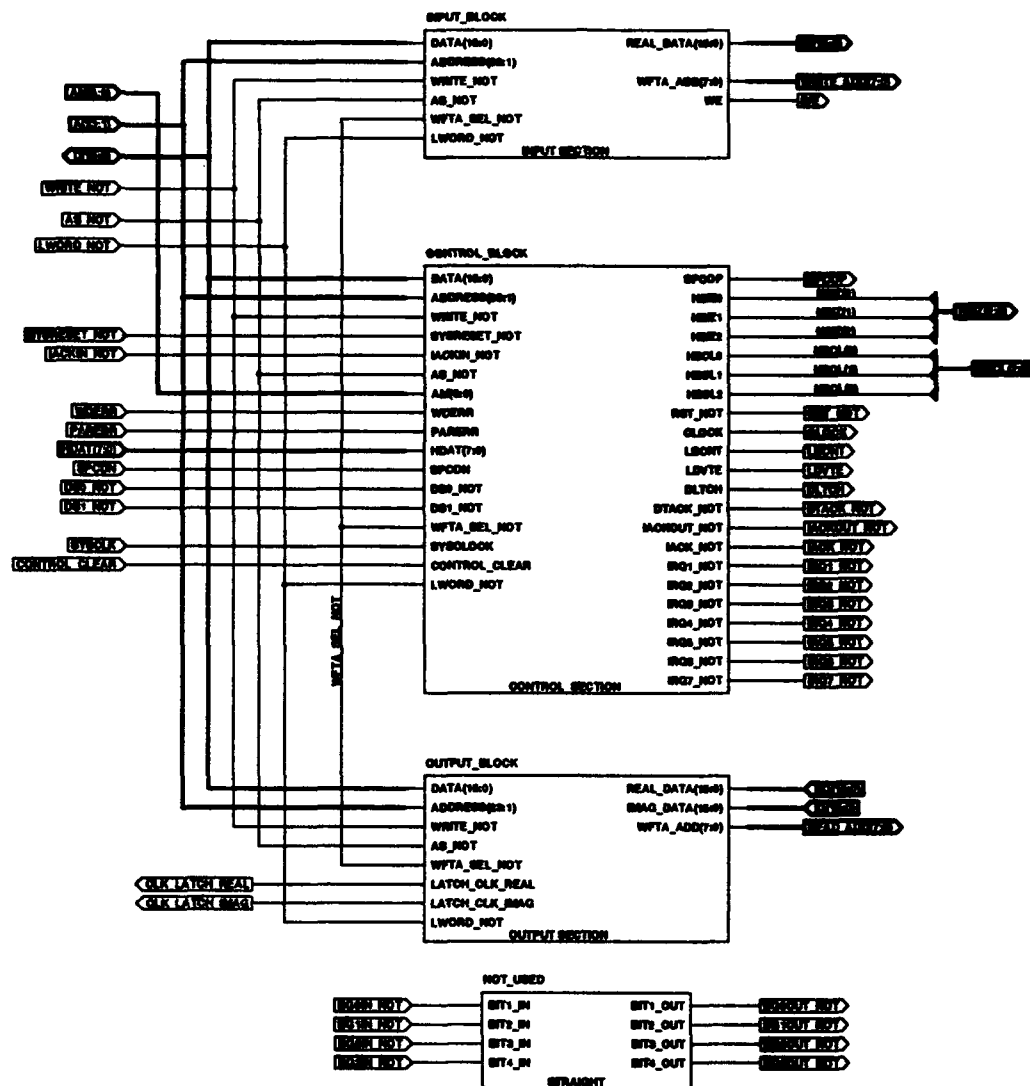


Figure 8. Bus Interface Schematic

The remaining SN74LS121 is used to generate the write enable pulse for the real input memory. The output of the comparator triggers the one-shot and the generated write enable pulse is sent to the input memory. This pulse width is 40 ns, which satisfies the write enable pulse requirements for the memory chips used in the design. Since the comparator is monitoring the VMEbus lines associated with a write to the input memory, no other conditions can cause an inadvertant write enable pulse to be sent to the memory.

The timing diagram for the significant signals of the input section is shown in Figure 35 of Appendix B. After the *REAL_DATA_ENABLE* signal goes low, the *REAL_DATA* bus output (AAAAh) reflects the data from the VMEbus. The *WE* pulse is not generated

until after the output data from the input section is valid. The only signal here which needs further explanation is the *WFTA_ADD* address. The address on the VMEbus is shown as 700004h and the address that is output from the input section is 02h. This seeming discrepancy is caused by the VMEbus addressing scheme. The VMEbus is byte-addressable while the WFTA is word-addressable. Address 4 on the VMEbus corresponds to the first byte of the second word (or address 2) in the WFTA memory. So, the WFTA is operating correctly. This addressing difference will be also be evident in the output section.

It should be noted that since the comparator monitors the *WRITE_NOT* signal on the VMEbus, a read from the input memory is not possible. Additionally, given the design of the input memory, a read is not possible because no datapath exists back to the VMEbus from the input memory. Data can only move forward through the WFTA system.

4.3.3.2 CONTROL_SECTION block. This functional block provides the means for the host processor to control the WFTA system. The heart of this section are two registers called the control register and the output register. Through these two 16-bit registers the host processor starts the WFTA and determines when the WFTA is finished calculating the FFT. The schematic for the control section is shown in Figure 22 of Appendix A.

In order to decrease the decoding circuitry for the prototype WFTA system, three SN74LS520 decode those signals common to all WFTA system accesses. These signals are comprised of the top eight bits of the address lines, the address modifier lines, the *DS0_NOT* and *DS1_NOT* data strobe lines, and the *LWORD_NOT* lines. Since these signals are the same for all WFTA system accesses, they can be monitored centrally here in this section and the other sections (input and output sections) can be informed when the signals occur. Table 4 shows the VMEbus signals that are constant and do not change over all WFTA accesses. When the WFTA system is addressed, these comparators generate a signal (*WFTA_SEL_NOT*) through a series of OR gates which are sent to the other two sections of the bus interface. All three sections use the *WFTA_SEL_NOT* signal in conjunction with other signals specific to their operation to determine whether they are being addressed by the host.

Table 4. Common VMEbus Signals Interfaced to the WFTA

VMEbus Signal	Value
Address (A23 - A16)	"01110000"
Address modifier (AM5 - AM0)	"111101"
DS0_NOT	'0'
DS1_NOT	'0'
LWORD_NOT	'1'

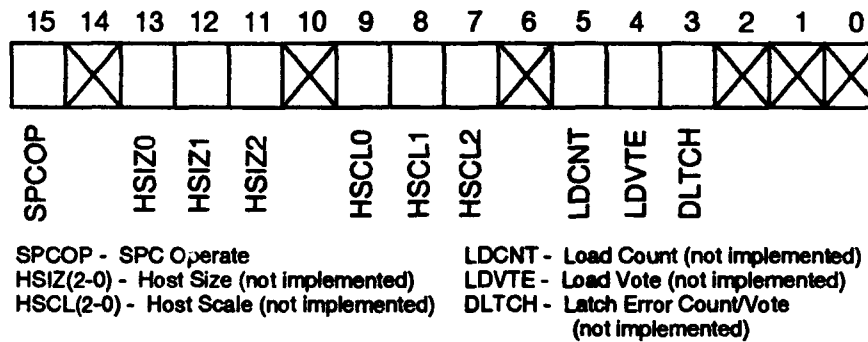


Figure 9. Data Format for Control Word

The control register of the control section is how the host processor tells the WFTA it has written a set of data points to the input memory and the WFTA may begin calculation of the FFT. Presently there is only one signal (*SPCOP*-SPC Operate) that is used with the WFTA system, though the design allows for future expansion. Table 9 includes the signals for future expansion described in [2]. For example, in the reconfigurable WFTA design, certain data, such as the size and scale of the FFT, must be transmitted to the MSPC for proper control signal generation. The single SN74LS520 decodes the three address bits (A15-A13) and latches the sixteen data lines through two SN74LS116 to the MSPC. The data format for the control register is indicated in Figure 9.

By polling the output register of the control section, the host processor knows that the WFTA has computed the FFT and has written a set of points to the output memory. Presently there is only one signal (*SPCDN*-SPC Done) used in the WFTA system of this thesis, though the design allows for future expansion. Table 10 includes the signals for

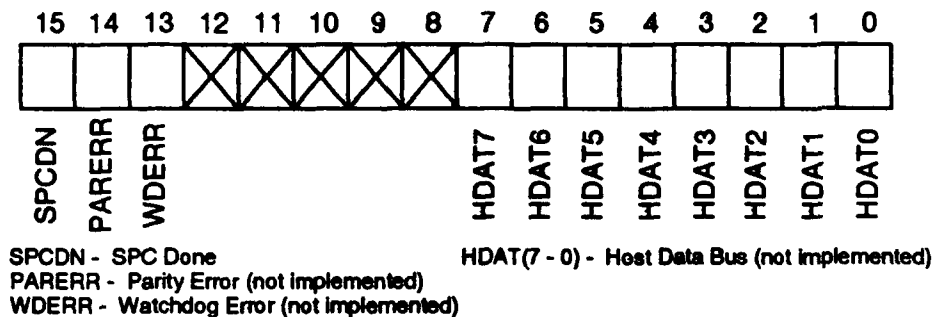


Figure 10. Data Format for Output Word

future expansion described in Scribner's thesis. For example, in the original WFTA design, a parity error can be detected by the APU or WFTA processor and can alert the MSPC that a parity error has occurred and the output is incorrect. The single SN74LS520 decodes the three address bits (A15-A13) which allows the output of the MSPC to be transmitted to the data lines through two SN74LS747. These line drivers are needed to provide enough drive current for the VMEbus. Further, the drivers satisfy the IEEE standard, which indicates the data lines must be driven by a tri-state device [7]. The data format for the output register is indicated in Figure 10.

As mentioned earlier in this section, the VMEbus is an asynchronous bus, which means that the slave, in this case, the WFTA, must somehow notify the host when it is finished processing the data. The VMEbus signal used in this handshaking procedure is the DTACK_NOT signal. The host processor starts a read or write cycle and waits for the slave to assert DTACK_NOT. At this time the slave has indicated the data transfer is complete and the host processor can continue with its operations. When the AS_NOT signal goes high, the slave releases the DTACK_NOT line.

The DTACK_NOT line is permanently tied low in this thesis, which seems to contradict the handshaking procedure discussed in the previous paragraph. The memory or control section does not have enough time to react to the host's addressing. This contradiction is easily explained when the type of host processor is discussed. For this thesis, the host processor is a Motorola 68010 16-bit microprocessor. This processor does not look for

the DTACK_NOT signal assertion until the falling edge of its own state 4, which is 250 ns after the cycle has begun [29]. This 250 ns time is enough for either a read or write to memory or a read or write to the control and output registers. Simply stated, the WFTA system is able to finish the cycle before the 68010 can reply. With a faster processor this convenience might not be possible.

The DTACK_NOT signal, tied low, goes through a SN74LS757 which is enabled when any part of the WFTA is selected. This line driver is necessary to provide adequate current to the VMEbus line. Furthermore, the DTACK_NOT line must be an open collector output [7].

The RESET block simply routes the VMEbus SYSRESET line to the WFTA. When the VMEbus resets, the WFTA system is forced to a known start state. This reset signal (*RST_NOT*) propagates through the design to drive flip flops and the finite state machine of the MSPC to a known state. Initially when the system is first powered up, the bus master propagates this signal to the entire bus.

The VMEbus SYS_CLOCK signal operates at 16 MHz. The clock block of the control section is simply a frequency divider which takes the 16 MHz and generates an 8 MHz system clock for the WFTA. This frequency divider is a SN74LS109 in a toggle configuration. The 8 MHz gives the WFTA a 100 nanosecond period with approximately a 75 % duty cycle. The signal is asymmetrical because of the propagation timing of the SN74LS109. The propagation time for a low to high transition of the output is 13 ns and for a high to low transition of the output is 25 ns. The WFTA system operates correctly using a clock with a 75 % duty cycle. This clock has been left as a block for future expansion when the WFTA will be required to operate at faster speeds and a different clock will have to be used.

The timing diagram for the significant signals of the control section are shown in Figure 36 and Figure 37 of Appendix B. The timing diagram is broken into two parts; Figure 36 shows a write to the control word and Figure 37 shows a read from the output word. In Figure 36, the VMEbus address lines are 704000h which maps to the control word access and the VMEbus data lines read 8000h which corresponds to the host telling the

MSPC to begin operation. The control section responds by driving the *SPCOP* signal high after approximately 20 ns. In Figure 37, the VMEbus address lines are 708000h which maps to a output word access. The control section responds by driving the VMEbus data lines to an arbitrary 8055h. If the host were polling this would indicate that the MSPC has completed the FFT calculation. Notice in both figures that the VMEbus clock has been divided and the WFTA system clock is operating at twice the period.

The interrupt handler has already been mentioned in the behavioral section and has not been implemented in this thesis cycle. It is only here to provide room for future expansion.

4.3.3.3 OUTPUT_SECTION Block. This functional block decodes the appropriate bits for a memory read from the host processor to the real and imaginary output memory of the WFTA system and passes the appropriate address lines. It also generates a latch signal which tells the memory when to output data to the output section and through bus drivers to the data lines on the VMEbus. The schematic for the output section is shown in Figure 23 of Appendix A.

There are two SN74LS520's to decode whether the host is addressing the real output memory or the imaginary output memory. The two outputs of the identity comparators are tied to an AND gate which enables and clocks a SN74LS374 transmitting the desired address to the output memory.

Due to the design of the memory, the output section must also transmit a control signal to the output memory indicating when the multiplexers are to latch data from the memory chips. The two SN74LS31 are used to delay the outputs of the identity comparators long enough for the memory to be accessed. These two control signals are the *LATCH_CLK_REAL* and the *LATCH_CLK_IMAG* signals. The outputs of the identity comparators are asserted low and requires two inverters to latch the positive edge-triggered SN74LS374 latches.

The two sets of two SN74LS747's drive the VMEbus data lines with the output of the real and imaginary output memories. Again, as mentioned previously, the data lines must be driven by a tri-state device.

The timing diagram for the significant signals of the output section are shown in Figure 38 and Figure 39 of Appendix B. The timing diagram is broken into two parts; Figure 38 shows a read from the real output memory and Figure 39 shows a read from the imaginary output memory. In Figure 38, the VMEbus address lines are 70C004h which maps to a real output memory access. The difference in the VMEbus address lines and the *WFTA_ADD* lines was discussed in the input section previously. In Figure 39, the VMEbus address lines are 70E0004h which maps to an imaginary output memory access. In both figures, the output section responds by sending a latch signal (either *LATCH_CLK_REAL* or *LATCH_CLK_IMAG*) to the output memory and then driving the VMEbus data lines with the memory output.

It should be noted that since the comparator monitors the *WRITE_NOT* signal on the VMEbus for logic high, the host cannot execute a write to the output memory. Additionally, given the design of the output memory, a write is not possible since a datapath to the output memory from the host does not exist. Data can only flow from the APU to the output memory.

4.3.4 Input and Output Memory. The memory functional blocks include both the input memory and the output memory. Data is written by the host into the input memory and, conversely, data is read by the host from the output memory. The problem with the memory was to construct a dual bank of memory that is switchable, that is, with one bank accessible by the host processor over the VMEbus and the other bank holding data for the APU with both banks accessible at the same time. While the APU is operating with a set of data, the host is loading a new set of points into the next bank. This bank switchable feature increases the overall throughput of the system.

The original WFTA design called for an application-specific memory chip which would perform this dual access with one bank of memory always accessible from either the host or the APU. However, this component was not available at the time of this thesis and had to be constructed discretely with commercially available chips.

In this design, 12K of VMEbus address space has been allocated to the memory in consideration of the 4080-point processor that was envisioned by earlier designers. In

this design, only 16 locations of the address space is used, but addresses has been made available for future enhancements. There is 4K of memory for each of the three memory components in the system; real input memory, real output memory and imaginary output memory. As previously discussed, there is no imaginary input memory. The 4K VMEbus address space has been allocated for the imaginary input memory to ease address decoding.

All memory is addressable from the VMEbus, but access is limited. The host cannot read from the input memory or write to the output memory due to the VMEbus read and write decoding.

The input memory (MEM_IN component) and output memory (MEM_OUT component) for this system are essentially the same, and the differences in the VHDL code can be attributed to the 24-bit to 16-bit datapath design decision discussed previously. Figure 11 shows the Synopsys schematic for the MEM_IN component. Figure 12 shows the Synopsys schematic for the MEM_OUT component. Note that the only difference between the two is in the DEMUX1 and MUX2 components in the MEM_IN schematic and the DEMUX1a and MUX2a components in the MEM_OUT schematic.

There are two signals that require additional explanation in Figures 11 and 12. The first signal is the *CS_NOT* signal on the BANK0 and BANK1 instantiations of both figures. In actuality, *CS_NOT* is not a chip select signal as the name implies. The *CS_NOT* signal is an output enable for the memory chip used in this design. When *CS_NOT* is low, the output of memory is disabled and the memory is configured to perform a write operation. When *CS_NOT* is high, the output of the memory is enabled and the memory is configured to perform a read operation.

The second signal that might be confusing in Figures 11 and 12 is the *SEL* signal on the DATA_MUX instantiation. Due to the selection of integrated circuits, the *SEL* signal is opposite in function to the one used in the DEMUX1, DEMUX2, and DEMUX3 blocks. When *SEL* is high the IN1 input lines are routed through to the output of the multiplexer. When *SEL* is low the IN0 input lines are routed through to the output of the multiplexer.

The original intent of the WFTA design had the memory implemented using both error detection and correction circuitry; however, there is no error detecting or correcting



logic in this design. This circuitry is missing due to space and chip count restrictions on the size of the finished prototype.

The memory is functionally decomposed into five subsections, to be discussed in detail in the sections that follow. The demultiplexer blocks route the address, data, and write enable signals to the appropriate bank of memory, while the multiplexer block routes the data from one of the banks to the APU. The schematics for these functional blocks are shown in Appendix A. After all of the functional blocks are discussed and the major signals introduced, there is a short discussion of the timing diagrams of both the input and output memory. The timing diagrams for the memories are shown in Figures 40 and 41 of Appendix B.

4.3.4.1 DEMUX1 & DEMUX1a Block. This block routes the incoming data lines to the appropriate bank of memory. Depending on the control signal generated by the MSPC, the incoming data is routed and written to the only one bank of memory. The other bank of memory is oriented towards the ACU and APU. The schematics for the DEMUX1 and DEMUX1a blocks are shown in Figures 24 and 25, respectively, of Appendix A.

This is one of the blocks which is different between the input memory and the output memory. The DEMUX1 block is used in the input memory while the DEMUX1a block is used in the output memory. Both use four SN74ALS373's. This block allows data to pass to all four SN74ALS373's but enables the output of only two of them based on the select signal generated by the MSPC. Only two of these latches are enabled at one time due to the inverter gate which separates the two enable pins. Two latches are necessary for the 16 bits of data—one for the upper eight bits of data and the other for the lower eight bits of data.

The only difference between the two blocks is the number of data bits that are input into the memory. In the case of DEMUX1a block, there are 8 bits of data from the APU which are never used as the APU still sends 24 bits of output data instead of the 16 bits which the system was designed to accept. Bit 7 through bit 0, which are the least significant in this data format, are the bits which are discarded. Functionally, there are no other differences between the two components.

4.3.4.2 DEMUX2 Block. This block routes the incoming address lines of the memory to the appropriate bank of memory. There are two of these blocks in the input memory and output memory schematics because the memory has the ability to read and write from the separate banks at one time. The structural configuration of the memory and the select line from the MSPC make this simultaneous transfer possible. Again, depending on the control signal generated by the MSPC, the incoming address lines are routed to the appropriate bank of memory. The schematic for the DEMUX2 block is shown in Figure 26 of Appendix A.

This block is similar to the previous section in its implementation. Instead of four SN74ALS373, there are only two latches because the number of bits of data in this case is eight instead of sixteen. Again only one of the latches is enabled at one time due to the inverter gate which separates the two enable pins. Although, technically, the memory for this system needs only four bits of address for the 16 words that are written to memory, eight bits were passed for future enhancement.

4.3.4.3 DEMUX3 Block. This block routes the incoming positive logic write enable pulse to the appropriate bank of memory. Depending on the control signal generated by the MSPC, this block routes the write enable pulse to correct bank of memory. The schematic for the DEMUX3 block is shown in Figure 27 of Appendix A.

There is a subtle difference in this block versus the other DEMUX blocks discussed above because instead of a high impedance output on the non-selected signal there must be a high output. This is necessary to prevent unwanted writes to the non-selected bank of memory. Since the write enable for the memory is negative logic, this block also serves to translate the positive write enable pulse from the ACU into a negative pulse that can be used by the memory. For this reason a SN74LS74 was used. It is used asynchronously with the control signal either enabling the clear or preset function of the flip flop. An inverter between the two pins prevents enabling both the clear and the preset pins at the same time. However, there exists a finite time (propagation delay of the inverter) when the clear and preset are momentarily the same. This is not a problem because it does not generate a write enable pulse. According to the specifications for the SN74LS74 [26], when both

clear and preset are high the output is the stored value and when both clear and preset are low the output is high on Q and Q_NOT. The write enable pulse from the ACU or the VMEbus interface is not generated for approximately 100 ns, which allows enough time for the signals in this block to transition to their proper values.

The two outputs of the flip flop (Q and Q_NOT) are input to two OR gates and, depending on which output is zero, the active low write enable pulse from the ACU or VMEbus interface is directed to the correct bank of memory. Since Q and Q_NOT are not the same, only one of the OR gates will allow the write enable pulse to pass through to the memory chips.

4.3.4.4 MEM_MCM6264 Block. This block is essentially a bank of memory using two Motorola MCM6264 chips to store a single 16-bit word. One of the chips stores the upper eight bits of data while the other stores the lower eight bits of data. Although only the lower seven addresses are used for this chip, only 16 words are stored at one time for this single configuration architecture leaving a large amount of memory left for future enhancements. The schematic for the MEM_MCM6264 block is shown in Figure 28 of Appendix A.

This additional memory bandwidth was necessary because of the lack of commercially available chips that would have been more suitable for the WFTA. There is apparently no commercial demand for a 16 word 16-bit memory. The design decision was to use a larger capacity chip which could store a longer word of memory and be relatively fast. After careful consideration of the available choices, the Motorola MCM6264 8K X 8 Static random access memory (SRAM) chip was chosen as it satisfied these requirements. After searching available memory chips, the "ideal" memory chips for this thesis are scarce in the industry.

Static RAM was selected over dynamic RAM for a number of reasons. The increased speed of memory access for both reads and writes, although for this particular host processor are not critical, is desirable for increased speed of the overall device. Some dynamic RAM memories also require additional chips for control and refresh circuitry which would have added additional chips to the total chip count which was undesirable. Further, dy-

dynamic RAM is more dense with generally more words of storage of shorter word length. The memory required must be able to store 16-bit words from the host and using dynamic RAM would have wasted memory versus less waste for any static RAM configurations.

4.3.4.5 MUX2 & MUX2a Block. This block is the interface between the output of the memory banks and the output of the memory component. Based on the control signal from the MSPC discussed below, the correct input is selected between the two memory banks outputs and multiplexed out of the memory. The schematics for the MUX2 and MUX2a blocks are shown in Figures 29 and 30, respectively, of Appendix A.

These blocks are structurally different between the input memory and the output memory. The MUX2 block is used in the input memory while the MUX2a block is used in the output memory. Both blocks use two SN74ALS604, one for the upper eight bits and the other for the lower eight bits. The difference between the two blocks is in the addition of two SN747180 in the MUX2 block which are used to generate the odd parity bit (bit 0) needed for the APU. One calculates the odd parity of the upper eight bits, and the other calculates parity for the lower eight bits. These two outputs are fed into an exclusive-OR which then calculates the entire parity of the 16 bit word. The remaining seven bits of the output of the memory input have been grounded, to account for the difference in the 24-bit versus 16-bit data words.

4.3.4.6 Input and Output Memory Timing Diagrams. The timing diagram for the input memory is shown in Figure 40 of Appendix B and the timing diagram for the output memory is shown in Figure 41 of Appendix B. The two timing diagrams are similar because, functionally, both of the memories operate exactly the same and the two test benches used to generate these timing diagrams used similar input test vectors. The only differences have already been discussed in Sections 4.3.4.1 and 4.3.4.5. The input memory reads in 16 bits of data and outputs 24 bits of data with a generated parity bit, while the output memory reads in 24 bits of data and outputs 16 bits of data. The other signals are the same, only the sources of the signals are different.

In both timing diagrams, the input data (*DATA_IN*) changes halfway through the simulation. Also notice that the *MEM_FLIP* signal changes at the same time that the data changes. The two addresses to both memories (*BANK1_ADD* and *BANK0_ADD*) remain the same for these simulations. *MEM_FLIP* is the most important signal in the memory because it controls the flow of data to and from the correct bank of memory. All the inputs of the two banks of memory are also shown in both timing diagrams.

In Figure 40, the input memory initially receives 16 bits of data (5555h) from the VMEbus interface. *MEM_FLIP* is high which routes the data to memory bank 1 (*DATA1*). The *WE* pulse from the VMEbus interface gets routed to memory bank 1 (*WE_1*). This causes the input data to be written to address 3 (*BANK1_ADD*) of memory bank 1. Meanwhile, memory bank 0 is reading from address 8 (*BANK_ADD*) and after the odd parity bit is calculated outputs this to the APU (*DATA_OUT*). During the second half of the simulation, the *MEM_FLIP* signal is low, which causes the input data (AAAAh) to be written to bank 0 (*DATA0*) and the output data to be read from bank 1 (*DATA_OUT*). Except for the differences in size of the input and output data, and the generation of the parity bit, Figure 41 describes the same operations described above.

4.3.5 ACU. The Arithmetic Control Unit (ACU) was one of the functional blocks which is ultimately destined to be an application-specific integrated circuit for incorporation into the WFTA system. However, since this module is presently not available for this thesis, it has been designed using discrete components. Many of the functions of the ACU described in earlier theses, such as the watchdog functions, are not implemented in this discrete design for simplification reasons.

The ACU works hand-in-hand with the APU and provides the necessary address lines to both the input and output memory, as well as the write enable pulse to the output memory. Timing is critical between the ACU and the APU and is based solely on a count of clock cycles. The ACU also provides a done signal to inform the MSPC that the FFT has been calculated and loaded into the output memory.

For this single processor architecture, the memory access is sequential or data points are read one after the other into the APU. This is true for the 15, 16, and 17-point trans-

form sizes, however, this is not true of the ACU that is used in the reconfigurable WFTA architecture which calculates larger transform sizes. The Prime Factor Algorithm (PFA) demands that the addressing of data be in a non-sequential but determinable pattern. This ACU only works in the single processor architecture described by Figure 6.

The ACU is functionally decomposed into four subsections discussed in detail in the sections that follow. The initialize block waits the appropriate number of clock cycles necessary before the APU is prepared to accept data. The counter block counts the necessary number of clock cycles before enabling addresses to the output memory. The two address blocks output the addresses and write enable to either the input or output memory at the correct time. Figure 13 shows the schematic indicating the relationship of these functional blocks.

Presently, the ACU has been designed to be used with only one of the WFTA processors, the 16-point processor. The different latency times of the other FFT processors and different number of addresses used by each make a configurable discrete ACU more complicated to design. In order to keep chip count of the design a minimum, this ACU was only designed to work with a single processor.

Since the APU takes inputs and outputs on the falling edge of every second clock pulse, the SN74109 pictured in the schematic divides the clock signal. This chip was needed to provide the two sub-components, ACU_ADD and ACU_ADD1, with a signal required to change their respective memory addresses.

The *CONTROL_CLEAR* control signal is sent back to the bus interface to clear the control register which controls the MSPC. This signal is necessary because if the signal is not present the MSPC, in its current design, would continue to calculate FFT's without termination.

After discussing the four subsections composing the ACU, the timing diagrams for the ACU are discussed in Figures 42 and 43 of Appendix B. These timing diagrams can be referenced during the discussions of the four subsections for specific relationships.

4.3.5.1 ACU_INIT Block. This functional block delays the ACU six clock cycles before enabling the addresses to the input memory. The APU needs this six clock

cycle initialization every time it calculates a new FFT in order to correctly start its own internal counters. The clock signal in this block is the system clock signal generated by the VMEbus interface and not the frequency divided signal introduced above. The clock signal used is the same as the one that drives the APU so the two events are synchronized for the sixth clock cycle. The schematic for the ACU_INIT block is shown in Figure 31 of Appendix A.

When the control signal *OP* from the MSPC is low, it clears the six flip flops in this block. The output of the sixth flip flop is a low to the next functional block or the ACU_ADD block. When the WFTA is told to begin operation, the *OP* control signal goes high, and in conjunction with the system clock, propagates a high through the six SN74LS74. After six clock cycles, the output (*ACU_EN1*) becomes high going to the ACU_ADD block shown in Figure 42.

4.3.5.2 ACU_ADD Block. This functional block generates addresses used by the input memory to output data before the APU latches the data. Using the enable signal from the ACU_INIT block, the ACU_ADD block simply counts through the addresses to the input memory. The schematic for the ACU_ADD block is shown in Figure 32 of Appendix A.

The clock signal has already been divided and the SN74161 only counts on every other clock cycle, which synchronizes it with the APU. This counter is a four-bit counter, making it ideal for the 16-point processor. When the counter reaches address sixteen, which is the last address, the ripple carry-out (RCO) pin on the SN74LS161 goes high for that sixteenth count before starting at zero once again as shown in Figure 42¹. When RCO falls, it clocks the SN74LS74 through the inverter gate and this low clears the counter. This keeps the counter clear for the rest of the ACU cycle. When the *ADD_EN* signal goes low again at the end of the ACU cycle, the D flip-flop is preset to enable the counter for the next ACU cycle.

¹There are two RCO signals shown in Figures 42 and 43 of Appendix B. The first RCO signal is for the ACU_ADD block and the second RCO signal is for the ACU_ADD1 block discussed later.

Due to the design of the memory, the ACU_ADD block must also transmit a control signal to the input memory indicating when the multiplexers are to latch data from the memory chips. The *ADD_EN* signal and *CLOCK* signal are input to an AND gate to determine when the counter generating the addresses increments the address count. The SN74LS31 is used to delay this signal long enough (100 ns) for the data to be output from the memory chips.

Since the memory for this design allows seven bits for addresses, the top three bits, which are not used, have been grounded inside the ACU_ADD block. The schematic for the ACU_ADD block is located in Appendix K.

An important note for both this section, and the ACU_ADD1 block section is the host processor must write to and read from the lowest sixteen locations in the memory. Programmers driving the WFTA system must be aware of this limitation. These sixteen addresses are the only locations addressed by the ACU.

4.3.5.3 ACU_COUNTER Block. This functional block of the ACU performs a similar function to the ACU_INIT block in that it enables the next block, which is the ACU_ADD1 block, to begin outputting addresses and write enables to the output memory. However, in this case, instead of just the six clock cycles associated with initialization, the ACU_COUNTER block must wait for the six clock cycles plus the time it takes the APU to complete the FFT. For the APU16 processor, this time is 124 clock cycles. After this time, the APU starts storing the calculated data on every other falling clock edge. The schematic for the ACU_COUNTER block is shown in Figure 33 of Appendix A.

The two SN74161 are connected in tandem to count to the required clock cycles. The outputs of these two chips are fed into a SN74LS520 and when the count reaches 124 clock cycles, the counters clock the SN74LS74 through an inverter to output a high to the next block, which is the ACU_ADD1 block. The 124 clock cycles are required to synchronize the APU and the ACU. This flip flop is cleared when the control signal *OP* goes low after the ACU cycle. The SN74LS31 is necessary because the *ADD_EN* enable signal is tied into the *DONE* signal generated by the ACU. Without this delay, the *DONE* signal would not be long enough for the MSPC to transition to the next state.

4.3.5.4 ACU_ADD1 Block. This functional block is also similar to the the ACU_ADD block already discussed. This block outputs addresses to the output memory; however, there are two additional signals which must generated here: a write enable pulse for the memory and the DONE control signal which goes back to the MSPC. The schematic for the ACU_ADD1 block is shown in Figure 34 of Appendix A.

The configuration for the address output is slightly different from the ACU_ADD block described above, and the common elements are not discussed again. The *CLOCK_DIV* signal and the *ADD_EN* signal are input into an AND gate to generate the write enable for the zero address. This signal must be delayed for one clock cycle, which is the purpose for the two SN74LS74 cascaded from the output of the AND gate. When the count reaches sixteen, the output of the ripple carry-out (RCO) pin of the counter goes high, as shown in Figure 43. The inverter is used to makes this signal a negative going pulse. The output of the inverter clocks a high through the SN74LS74 to form the *DONE* signal, used to instruct the MSPC that the ACU and APU have completed a FFT calculation. This flip flop is cleared when the enable signal from the ACU_COUNT block goes low.

The write enable pulse to the output memory is generated using a SN74LS121 which is triggered from the same signal that triggers the counter described above, the output of the AND gate with the *CLOCK_DIV* and the *ADD_EN* input signals. The SN74LS31 is used to delay this *WE* pulse long enough for the new address to propagate through to the memory. Since the *ADD_EN* signal for this block lasts a little longer after the *DONE* signal is generated, an AND gate uses the output of the latch that clears the counter to prevent an additional write enable. Since the memory for this design allows seven bits for addresses, the top three bits, which are not used, have been grounded inside the ACU_ADD1 block.

4.3.5.5 ACU Timing Diagrams. The timing diagrams for the ACU are shown in Figures 42 and 43 of Appendix B. The two timing diagrams are from the same VHDL simulation. In Figure 42, the ACU is generating the addresses for the input memory (*IN_ADD*). After *OP* goes high, the addresses are generated in sequence, changing every two clock cycles. The WFTA system clock (*CLOCK*) is divided (*CLK_DIV*) in order to synchronize the ACU with the APU. Notice that the *CONTROL_CLEAR* signal, which

clears the VMEbus interface control word register, goes low after six clock cycles. In Figure 43, the ACU starts generating the addresses and write enable pulses for the output memory, after 124 clock cycles from the *OP* signal going high. Again, the addresses are in sequence and generated every two clock cycles. After all the addresses are generated, the *DONE* goes high to inform the MSPC the FFT calculation is completed. The *ADD_EN1* signal enables the ACU_ADD block after the six clock cycle initialization for the APU and the *ADD_EN2* signal enables the ACU_ADD1 block after the 124 clock cycle processing time for the APU. Although not pictured in Figure 43, both of these signals (*ADD_EN1* and *ADD_EN2*) returns to zero when the *OP* signal goes low.

4.3.6 APU - WFTA16 Processor. The APU is the workhorse of the entire system. It is the functional block which actually calculates the FFT and is also the only block described behaviorally in VHDL prior to this thesis. The behavioral description of the APU used was created by Baker [17] as modified by [2]. The VHDL description is separated into three major functional blocks; the PISO (parallel-in, serial-out), the MATRIX (which performs the FFT), and the SIPO (serial-in, parallel-out). With the minor modification of adding a six clock delay associated with the internal counters of the APU and a few type conversion functions, this code is the behavioral description used in this thesis for the APU. Since Scribner used different names and, more importantly, types for his signals, a few type conversion functions had to be written for compatibility. These type conversions are located in the *wfta_types.vhd* file. The configuration file was modified and is located in the structural VHDL code for the entire WFTA system (*wfta_sys.vhd*).

However, before using this complete behavioral description of the APU, a stub was used for testing the system. The stub is described in the *apu_ent_dummy.vhd* file and simulates the APU reading data from the input memory and storing data to the output memory after the required number of clock cycles (124). This VHDL code models a hardware stub which was to be used in place of the APU on the system breadboard of since the real 16-point processor was not be ready before the end of this thesis cycle.

The stub in VHDL is fundamentally different than the stub used in the actual construction since construction of a sixteen register device with appropriate logic to simulate

the real APU is not feasible given space and time limitations. The actual stub was a single register device which latches only one of the sixteen points and outputs that data point to memory. A simple wired header would not work because input and output to the APU processor is offset by the 124 clock cycle processing time.

Although the data path has been reduced to 16 bits, the APU still reads in 24 bits of data, which means that seven of the real input pins are grounded. The eighth bit is the parity bit which is generated by the input memory. The data is in a normalized 2's-complement format, which means that bits 22 through bit 16 will be grounded. Bit 23 is a parity bit which is generated by the input memory. Tests on the data from previous theses by the WFTA design team have shown that the loss of 7 bits of data does not significantly affect the calculation of the FFT for this application [21].

In addition to these seven pins on the input of real data, all of the imaginary input data pins have been grounded. This decision to eliminate the input imaginary memory was based on the design goal of minimizing the number of integrated circuits on the two breadboards. Further, since the WFTA system is expected to calculate the FFT of real signals, which means that the imaginary components are equal to zero, having no input imaginary memory does not have a significant impact on the operation of the system.

4.3.7 MSPC. If the APU is the workhorse for the WFTA system, then the MSPC is the "brains" of the system. This functional block is also being built discretely for this thesis, though it will ultimately be implemented in a single ASIC. This finite state machine, which is even more complicated in the originally designed system described by [15], provides the necessary control signals for all the different components of the WFTA system.

The SPC described in [2] is too complicated and involved for the smaller system of this thesis. In the effort to decrease complexity and chip count to build a working system, a simpler finite state machine was required. Subsequently, the Minimal SPC (MSPC) has been developed. This MSPC is a state machine which provides the minimum number of control signals necessary in order for the system designed for this thesis to operate correctly. Many of the features of the SPC are not implemented. For example, the MSPC does not react if there is a parity error discovered by the APU16 processor. The signals generated

by the original SPC in [2] not used in this thesis are accounted for in the `APU_NOT_USED` block of the VHDL code discussed in the discussion of the behavioral description.

4.3.7.1 Design of the MSPC. There was a different approach used in the design of this component than the one used in the other discrete components. Included with the Synopsys package is a synthesis tool, called the Design Compiler, which among other things, can take a behavioral description of a finite state machine (FSM) and synthesize a schematic with gates and flip flops that implement the behavioral description [30].

Using a design library created by Brothers [31] which uses CMOS technology instead of default TTL library the Design Compiler normally uses, a finite state machine was synthesized from a behavioral description in VHDL. This design was then saved in the EDIF file format and translated to SGE file format which can be read into the SGE environment using the `edif2sge` utility provided by the Synopsys software package. When this is completed, the SGE tool will generate the structural VHDL code automatically.

However, in order to start this process, the minimal set of signals necessary for operation of the WFTA was identified. There are six signals identified in the design that are necessary. The input signals to the FSM are the *SPCOP* (SPC Operate), the *WFTA16_DONE*, and the *RST_NOT* signals. The output signals to the FSM are the *WFTA16_OP* (WFTA16 Operate), the *MEMFLIP* (memory bank flip) and the *SPCDN* (SPC Done) signals.

Using these signals, the FSM construction is shown in Figure 14. There are five states for this FSM: the START state; the OP1 (Operate One) state; the DONE1 state; the OP2 (Operate Two) state; and the DONE2 state. After the WFTA system has been reset, the FSM enters the START state to begin operations. If the *RST_NOT* signal is asserted any time during the state transitions through the states, the FSM returns to the START state. When the *SPCOP* signal is asserted high, the FSM moves to the OP1 state and remains there until the *WFTA16_DONE* signal is asserted, which indicates that the WFTA processor has finished calculating the FFT. The FSM then moves to the DONE1 state. Since this is a pipelined device, the SPC continues moving through the OP1-DONE1-OP2-DONE2 states until the host is finished doing multiple FFT's.

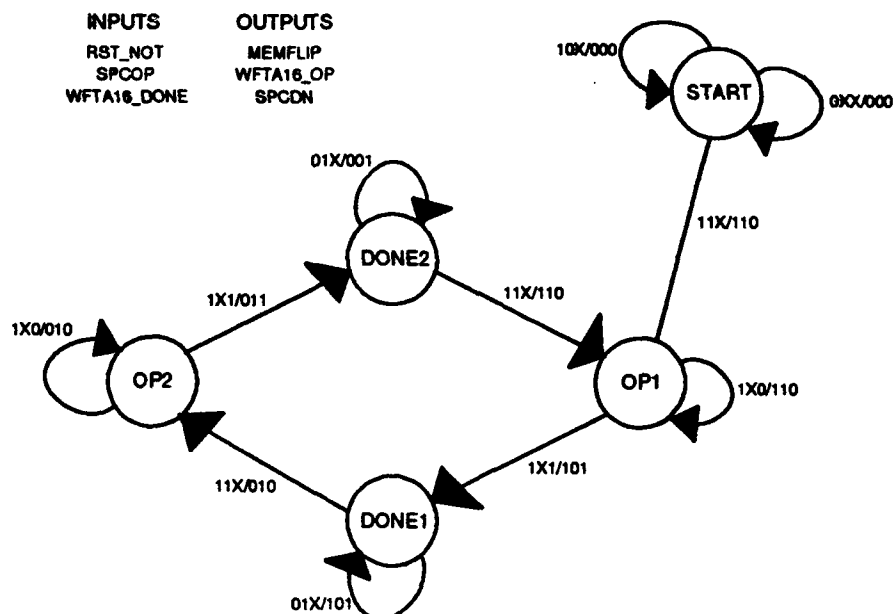


Figure 14. State Diagram for Minimal SPC

The *MEMFLIP* signal alternates values throughout the FSM cycle changing only when the MSPC moves to one of the operate states (OP1 or OP2). This allows the host to access the correct bank of output memory containing the output of the APU.

Note that the *SPCOP* signal must be negated after the MSPC moves to one of the operate states. Otherwise, the MSPC would continue moving through the cycles regardless of the host's commands. This signal is negated using *CONTROL_CLEAR* signal previously discussed. After the six clock ACU initialization cycle, *CONTROL_CLEAR* goes low and clears the output of the control register in the bus interface.

4.3.7.2 MSPC Timing Diagrams. The timing diagram of the MSPC is shown in Figure 44 of Appendix B. The timing diagram shows all the inputs (*RST_NOT*, *SPCOP*, and *WFTA16_DONE*) and outputs (*MEMFLIP*, *WFTA16_OP*, and *SPCDN*) to the FSM, as well as the outputs of the three flip flops used (*Q0*, *Q1*, and *Q2*). The inputs are changed to stimulate actual conditions that could occur in the WFTA system. For example, at the first clock edge, the *RST_NOT* signal is high, the *SPCOP* signal is high, and the *WFTA16_DONE* signal is low. These signals would occur when the host has told the

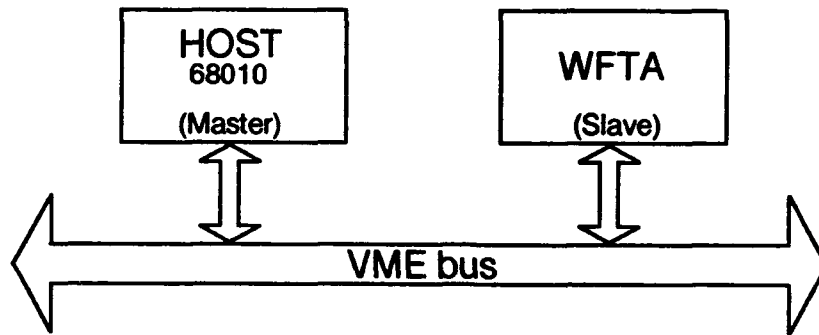


Figure 15. Host-WFTA Relationship

WFTA to begin operations. Table 7 of Appendix B shows the transitions of the timing diagram with the associated states. Comparing Table 7 with the state diagram of Figure 14, shows that the MSPC operates correctly during this VHDL simulation.

4.4 Host

The host VHDL code simulates the read and write cycles of a Motorola 68010 microprocessor, which is to be the test processor used in this thesis. This host processor, which controls the WFTA system operation, is interfaced to the WFTA system through the VMEbus, which allows it to control WFTA system operation. The relationship between the host and the WFTA is depicted in Figure 15.

Using the timing information from the Motorola 68010 data book [29], reasonable times were established for normal read and write cycles. The Motorola 68010 is tailored for use with the VMEbus and has signals which almost directly translate those of the VMEbus. For example, the AS_NOT (address strobe) of the 68010 processor corresponds to the AS_NOT of the VMEbus.

The first thing the host processor must do is to fill the pipeline. The host must write to the first bank of real input memory and then tell the WFTA to begin operation by writing to the control register. While the WFTA is calculating the FFT using this data, the host may write a new set of data points to the second bank of real input memory. The host polls the output register to determine when the WFTA's operations are completed.

When they are complete, the host must tell the WFTA system to begin the operation a second time so the output memory bank switches for the host to read. To maximize throughput on the system, the host must read the output memory during the time that it takes the APU to calculate a FFT and, if additional points are necessary, load the real memory input. Then the polling process starts again.

The important point here is the host must tell the WFTA system to operate one last time to read the last set of output data. When the WFTA has completed an FFT, the FFT data in the output memory is oriented toward the APU and not toward the VMEbus. There is no way for the host to access the output data. Telling the WFTA to start again, flips the memory and orients the memory bank that holds the FFT data toward the VMEbus and the host. The host can now access the data and read it out to the host memory. This means that "garbage" data was input to the APU and output to the memory. However, this is the only way to get data from the output memory.

The host VHDL code does not reflect the entire handshaking protocol used in the data transfer functions of the VMEbus. The behavioral description of the 68010 is by no means complete, but it is complete enough to provide the WFTA system with the required signals from the VMEbus so that the system can be demonstrated.

Apart from the VHDL behavioral description, two files are necessary for proper operation (the data input file and the data output file). The code reads data from an input file called "*fourier_input*" and writes data to an output file called "*fourier_output*". The complete VHDL code for the host is located in Appendix K of this thesis.

4.5 Test Plans

The design process is typically an iterative process, with each step of the process being tested to be sure each design entity is checked with a "test bench" used to demonstrate the entity was operating correctly. Each level of hierarchy was tested and results validated before continuing on to the next level of design. An independent tester should be able to reproduce the results of this thesis with these test benches. Table 5 lists the test benches used against each particular entity.

Table 5. Test Benches

<i>Entity</i>	<i>Test Bench</i>
acu.vhd	tb_acu.vhd
acu_add.vhd	tb_acu_add.vhd
acu_add1.vhd	tb_acu_add1.vhd
acu_counter.vhd	tb_acu_counter.vhd
acu_init.vhd	tb_acu_init.vhd
bus_inter.vhd	tb_bus_inter.vhd
control_section.vhd	tb_control_section.vhd
demux1.vhd	tb_demux1.vhd
demux1a.vhd	tb_demux1a.vhd
demux2.vhd	tb_demux2.vhd
demux3.vhd	tb_demux3.vhd
input_section.vhd	tb_input_section.vhd
mem_in.vhd	tb_mem_in.vhd
mem_mcm6264.vhd	tb_mem_mcm6264.vhd
mem_out.vhd	tb_mem_out.vhd
mux2.vhd	tb_mux2.vhd
mux2a.vhd	tb_mux2a.vhd
output_section.vhd	tb_output_section.vhd
spc.vhd	tb_spc.vhd
wfta_clock.vhd	tb_wfta_clock.vhd
wfta_sys.vhd	tb_wfta_sys.vhd

Test bench is a VHDL term used to describe code that takes the entity, or unit, under test and uses in a higher level configuration. The test bench instantiates the entity and drives the inputs going to this entity. The testing process continues with taking the outputs and comparing them with expected results. The set of inputs driven to the entity is typically called a test vector.

These test benches contain relatively straightforward VHDL code with a simple process statement generating the appropriate signals. The test vectors used testing the entities were not exhaustive, but were selected to represent control signals as they appear in the WFTA system. The test bench for the entire WFTA system (*tb_wfta_sys*) is described in the next section because the results from this test bench were used to verify the design.

Prior to testing a particular entity, both the file containing the entity and the test bench, in that order, must be re-analyzed using the Synopsys package. This re-analysis is necessary because the test benches use the same entity name, the same architecture, and the same configuration declaration for the testbench. Therefore, the simulation file that is created for each test bench has the same name and overwrites the simulation file that existed prior to the re-analysis.

The complete VHDL code for all the test benches and results using the trace option in the simulator are located in Appendix K of this thesis. Some of the results of the test benches were used to illustrate the design and can be found in Appendix B.

4.6 Evaluation of VHDL Development

The first two objectives of this thesis, the design of a VMEbus interface and development of VHDL code describing the WFTA system were incorporated into this chapter, because they were closely tied to each other. This section evaluates the two objectives jointly. The design of the WFTA system was completed and provides a platform for the testing and proof of concept for the WFTA16 processor in a total system. Using a chip-level VHDL simulation which directly reflects the design of the WFTA system, the design was validated for several test cases.

The test bench for the entire WFTA system (*tb_wfta_sys*) was different in structure from the other test benches. Instead of a process statement, the host VHDL code was inserted. This test bench models the physical configuration that the WFTA would normally use, with the host processor controlling the WFTA system. Since this closely models the physical world, the results from this test bench simulation were used to verify the system design.

4.6.1 Input Test Vector Selection. The first test vector used in verifying the system design was the sixteen points representing a 1 Hz sine wave. This signal was used because both the inputs and outputs were available from previous theses. The inputs used are shown in Table 8 of Appendix C. Since this is a real signal, the input imaginary points are

all zero and the imaginary input test vectors are not shown. This models the imaginary inputs to the APU being grounded in the design.

4.6.2 Simulation of the WFTA System. Using the single test vector for a 1 Hz sine wave, the entire WFTA system was simulated. The timing diagram generated for the WFTA system is not shown in its entirety because the simulation took approximately 80000 ns. Rather, sections of the timing diagram have been extracted to verify that the design of the WFTA system operates correctly. The timing diagrams used in the discussion of this section are shown in Appendix D.

Since it is impractical to trace every signal in the WFTA system simulation, the correct data flow can be used to verify the design. Furthermore, the data can be easily traced around the entire system. For specific details of the data flow when it enters one of the major functional blocks, refer to the appropriate section in this chapter. Figure 45 shows the host writing the 16 data points to the input memory. The first address shown, 70001Eh (*VME_ADD*), is actually for the sixteenth point of data because the host VHDL code writes the data in reverse order. The address 70000Fh might have been expected, but the VMEbus is byte addressable while the WFTA system is word addressable. Each point of data takes two bytes (one word). The address 70001Eh corresponds to the sixteenth word in the input memory. The address from the VMEbus interface going to the input memory is *WRITE_ADD* and the data from the VMEbus interface going to the input memory is *RI.1*. Although the host VHDL code writes the data to the input memory in reverse order, with the sixteenth data point written first to the sixteenth location in the input memory, the data is accessed in ascending order through the WFTA system. The first data point assessed by the ACU is located in the first location in the input memory. After the host is finished with loading the input data, the host tells the WFTA to begin operation by writing to 704000h which corresponds to the control word register. Notice that *SPCOP* goes high and *MEMFLIP* changes from low to high. The *MEMFLIP* must change so that the input data is oriented towards the APU. Also notice that *SPCOP* goes low after a short time. This is caused by the *CONTROL_CLEAR* signal from the ACU which clears the control word register.

Figure 46 shows the ACU addressing the input memory and data flowing to the APU. The addresses generated by the ACU are *IN_ADD*, in ascending order, and the data from the the input memory to the APU is *RI_2*. The VMEbus addresses (*VME_ADD*) can be disregarded. The VHDL host code is simply loading another set of data points in the input memory demonstrating the pipelining features of this design.

Figure 47 shows the ACU addressing the output memory and data flowing from the APU to the output memory. The addresses generated by the ACU are *OUT_ADD*, in ascending order. The real FFT data from the APU to the output memory is *RO_1*, which corresponds to the actual real output test vectors of Table 9 of Appendix C. The imaginary FFT data from the APU to the output memory is *IO_1*, which corresponds to the actual imaginary output test vectors of Table 10 of Appendix C. Notice that both *RO_1* and *IO_1* are 24-bits wide coming from the APU to the output memory and the table entries of Tables 9 and 10 are 16-bits wide. The 16 most significant digits of the *RO_1* and *IO_1* data busses are the bits that compare to the table entries. Although the design decision was made to change the datapath from 24-bits to 16-bits in Section 3.3, the APU still outputs 24-bits of FFT data.

When the ACU and APU are finished loading the output memory, the *SPCDN* signal goes from low to high, telling the host that the WFTA has completed the FFT. The host VHDL code is not polling at this time because there is a busy loop in the VHDL code which executes prior to polling the output word register.

Figures 48, 49, 50, and 51 shows the host reading the output memory for the FFT data. The VMEbus address (*VME_ADD*), 708000h, maps to the output word register. The host, which has been in a busy loop, only polls once because the WFTA has already completed the FFT. When the host determines that the WFTA is finished, the host tells the WFTA to calculate another FFT by writing to the control word register (704000h). This write operation orients the data in the output memory towards the host. Notice that the *MEMFLIP* signal goes from high to low. The host then reads the output memory. The host code alternates reading the output memory, first reading from the real output memory (70C000h), and then reading from the imaginary output memory (70E000h). The host reads the 16 points of real FFT data and 16 points of imaginary FFT data. The

address from the VMEbus interface going to the output memory is *READ_ADD*. The data going from the output memory to the VMEbus interface is *RO_2* for the real FFT data and *IO_2* for the imaginary FFT data.

4.6.3 Results of WFTA System VHDL simulation. The host takes the FFT data from the output memory and writes them into a file (*fourier_output*). The results from the VHDL simulation were compared to the expected FFT values. This comparison is shown in Tables 9 and 10 of Appendix C. The WFTA system VHDL simulation results are exactly the same as the expected values. Similar tests to the one described above were conducted on a 1 Hz cosine wave, a 2 Hz sine wave, and a 2 Hz cosine wave. In all these tests, the results from the simulation matched the expected values. The WFTA system design was verified in VHDL using the results from these simulations.

4.7 Summary

This chapter has covered the VHDL development for the WFTA system described in Chapter III. The design of each of the major functional blocks is discussed in detail. Behavioral VHDL descriptions of integrated circuits were developed and used as the basic building blocks of the structural VHDL description of the WFTA system down to the integrated circuit level. Through the use of a set of comprehensive test benches, the design was verified for correct operation in simulation. A rudimentary model of the host processor in VHDL was developed to simulate the control signals from the host to the WFTA system via the VMEbus. The next chapter describes the WFTA system construction.

V. Construction of the WFTA System

5.1 Introduction

There is a tremendous difference between a paper design and actually wirewrapping chips to a VMEbus breadboard. The physical world has such things as capacitance, current drive requirements, fan-in, and fan-out. Rarely are signals as "clean" in VHDL as they are in the digital lab. Although VHDL can be made to account for these physical actualities, the VHDL design becomes more intricate and complicated. Lack of time during this thesis cycle made modelling these physical considerations impractical.

Furthermore, a design developed in VHDL is only as good as the behavioral descriptions that form the foundation of the simulation. Actually, the behavioral descriptions are not complete in that they do not totally reflect the ideal specifications of the datasheets. Differences in expected behavior versus actual behavior can often result in errors in the construction. This was the case in this thesis, which resulted in changes to the VHDL model to reflect actual behavior observed.

These two factors forced the design of the system to be modified during this phase of the thesis. Errors not detected during VHDL development manifested themselves in the actual construction. One example of this modification was the elimination of a latch used in the original design between the VMEbus interface and the input memory. Although the original design would have worked with the latch, the elimination of the latch decreased the chip count, which was critical during the entire design. As stated previously, the design that was discussed in Chapter IV represents the final design describing the device after all the design iterations.

Since the design of the WFTA system has already been discussed in Chapter IV, this chapter deals with the specifics of the equipment and procedures used in the digital lab and other documentation that will help clarify and continue any future work in this area.

The same schematics used in the VHDL development also document the construction phase of this thesis. The schematic produced with the Synopsys SGE tool provides the ability to label pin and chip numbers. There is no single level schematic which contains all

the gates and connections. Rather, the schematics are hierarchical. As mentioned before, all the schematics used for this design are located in Appendix K of this thesis.

Due to time and resource constraints, the WFTA system described by Chapter IV was not completely built. The input memory and MSPC functional blocks were totally completed along with a partial construction of the VMEbus interface.

This chapter starts with a discussion of the resources used in the construction, followed by a section on the construction methodology and the testing procedures for those blocks that were built. Then specific problems concerning construction are discussed, followed with an evaluation of this phase of the thesis against the stated objective.

5.2 Resources

The following sections discuss some of the peculiar resource requirements for the WFTA prototype system that was assembled in the digital lab. Specific equipment and tools used are discussed first, followed by the types of integrated circuits composing the system. Additionally, there were many parts needed particular to wirewrapping and the VMEbus. Whenever possible, the make, model, or part number is listed in the discussion.

5.2.1 Equipment and Tools. The chassis used for this thesis which contains the VMEbus backplane was the MVME945-1 Chassis from Motorola Incorporated. All the specifications for this chassis are discussed in the User's Manual [32]. Usually, the 945 chassis contains one 12-slot, full 32-bit VMEbus backplane using the bus connectors P1 and P2 to connect to the bus lines. However, the version used for this thesis only contained the P1 connector on the backplane, forming a 16-bit VMEbus backplane. Using this chassis to hold particular VMEbus cards, total processing systems can be implemented onto the backplane.

One of the cards used in this thesis is the processor card or MVME120, VMEbus Microprocessor Module, produced by Motorola [33]. The microprocessor used in this card is the Motorola 68010. However, this entire VMEbus card houses a complete processor system with RAM, ROM, interrupt handler, and bus requester. This was the host processor discussed in previous chapters of this thesis. The other VMEbus card used in the chassis

was the controller card, MVME050, also produced by Motorola. This card assumes the duties of bus master upon power up and arbitrates bus requests on the VMEbus. This controller card must be used in conjunction with the MVME120, Microprocessor Module, as it also provides the power, ground and clock used on the VMEbus.

The most important tool used during the testing of this phase was the HP-1631A/D logic analyzer produced by Hewlett Packard [34]. The logic analyzer is general purpose machine capable of performing state, timing, and analog waveform measurements. For this thesis, the logic analyzer was used for making only digital timing measurements. The logic probes were attached to specific signals and the waveforms were compared with the expected results from the VHDL development.

In order to communicate with the Motorola 68010 on the MVME120 VMEbus card a dumb terminal with RS232 interface was needed. The terminal used for this thesis was the Heath H-29 Video Display Terminal [35]. The RS232 interface is located on the front of the MVME120 Microprocessor Module. This terminal provides input/output functions from the user to the resident debug monitor program in the MVME120 Microprocessor Module. Without this monitor and keyboard, there is essentially no way for the user to control the 68010 in the MVME120 card. The debug monitor is a ROM resident program that acts a rudimentary operating system for the host 68010 [36].

5.2.2 Integrated Circuits. In construction of the actual WFTA system, the integrated circuits were the most numerous resource and also the most difficult to acquire. In total, there were 160 integrated circuits needed for this design which were obtained from different sources.

In Table 1 of the last chapter, the type of chips used in this design were listed but not broken down in any manner. In this chapter, the number and location of use for these integrated circuit chips is important, and Table 6 provides a better indication of this distribution between the different functional blocks. The total number of chips in the previous paragraph is somewhat deceiving since some of the chips have more than one gate in the package. For example, the SN74LS04 inverter gate has six inverters on a single

Table 6. Integrated Circuit Requirements with Functional Blocks

<i>Type</i>	<i>Total Number</i>	<i>Used in Functional Block</i>
MCM6264	12	Input and Output Memory
SN74LS00	14	MSPC
SN74LS02	1	MSPC
SN74LS04	28	ACU, Bus Interface, Input and Output Memory
SN74LS08	7	Bus Interface, ACU
SN74LS10	5	MSPC
SN74LS31	5	ACU, Bus Interface
SN74LS32	7	Bus Interface, Input and Output Memory
SN74LS73	3	MSPC
SN74LS74	14	ACU, Input and Output Memory
SN74LS86	1	Input Memory
SN74LS109	5	ACU, Bus Interface
SN74LS116	2	Bus Interface
SN74LS121	2	ACU, Bus Interface
SN74LS161	4	ACU
SN74LS180	2	Input Memory
SN74LS373	24	Input and Output Memory
SN74LS374	4	Bus Interface
SN74ALS520	7	Bus Interface, ACU
SN74ALS604	6	Input and Output Memory
SN74ALS747	6	Bus Interface
SN74ALS757	1	Bus Interface

chip. Whenever possible during construction, gate requirements were combined on the same VMEbus board.

The common gate chips like OR and NAND gates were obtained from the digital logic lab bench stock, while the other standard Transistor-Transistor-Logic (TTL) chips had to be ordered from different area suppliers. In Appendix E, a short list of distributors with phone numbers is provided for future researchers in order to minimize the amount of time needed to locate integrated circuits in the future.

5.2.3 Other Parts. Integrated circuits were only one part of the numerous materials needed for construction of the WFTA system. Specifically, the VMEbus requires certain parts to be used, such as cards for the slots in the chassis. The WFTA system occupied

two separate VMEbus boards and required a means to connect certain signals between the two boards. Finally, the wirewrap construction technique requires particular tools and resources. Part numbers and manufacturers are documented, since many of these parts might be needed in the future for VMEbus design work. A major company that specializes in VMEbus boards and interconnects is the Vector Electronic Company and their Vectorboard line of products. As mentioned above, any parts that are needed can generally be ordered from one of the area distributors in the list of Appendix E.

5.2.3.1 VMEbus Board and Interconnects. The chassis used for this thesis has 12 slots for VMEbus boards. The boards used for this thesis is the Eurocard from Vector Electronic Company, part number E220-6U-1. These cards are larger than the ones provided by the digital logic lab and are much more convenient to work with. The boards that actually fit into the chassis of the VMEbus backplane provided by the digital logic lab are smaller than the Eurocard described above and inconvenient in larger system prototyping.

The VMEbus interconnects are also provided by the Vector Electronic Company and the ones used for this thesis are the 96 pin DIN wirewrap connectors, part number RE96WSR. This connector is only used with the P1 connector on the VMEbus backplane. The pins are longer and at a right angle to the board in order to provide room for wirewrapping.

5.2.3.2 Interconnects between Boards. The goal in future construction should be to keep the WFTA system limited to a single board, eliminating the need for interconnects between two different boards. However, for this thesis, two VMEbus cards were needed and a means of connecting the two boards was required. A 50-wire ribbon cable is adequate for this need with the appropriate wirewrap connectors. The 50-pin wirewrap connectors were available from the digital logic lab bench stock and can be obtained through normal supply channels, NSN 5935-01-017-5825.

5.2.3.3 Wirewrap Parts. The programmable gate array (PGA) wirewrap sockets are necessary for the APU and possibly will be needed for the future implemen-

tations of the ACU, memory, and MSPC. Different PGA sockets will be needed for the different application specific chips. The staff of the digital logic design lab is searching for PGA sockets for one of the design classes here at AFIT and at the time of this thesis, were not successful in finding a company that provided these materials.

Additionally, wirewrap sockets for standard dual in-line package (DIP) integrated circuits are needed but the digital logic lab has an adequate and fairly complete supply of any of these sockets that might be necessary for any prototyping work. However, these should be ordered as well since the digital logic laboratory needs these sockets for some of the classes held there.

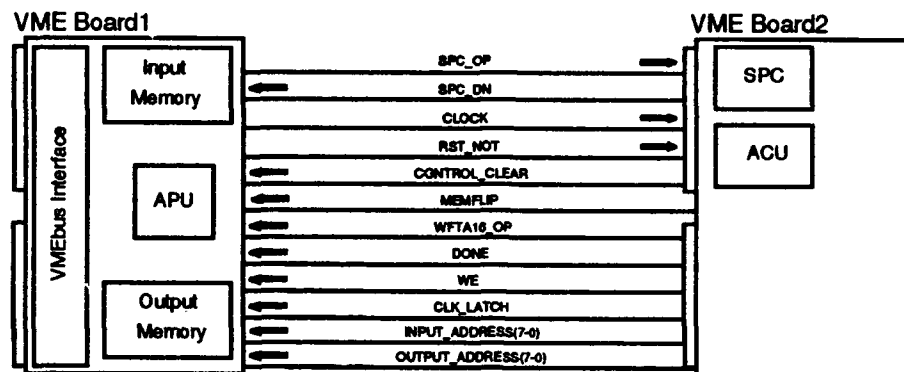
The wire and wirewrap tool is also available from the on-duty technician in the digital logic lab. The wire used in wirewrapping is a standard AWG-30 gauge wire and the wirewrap tool used for this thesis is produced by OK Industries, Incorporated, Yonkers, New York, part number WSU-30M.

5.3 Partitioning of Functional Blocks

Considering the number of chips necessary to implement the design, there was no other alternative than to use two VMEbus cards to house the WFTA system. With this in mind, and knowing the space on the two VMEbus cards was limited, a plan was necessary to partition the area of the boards to minimize the number of interconnecting wires required between them.

The first consideration was ease of maintainability and any future work to be performed with this board. The major functional blocks were kept together as much as possible. For example, the VMEbus interface block was located on a specific area of one of the boards. This makes replacement and modification of specific functional blocks easier. The second consideration dealt with minimizing interconnecting wires between the two boards. The 16-bit wide datapath for both the real and imaginary datapaths, had to be contained on one board.

These two considerations essentially solves the problem of the partitioning, by forcing the VMEbus interface, input memory, output memory and APU blocks to be restricted to



* NOTE: All connections are through a ribbon cable between the boards.

Figure 16. Partitioning and Interconnect Signals

one VMEbus card as they form the FFT datapath. This leaves the two other blocks, the ACU and the MSPC, to be constructed on the second VMEbus card. This separation is shown in Figure 16 with the interconnecting control signals between the two boards.

5.4 Construction Methodology and Testing

The WFTA construction was built using a modular approach with the "piecewise" testing of the prototype in mind. The number of inputs to the different modules made testing difficult in a modular fashion. Building testing circuitry would be as involved as building the actual system, and in the interest of time, this was not the testing methodology used. Furthermore, the availability of integrated circuits limited the sequence of construction. So, alternatively, using the host processor as the starting point and as the major testing apparatus, the WFTA system was built incrementally away from the host following the datapath of the architecture. Each step of the construction must be verified for proper operation before continuing to the next incremental step.

Starting with the input and control section of the bus interface, these functional blocks were built and tested before continuing on to the input memory. Then by continuing on the datapath, the input memory was built and tested to determine if the host was able to write to the input memory. The next functional block built was the MSPC to provide some of the control signals that were hardwired in the previous steps. The ACU, output

memory, and output section of the VMEbus interface were left for last in the construction, but were not completed due to time and resource constraints. The specific chip location and layout of the components on the two VMEboards is shown in Appendix F. These figures represent the extent of the construction of the WFTA system.

At each step of the incremental construction, tests were performed to insure proper operation before continuing on to the next step. However, this testing process was different for each one of the steps. For example, for the first step of constructing the input and control section of the VMEbus interface, the decoding signals and data lines were monitored. The second step of constructing the input memory, however, required some of the control lines of the input memory to be hardwired while the host processor wrote to the input memory. Then, the input signals to the memory chips, such as the write enable and data lines were monitored to insure proper operation. Since, the input memory could not be read due to the lack of a datapath back to the VMEbus, monitoring the inputs to the memory chip was the only way to verify operation. In the third and final step of construction, which was the MSPC, the *WFTA16_DONE* signal was tied low. After writing the control word, the output signals from the MSPC FSM were monitored to insure correct operation.

As the main testing apparatus is the host processor, the commands of the Motorola MVME-120 debug monitor were used [36]. In particular, the command used in the debugging environment provided was the Memory Modify (M or MM) command, whose function is to change data values in memory. The format for the command is MM <address> [<options>] where the address is in hexadecimal. With certain options set, this command can write a word to any location in the VMEbus address space. The first of the two memory change mode options that were needed was the ;W option which sets the size of the memory modify to word length or 16 bits and the ;N option which is the no verification option insuring that the debug monitor does not attempt to read data after updating. The word length option is necessary because access to the WFTA system is only even byte addressable. An example of this command is shown below.

MM 7000 ;W ;N

For each iteration of testing for this system, the memory modify command was used to insure proper operation by writing to a memory location in the WFTA address space. For example, writing to the control word started the finite state machine in the MSPC. After writing to a particular location in memory, the HP-1631A/D logic analyzer was used to monitor the important signals to insure expected behavior. The waveforms of significant signals were compared to the expected results of the VHDL simulation. A component was considered verified when the actual signals appeared similar to those predicted by VHDL. This ad hoc procedure constituted the testing plan during the construction of the WFTA system.

5.5 *Specific Problems*

There were a number of problems associated with the construction of the WFTA system which are discussed in this section. These problems included the user interface with the host, availability of parts, and the testing methodology.

5.5.1 Interface to Host. The host processor used for this WFTA system was Motorola 68010 on the MVME120 Microprocessor Module card. The debug monitor program in the ROM of the MVME120 is adequate for operation, but not extremely user-friendly. In many ways the debug monitor is functionally limited, making the interface to the host somewhat difficult. A different procedure will be used than the one discussed in this chapter for the interactive testing when the host driver program is introduced in the next chapter.

5.5.2 Parts. Although many of the chips and connectors were available in the digital lab, there were a number of uncommon items not currently stocked. Many of these parts were ordered prior to construction; however, the design was not yet complete and unforeseeable chip requirements forced a quick search to find the needed components. Even with last minute acquisitions, the parts list was not entirely fulfilled. This limited the completion of the construction of the WFTA system before wire-wrapping the first chip to the board.

5.5.3 Testing. The testing for this phase of the thesis was difficult because the number of inputs and time constraints forced the use of the host processor in the testing process. Construction was temporarily suspended for each test to insure correct operation before continuing. Building a test circuit every time a module was completed would have been prohibitive considering the time allocated for this effort.

5.6 Evaluation of Construction

The particular problems encountered during this phase of the thesis have already been discussed in this chapter. As mentioned in the beginning of this chapter, the entire WFTA system was not constructed onto VMEbus cards. The two major reasons for not finishing were lack of resources and time. Even with the necessary resources, additional time would be necessary to complete the WFTA system. Wirewrapping is a tedious and time-consuming process. This fact, coupled with the constant testing at each phase of the construction process, made assembling this prototype a prolonged process.

The parts of the WFTA system that were constructed and tested were the input and control sections of the bus interface, the input memory and the MSPC. Up to this point, the design was validated in actual hardware. However, before the entire WFTA system can be validated as operational, the remaining functional blocks need to be installed and tested—the output memories, the ACU, and the output section of the bus interface.

5.7 Summary

This chapter has covered the construction of the WFTA system in the digital logic laboratory and focused on particular problem areas. The WFTA system described in the design of Chapter IV was partially assembled and tested. The input memory and MSPC functional blocks were completely built while the VMEbus interface block was only partially built. Using the host processor as the primary testing apparatus, tests up to this point of the construction have verified the VHDL design. The WFTA system was not completed due to time constraints and a lack of resources. The next chapter deals with the development of the host processor code that drives the WFTA system.

VI. Development of the Host Driver Code

6.1 Introduction

The system host processor has the important responsibility of maintaining the WFTA pipeline and keeping it as full as possible. The program that performs this task is the host driver program running on the host. In order to provide an environment which will test and demonstrate the single WFTA processor, a rudimentary version of the host driver code was developed for this thesis.

The host processor for this system was the Motorola 68010 16-bit microprocessor located on the MVME-120 card of the VMEbus chassis. As already discussed in the last chapter, input and output of data with the host processor is difficult for several reasons. The processor itself has an embedded debug monitor with limited instruction set to control the processor. Additionally, the chassis used for this design did not have a file system, and any data which the FFT needs for calculation must be stored in system memory. This I/O limitation has driven the host driver code developed for this thesis to perform a single 16-point FFT problem. With a more powerful host processor or a more user-friendly environment, the pipelined nature of the WFTA system might be better exploited in the software.

Another design decision for this work with respect to the software was to use the C programming language for the host driver program. The major reason for this decision was the only compiler available for the 68010 was the Aztec C Compiler by Manx Software Systems, Inc. Another reason for this choice was in terms of software maintainability. Given the resources, the only other choice would have been to write the program in 68010 assembler language, which in general is harder to read and understand and more difficult to maintain.

This chapter discusses the development of the host processor code used to drive the WFTA system. The compilation and downloading procedures are discussed in Appendix redownload. This is followed by a discussion of the pseudocode version of the code. A section describing the data flow diagram is next and the chapter ends an evaluation of this objective against the goals stated in Chapter I.

6.2 *Compilation, Download, and Run Procedures*

This section discusses the procedures developed for compilation of the C source code, downloading to the host processor, and running the host driver program on the MVME-120. These three procedures are detailed in Appendix G.

6.3 *Pseudocode for the Host Driver Program*

Actually, the general nature of the code for the host driver program has already been discussed implicitly in Chapter IV on VHDL development, Section 4.4. In order to test the structural VHDL developed for the WFTA system, the signals generated by the WFTA system host had to be simulated. Essentially, the structure of the host driver program can be derived from this behavioral description of the host processor by using the commands necessary to create the simulated signals.

The pseudocode developed for the host driver program is listed in Figure 17. As stated earlier, this pseudocode has been written to operate on data for only a single FFT. The numbers located to the left of the statements in Figure 17 are associated with the data flow diagrams discussed in the next section and can be disregarded temporarily.

The pseudocode is fairly straightforward. The first *for* loop reads a set of sixteen points of data and writes that data into the input memory of the WFTA system. The address used by the host for system memory was arbitrary until the address for the WFTA was hardwired into the VMEbus interface. The memory for the WFTA must be from address location 700000h to 70001Fh corresponding to the bottom sixteen addresses of the input memory (the input memory is even-byte addressable) with the first data point going in the zero address location. This address is mandatory because this address is hard-wired into the VMEbus interface. The VMEbus and 68010 are both byte-addressable but each set of points written to the input memory consists of a "word" with two bytes (16 bits), therefore the first point of data is located at 700000h and the second point of data is located at 700010h.

```

1.1  for i in 1 to 16;
      read one data point from system memory;
      write one data point to input memory of WFTA;
    end for;

1.3  write control word to begin WFTA for first time;

    loop
1.4  poll WFTA for completion;
    end loop;

1.3  write control word to begin WFTA for second time;

1.2  for i in 1 to 16;
      read one real FFT point from output memory of WFTA;
      write one real FFT point to system memory;
    end for;

1.2  for i in 1 to 16;
      read one imaginary FFT point from output memory of WFTA;
      write one imaginary FFT point to system memory;
    end for;

```

Figure 17. Pseudocode for the Host Driver Program

After writing the data to the WFTA input memory, the host starts the WFTA system by writing a control word to the bus interface. The most significant bit, or bit 15, of the control word must be a “one” to start the SPC.

At this point, the WFTA calculates the FFT and the host processor polls the output word for completion. When the most significant bit, or bit 15, of the output word from the bus interface is a “one” the WFTA has finished calculating the FFT.

In order to get at the data, the host must write the control word to start the WFTA a second time. This operation “flips” the memory so that the host processor can access the data from the output memory of the WFTA system.

The host driver program then reads the FFT (sixteen points of real data and sixteen points of imaginary data) and writes to the system memory. The address used for system memory is again arbitrary as before but the address for the output memory of the WFTA is 70C000h to 70C01Fh for the real data and 70E000h to 70E01Fh for the imaginary data (the output memory is even-byte addressable).

The only modification required to change this pseudocode to implement a pipeline structure would be to add a loop for multiple operations after the first write operation to the input memory but before the start of the WFTA. Then, before polling for completion, a second write operation should be added to the input memory. Once the pipeline is full, repeated and sustained operations are possible. The changes necessary are illustrated in Figure 55 of Appendix H.

6.4 Data Flow Diagram for Host Driver Code

One of the many ways of representing information flow in the software engineering arena is through the use of a data flow diagram (DFD) [37]. A DFD is a graphical means of representing the flow of information, and the transforms applied to data, as it moves through the system. Using a number of DFDs, any system or software can be described to any level of abstraction.

The DFD has its own associated and accepted symbology. A rectangle represents an external entity, which is a source of inputs and a sink of outputs. A circle or bubble represents a process which performs some transformation of its input data to yield its output data. An arrow represents the flow of data with the arrow head indicating the direction of data transfer. Finally, a double line represents a data store which serves as a repository of data, such as memory.

DFD's are used to further document the software objectives associated with this design. Although this program is not especially difficult, the DFD provides future researchers with a basic understanding of the information flow of the system, which can be applied to any other host processor.

The context diagram or Level 0 DFD for the host driver code is shown in Figure 18. The data store represented is the onboard RAM of the 68010 microprocessor. The entire set of 16 points of input data and the 16 points of real and imaginary output data is represented in the diagram by the *DATA* and *FFT DATA* labels, respectively. The control word is the same word that starts the WFTA system, and the output word is polled for

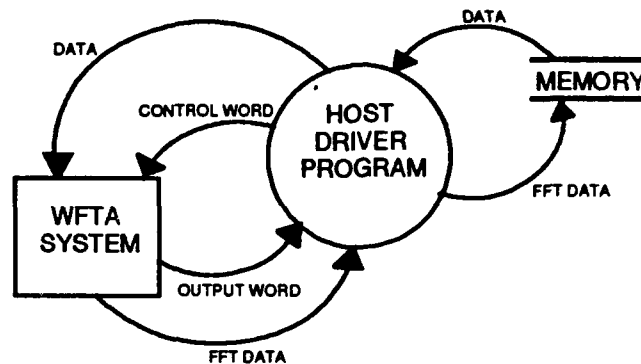


Figure 18. Context Diagram for the Host Driver Program

completion of the FFT. The DFD only shows the flow of data and does not depict the actual interchange, or handshaking, between the host processor and the WFTA system.

As seen in Figure 19, the Level 1 DFD, which is the lowest level DFD used in this design, the host driver program is functionally decomposed into its major modules. The four components describe the major functions of the host driver program. The LOAD DATA process (1.1)¹ reads a set of 16 real input points from the system memory and writes it to the input memory of the WFTA system. The LOAD MEMORY process (1.2) reads a set of 16 real outputs and a set of 16 imaginary outputs from the output memory of the WFTA system and writes to the system memory. The START WFTA process (1.3) writes to the control register of the WFTA to start the process, and the POLL WFTA process (1.4) polls the WFTA output register for completion of the FFT.

6.5 Coding and Memory Map

Using the DFD and pseudocode developed previously as guides, the host driver code was written. This program is listed in Appendix I and has been commented to correspond to the DFD and pseudocode. The location of both the host driver code and the input and output data in system RAM is arbitrary. However, the locations of the input and output

¹The numbers located to the left of the pseudocode program statements in Figure 17 directly correspond to the functional decompositions described in Figure 19. For example, the LOAD WFTA process (1.1) of the DFD is associated with the first *for* loop in the pseudocode.

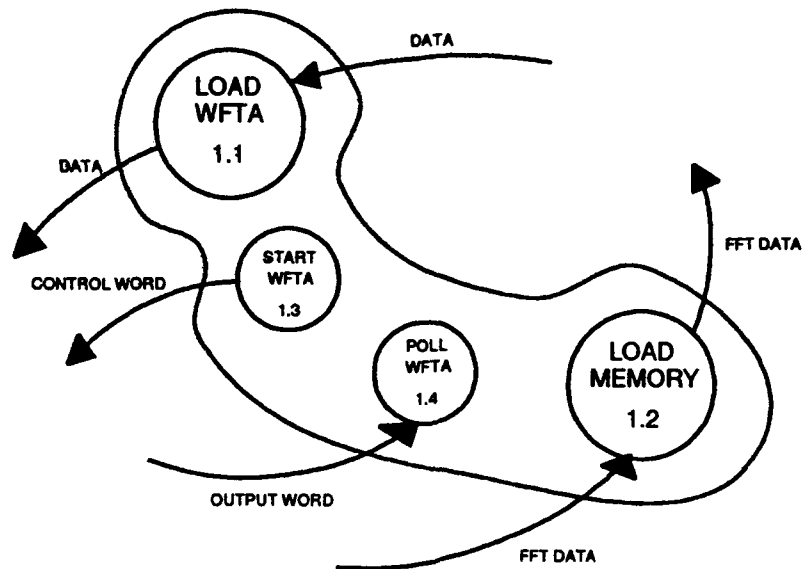


Figure 19. Level 1 DFD for Host Driver Program

data will be fixed by the code of the host driver program. The memory map used for this effort is shown in Figure 20.

The system RAM is located from 000008h to 01FFFFh [33]. The addresses for this thesis in the system RAM are arbitrary. From Figure 20 the host driver program will start at VMEbus address 005000h. There are 16 locations in memory for the input data at 001000h and 32 locations in memory (real and imaginary) for the output data starting at 010000h.

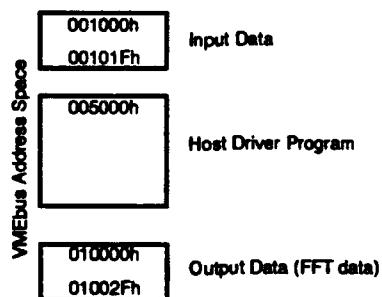


Figure 20. Memory Mapping for Host Driver Code and Data

6.6 Testing and Evaluation of Host Driver Program Development

The host driver driver program was written in C and is listed in Appendix I. The testing for the host driver code was not complete due to the unfinished construction of the system and time constraints. In order to fully test this code, the entire WFTA system is necessary to provide an environment which would react to coded instructions. The code has been left for future researchers to modify and improve. The code listed in Appendix I compiles but has not been run for this system. However, this program is simple enough to insure that the code should work correctly. All the host driver code does is reads and writes to addresses in the VMEbus address space.

6.7 Summary

This chapter has covered the development of the host processor code used to drive the WFTA system along with other considerations involved with this particular VMEbus system. The pseudocode and DFDs for the host driver program have been developed and document the behavior of the host driver program. The code for the host driver was written in C and compiles correctly but never tested due to time constraints. The next chapter discusses the conclusions for the research and the recommendations for future research.

VII. Conclusions and Recommendations

7.1 Introduction

Every year, progress has been made toward VLSI chips that implements the Winograd Fast Fourier Transform Algorithm. However, presently, there is a need for a platform into which the WFTA16 processor could be demonstrated. This research was an effort to solve that deficiency by designing and building a WFTA system that would provide an environment for WFTA16 processor operation. Specifically, the overall goal of this thesis was to design and build a working 16-point WFTA system that interfaces to the VMEbus standard as a proof of concept for the WFTA system designed and developed at the Air Force Institute of Technology.

In Chapter I, there were four objectives proposed to solve this problem. The first was designing an interface between the WFTA system and VMEbus. The second was developing VHDL code, down to the integrated circuit level, that implements the WFTA system design. The third was constructing the WFTA system onto VMEbus cards. The fourth was developing a host driver program to drive the WFTA system with data and instructions. As described in the separate Evaluation sections in Chapters IV, V, and VI, there were different levels of success with each of these objectives. This chapter presents the conclusions and recommendations derived from the research described in this thesis.

7.2 Conclusions

Conclusions are drawn logically from research providing an indication of the overall success of the solution to the problem statement. This section describes the conclusions drawn from this research effort.

7.2.1 Validation of WFTA System Design. The WFTA system design, as described in Chapter III and Chapter IV, was validated through VHDL simulations and tests conducted during construction. The structural VHDL was developed to directly model the WFTA system design down to the integrated circuit level. Appropriate timing of components were included in this VHDL structural description. Using this description of the

WFTA system, simulation results showed that the WFTA correctly calculated the FFT for a 1 Hz sine wave and other test signals. This simulation, along with results, are detailed in Chapter IV. These results support the conclusion that the WFTA system design was validated.

Although the construction was not complete, preliminary results indicate that the actual hardware seems to match those expected from the VHDL simulation. The input and control sections of the VMEbus interface, the input memory, and the MSPC were the only functional blocks which were constructed. The testing results from the partial construction further supports the conclusion of the WFTA system design validation.

Taking both the VHDL simulation results and partial construction results, the design of the single processor WFTA system built for this thesis was validated.

7.2.2 Continued Work in the WFTA System. The work on the WFTA system needs to be continued. The results of the partial construction of the WFTA system supports the validation of the WFTA system design, but the entire system needs to be constructed to be completely confident. Additionally, the host driver program was written but never tested. These concerns indicate that continued research is necessary for the complete development of a platform for the WFTA processors.

The architecture of the WFTA system used in this thesis is a scaled-down version of the original WFTA design. It was meant to be used in a single processor configuration. Research needs to be continued in the reconfigurable WFTA system architecture [2]. This thesis was a good starting point for system design issues and provides a stable foundation for continued work.

7.3 Recommendations

This section lists the recommendations for directions of further work or modifications to the original design. These recommendations come from strictly a systematic view and do not comment on the VLSI design of individual chips or original concept of design.

7.3.1 Further VLSI Work. One of the major problems with this thesis is there are no commercially available chips for the major functional blocks of the WFTA system. For example, for this thesis, there is no 16 X 16-bit word, dual-bank memory available which can be read from one bank while at the same time providing access for writing to the other bank. Consequently, using 8K X 8-bit chips in this design wasted a large amount of memory. This lack of convenient commercial chips comes as no surprise since the original WFTA design was based on a suite of application-specific integrated circuits. VLSI design work needs to continue on the memory, ACU, and the SPC in conjunction with the WFTA processors.

Assuming a working APU, a priority list of the needed components can be described. The first chip that needs to be fabricated is the ACU. This chip is closely tied to the APU and the timing between the two devices is critical. The next chip needed would be the memory chip which would greatly reduce the number of chips in the system. If the jump is made to a reconfigurable WFTA system with two or more WFTA processors, then the SPC must be the next chip fabricated. Building the SPC discretely for the more complicated WFTA system would not be feasible because the number of integrated circuits to implement the finite state machine would be prohibitive given the space constraints.

The recent AFIT acquisition of a field programmable gate array (FPGA) system will make the fabrication of some of the components of the WFTA a simplified process. The bus interface, the SPC, and the ACU could be constructed on a FPGA chip. This tool was not available for this thesis but should provide future WFTA system designers with the means to complete the system and significantly decrease the number of chips necessary.

7.3.2 Asynchronous Signals. Another problem is the lack of appropriate handshaking signals between the different components of the WFTA system. As shown in this design, some of the components will not necessarily be application specific and might have to be constructed discretely from commercially available chips. The problem of timing is critical and could be a significant problem when the actual WFTA16 processor is placed into the empty space left on the breadboard from this design. Presently, the only synchronizing signal between the two devices is the clock, the operate, and the done signal. There needs

to be additional asynchronous signals coming from the WFTA processor. When the actual ASIC ACU is completed, then the additional signals might be unnecessary. But in the interim, when using a discretely built ACU, additional signals might be beneficial and make system design easier. One signal that would be useful is a "START WRITING" signal which would indicate to the ACU when the WFTA processor is ready to start writing output to the memory. Presently, the only way to establish this synchronization is for the ACU to count a certain number of clock cycles before it outputs the addresses and the write enable pulses.

7.3.3 Different Host. For this thesis, the host selection was not particularly important, since it was only dealing with a 16-point transform. However, when the full-up WFTA is built, there needs to be a more powerful host processor driving the WFTA system. Writing 16 points to memory before the WFTA16 processor is completed with a previous set is not difficult using a 68010. But, looking toward the future, where the host processor will write 4080 24-bit data words to memory, the WFTA would be "starved" for data. Additional research into the WFTA project area needs to focus on an interface with a faster and more powerful host processor and bus standard.

7.3.4 Behavioral Descriptions of Chips. Using the behavioral descriptions of the chips used in the design of the WFTA system as a starting point, a library of behavioral descriptions of commercially available chips should be developed which can be used in the future for any design work of a similar nature to this thesis. In fact, this library might be coupled with the advanced microprocessor lab in order to prove designs in that lab prior to actual construction. The SYNOPSIS package with its SGE environment has eliminated much of the difficulty in VHDL design by providing configuration management and structural construction from the behavioral descriptions.

7.3.5 Supply of Resources. A hardware thesis such as this one is difficult to complete at AFIT, not because of complexity of design but because of the lack of proper support. For example, there was only one available VMEbus backplane for use in this thesis. Furthermore, many common ALS-series integrated circuits were unavailable and had

to be ordered or purchased. This deficiency has been corrected to some extent with the purchase of a FPGA system, but there remains a problem. Supplies supporting a VMEbus application should be stocked in the communications lab or digital lab if this standard is to be used in future work. Although this might seem like "technician" work, an engineer must be able to perform technical construction to a certain extent.

7.4 Lessons Learned

As discussed in this chapter, the objectives of Chapter I were not fully achieved. However, the effort has provided future researchers with some lessons learned.

7.4.1 Scheduling of Construction. There was an underestimation of the time required for the construction of the WFTA system during this thesis. Construction on this project started too late in the thesis cycle for completion. Do not make the same mistake in the future. Allow at least two months for any hardware construction using the wirewrap method. Resource shortcomings and testing will certainly fill this time. If an estimate is made for construction, take the pessimistic view rather than the optimistic view.

7.4.2 Construction Methodology. The testing of this prototype forced a piecewise construction methodology with functional blocks tested in system. Modular construction and modular testing is much more desirable with any prototyping. Future work in construction should use a modular approach, building the testing platforms necessary to fully test the modules before including them in the complete system.

7.4.3 Ordering of Parts. Another problem tied to the construction problems discussed is the late ordering of parts needed for the design. Parts for this thesis were ordered too late in the thesis cycle. Finish the design early enough to provide ample time for parts to be ordered and shipped. Be aware of the end of the government's fiscal year when funding for parts might become an issue.

7.5 Summary

This chapter has discussed the conclusions that were derived from this research, the recommendations for the future direction of research in the WFTA project area, the lessons learned during this thesis, and suggestions to improve the efficiency of hardware development.

Appendix A. *Schematics for Subcomponents*

This appendix provides the schematics generated for the WFTA system design which are discussed in Chapter IV. The schematics for the abstract, high-level functional blocks are located in the thesis. The schematics in this appendix describe the subcomponents of each of the major functional blocks of the WFTA system; the VMEbus interface, the input and output memory, and the ACU. All these schematics were generated in the Synopsys SGE environment.

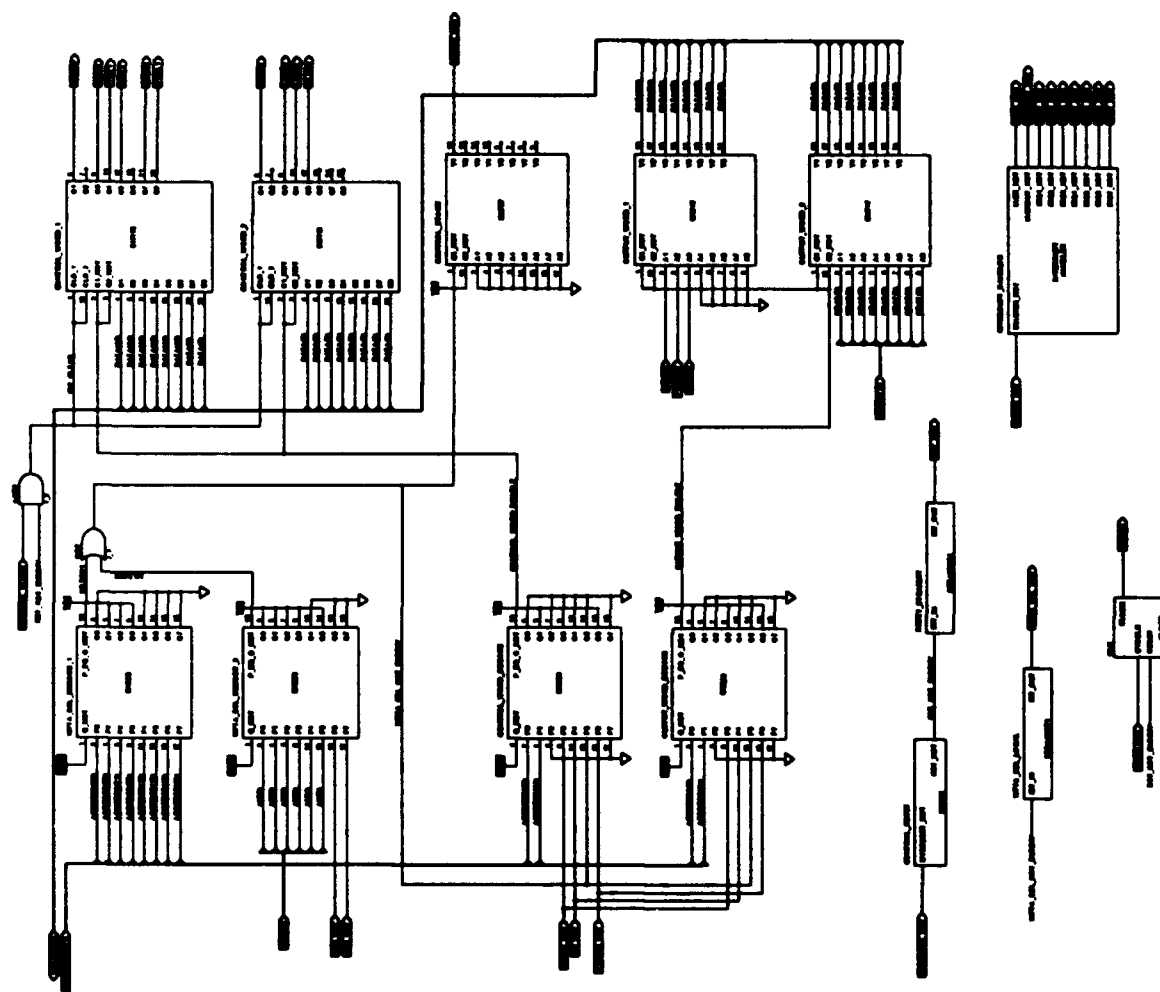


Figure 22. Control Section Schematic-VMEbus Interface

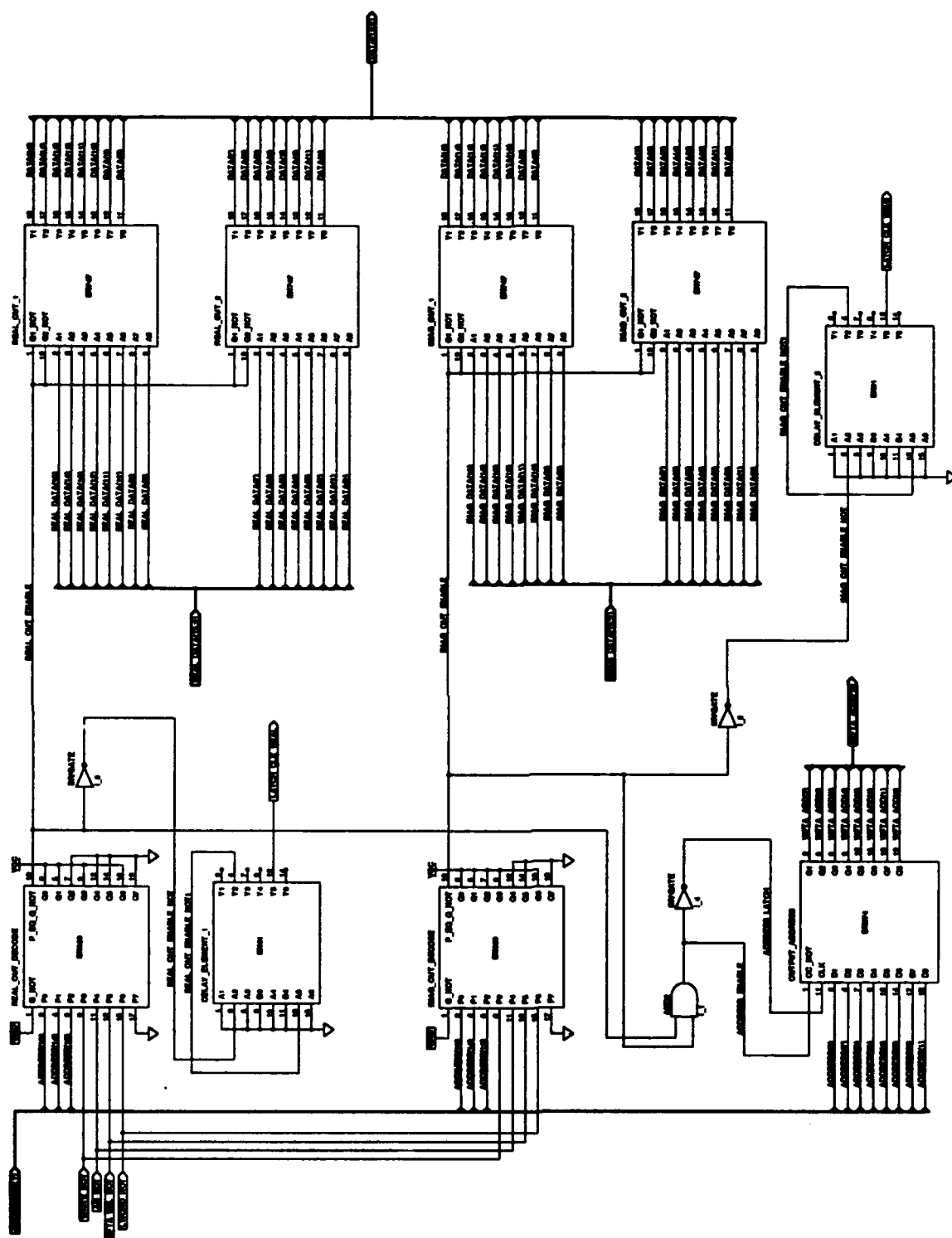


Figure 23. Output Section Schematic-VMEbus Interface

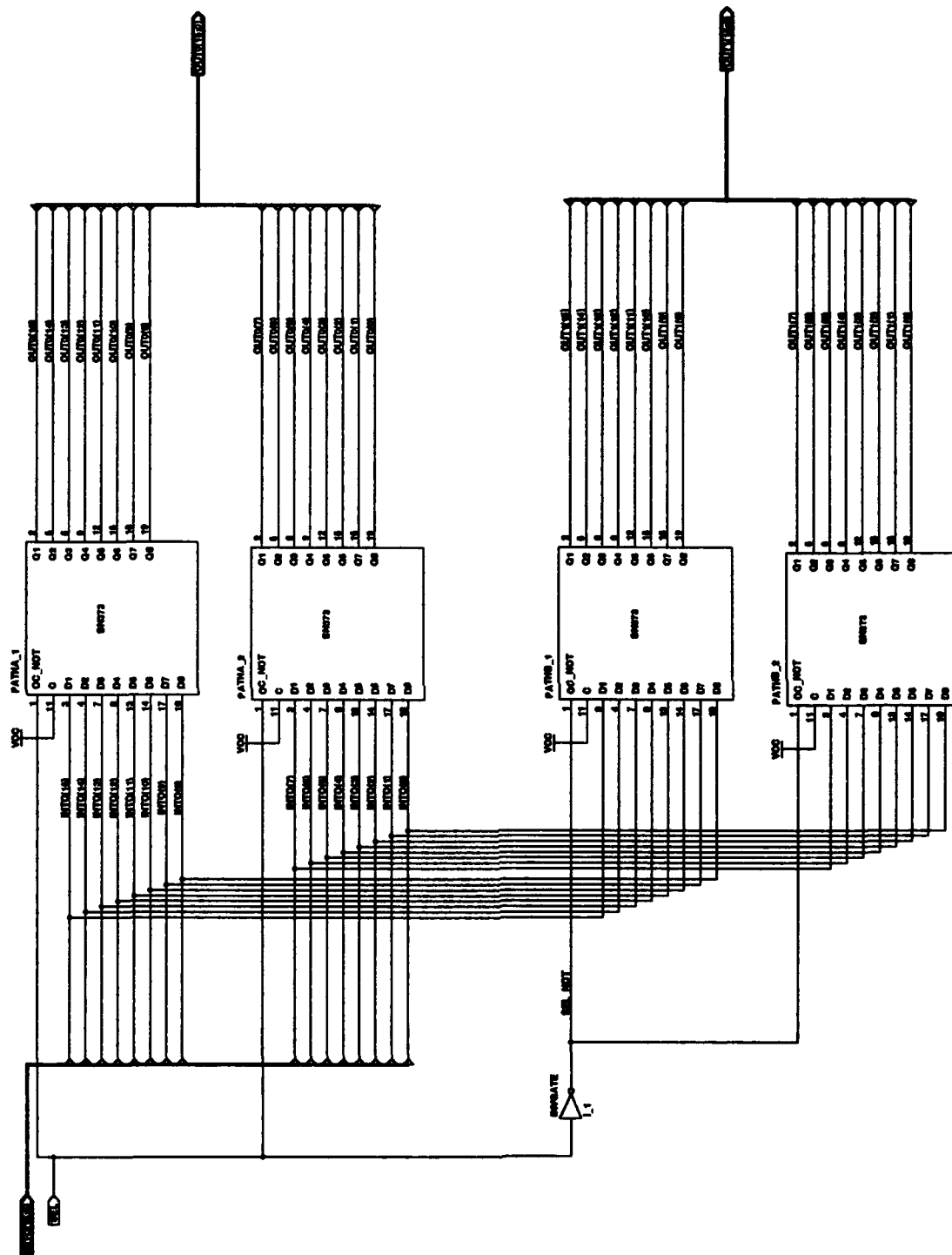


Figure 24. DEMUX1 Block Schematic-Input Memory

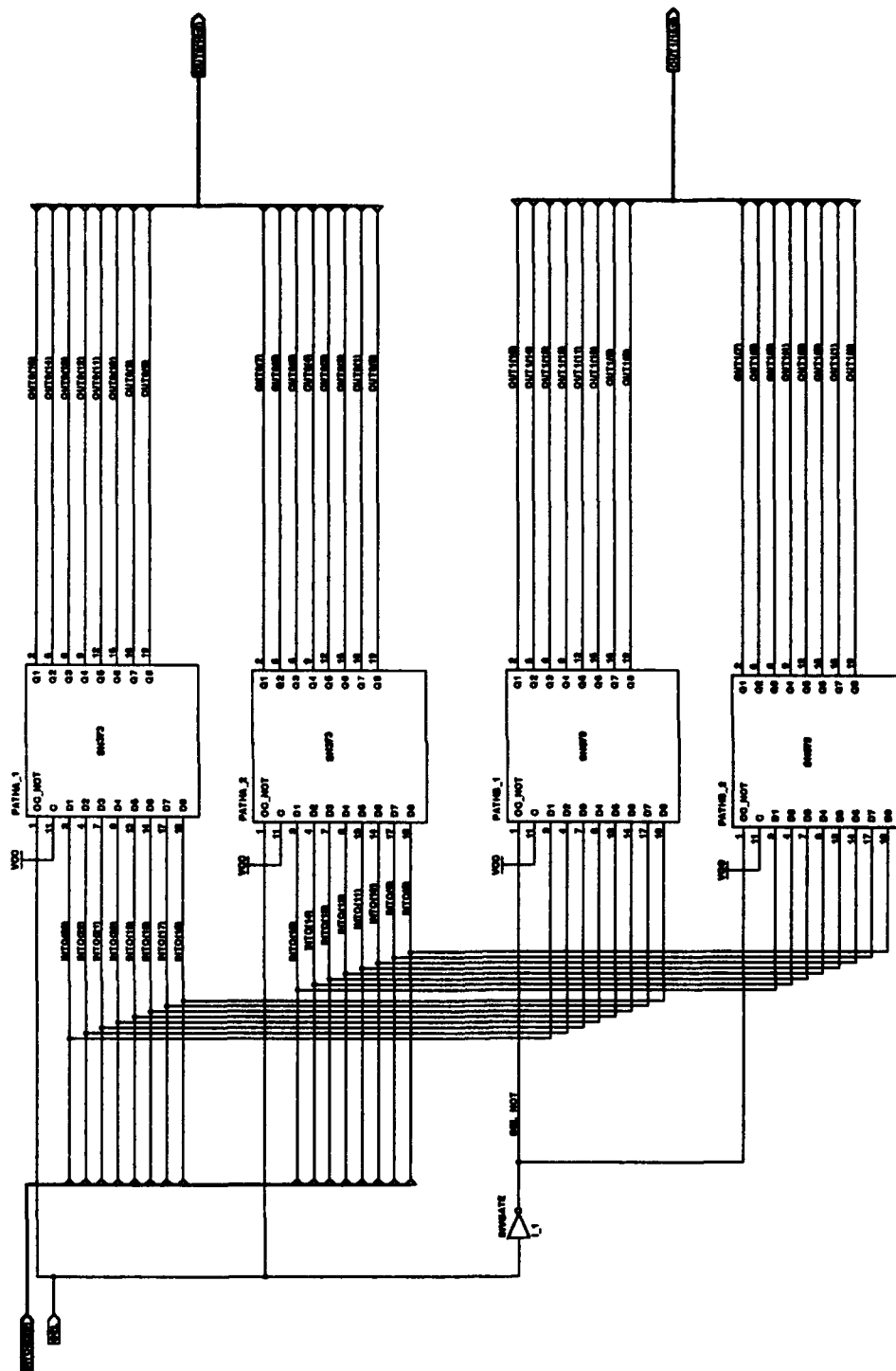


Figure 25. DEMUX1a Block Schematic-Output Memory

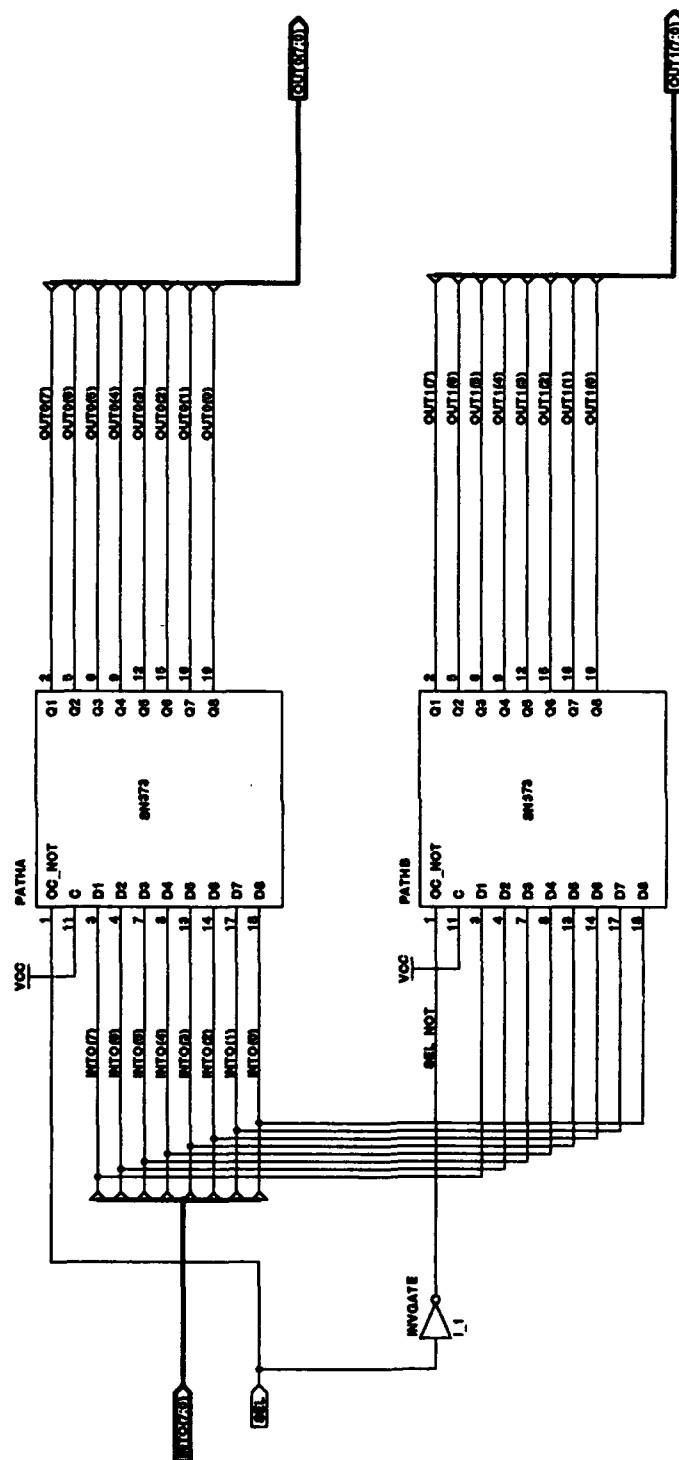


Figure 26. DEMUX2 Block Schematic-Input and Output Memory

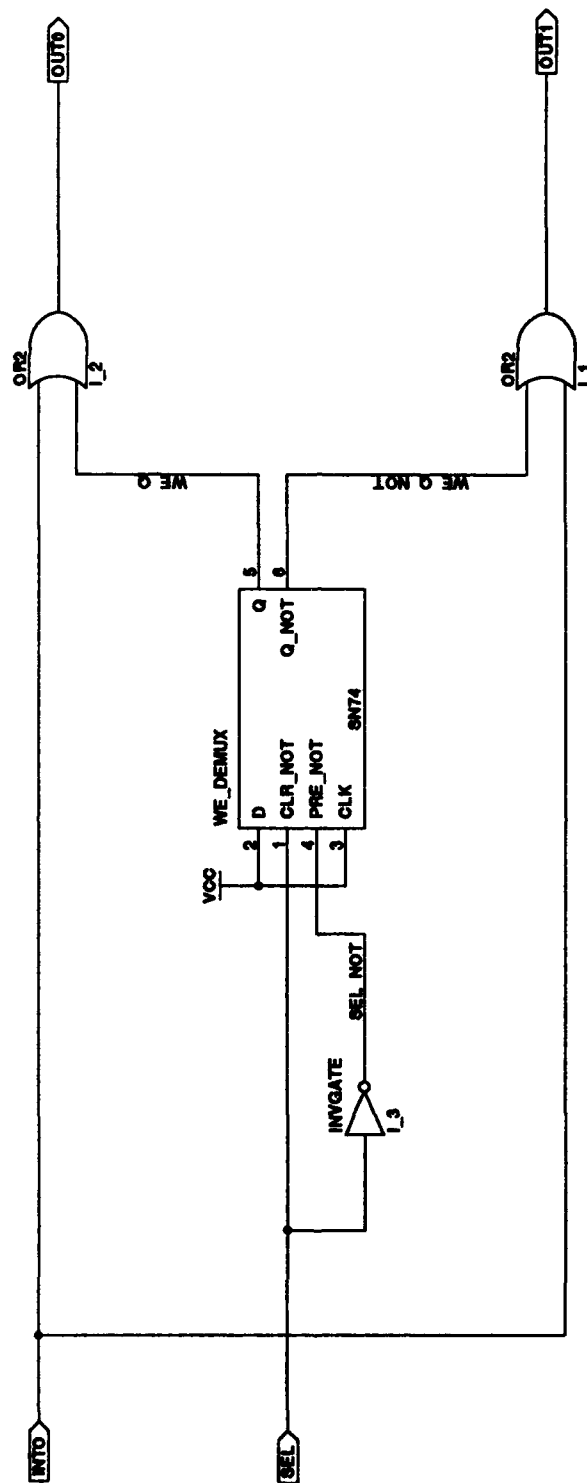


Figure 27. DEMUX3 Block Schematic-Input and Output Memory

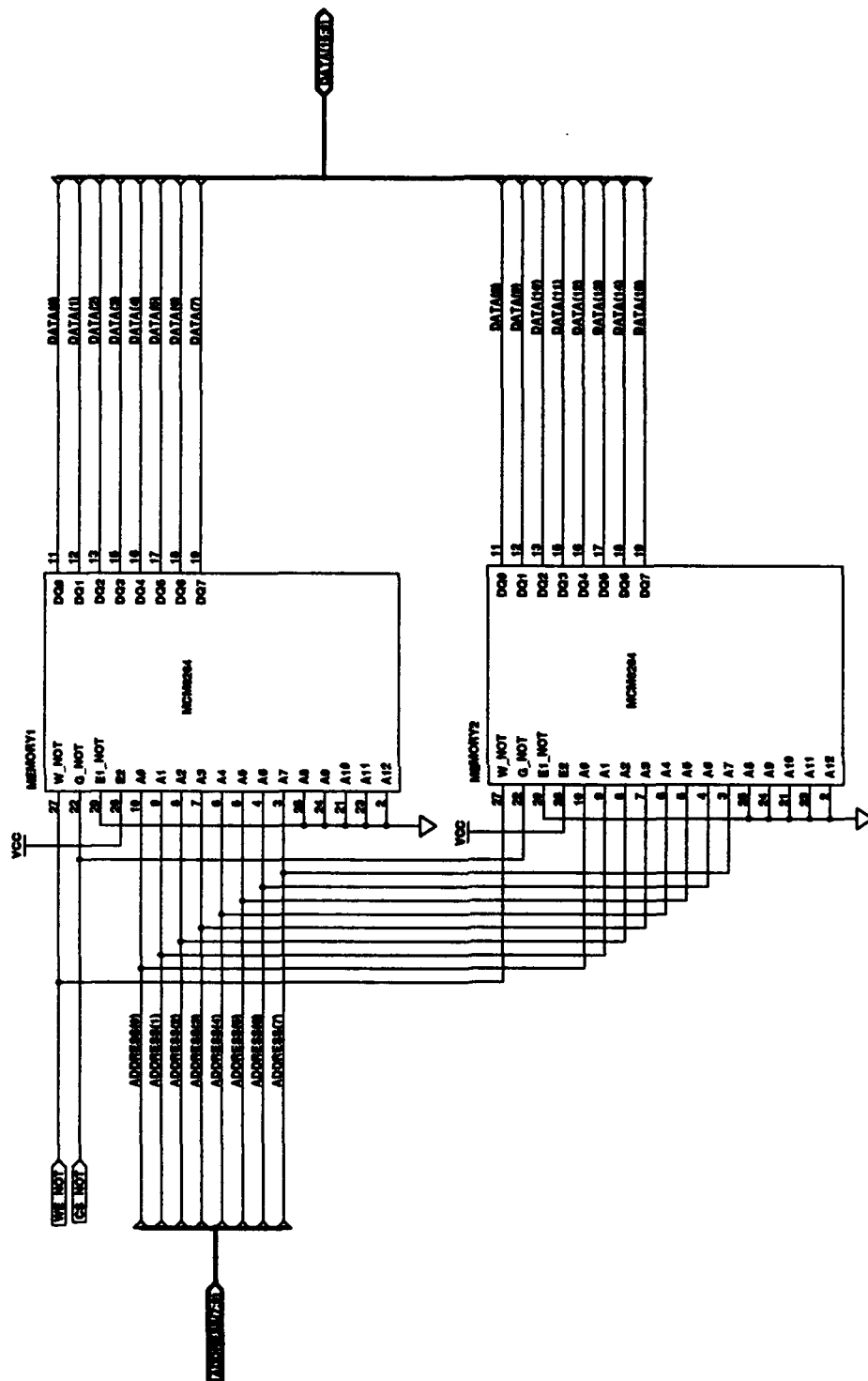


Figure 28. MEM_MCM6264 Block Schematic-Input and Output Memory

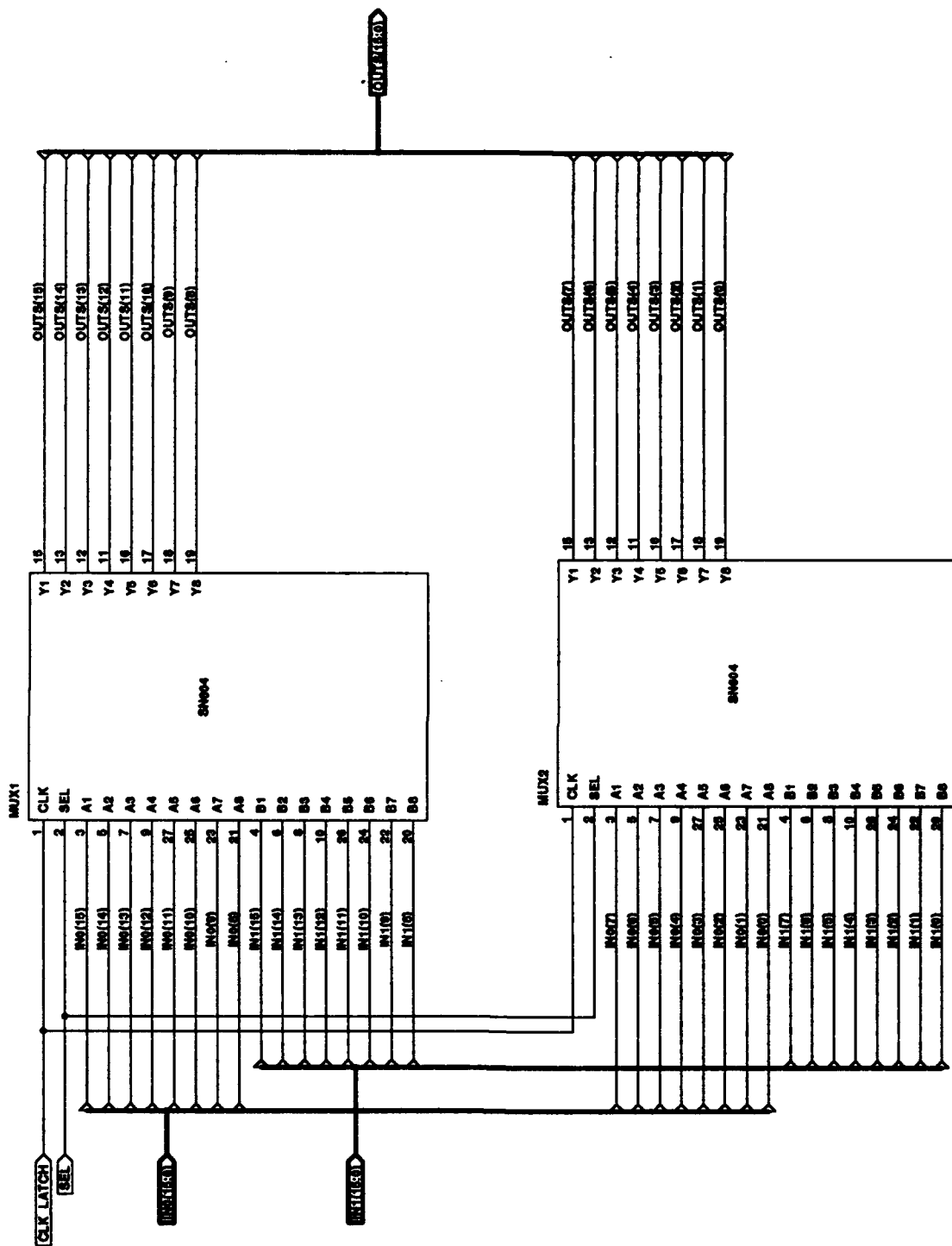


Figure 30. MUX2a Block Schematic-Input Memory

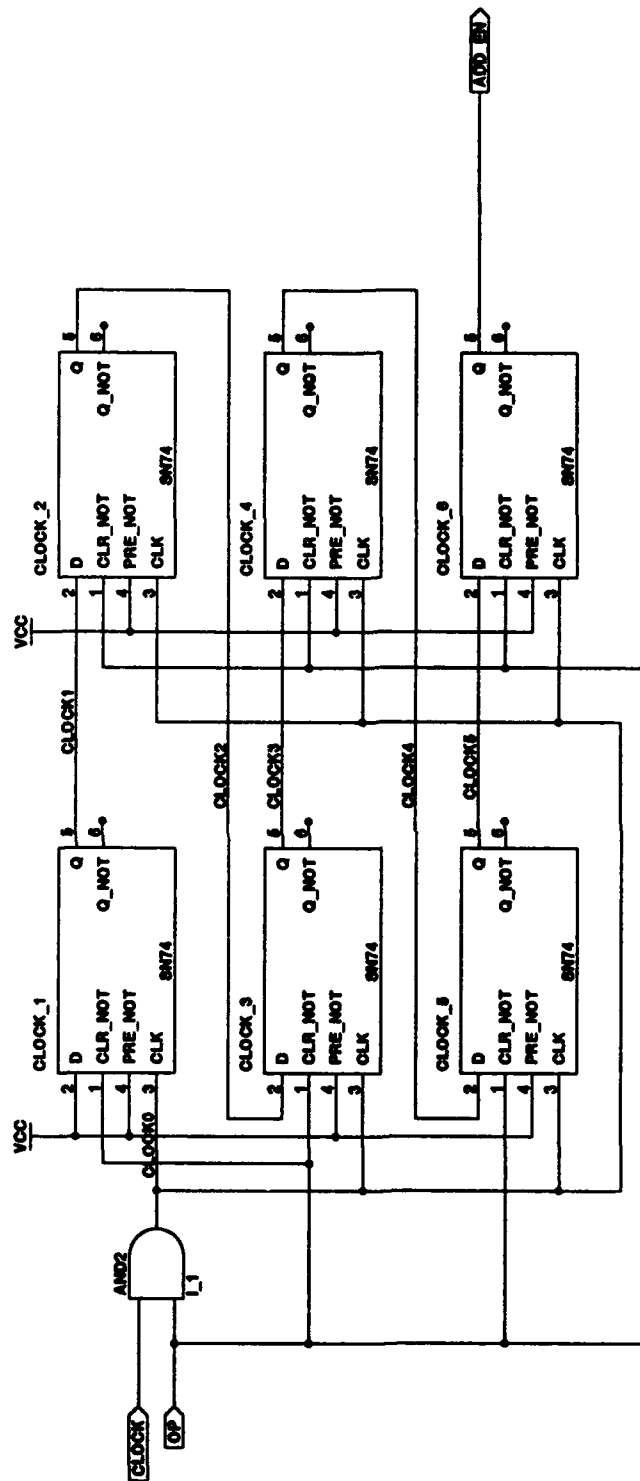


Figure 31. ACU_INIT Block Schematic-ACU

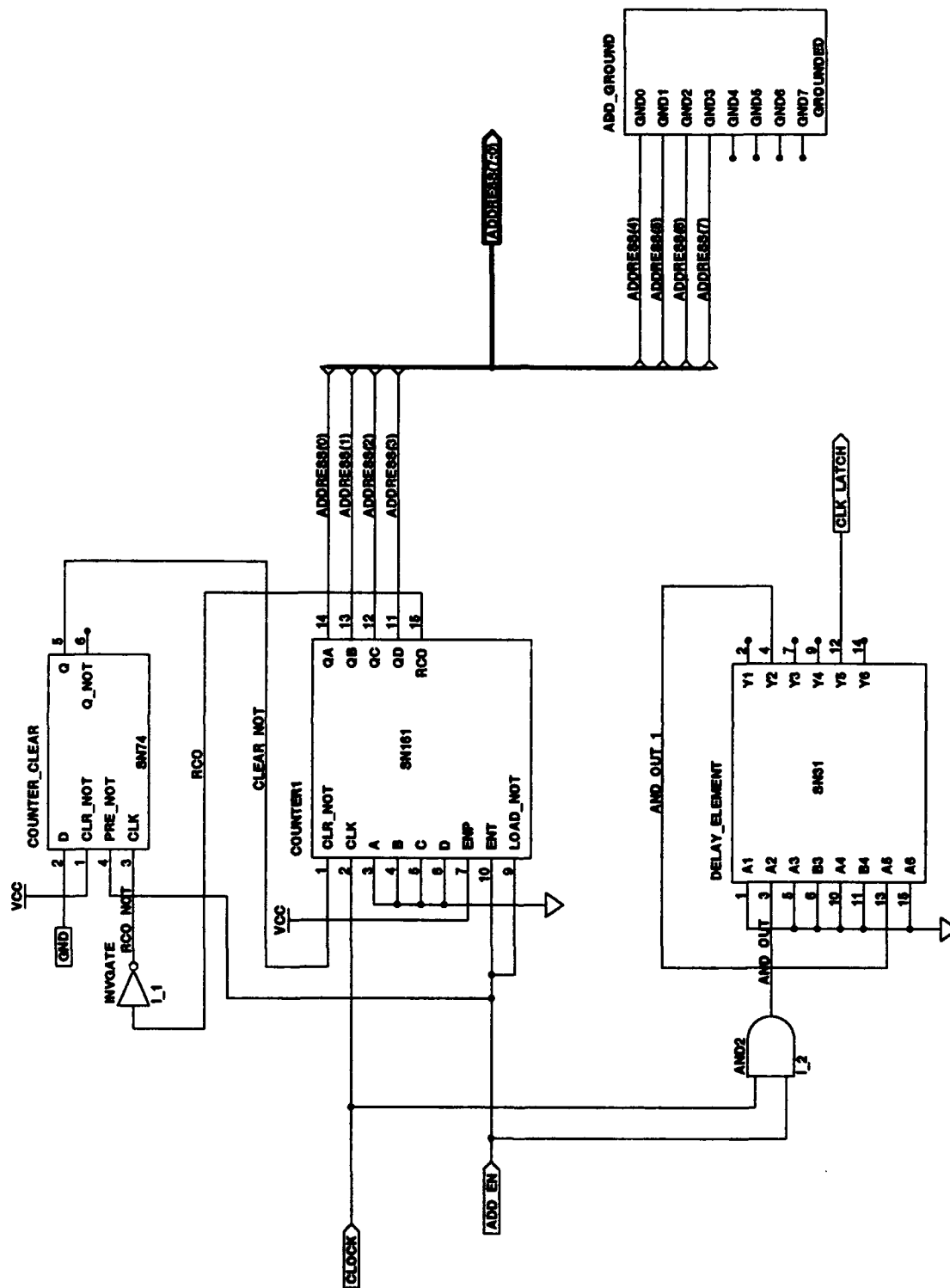


Figure 32. ACU_ADD Block Schematic-ACU

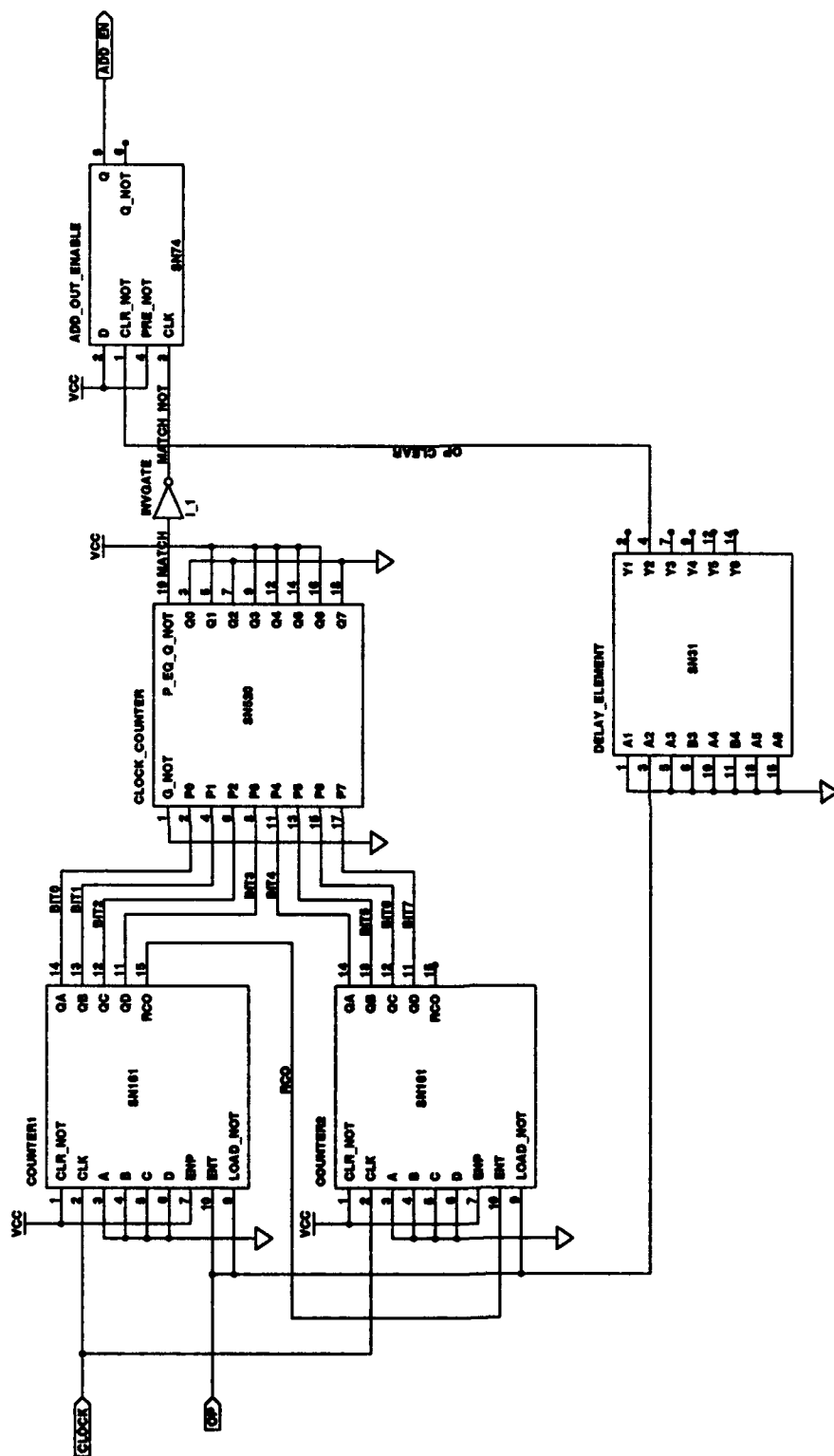


Figure 33. ACU_COUNTER Block Schematic-ACU

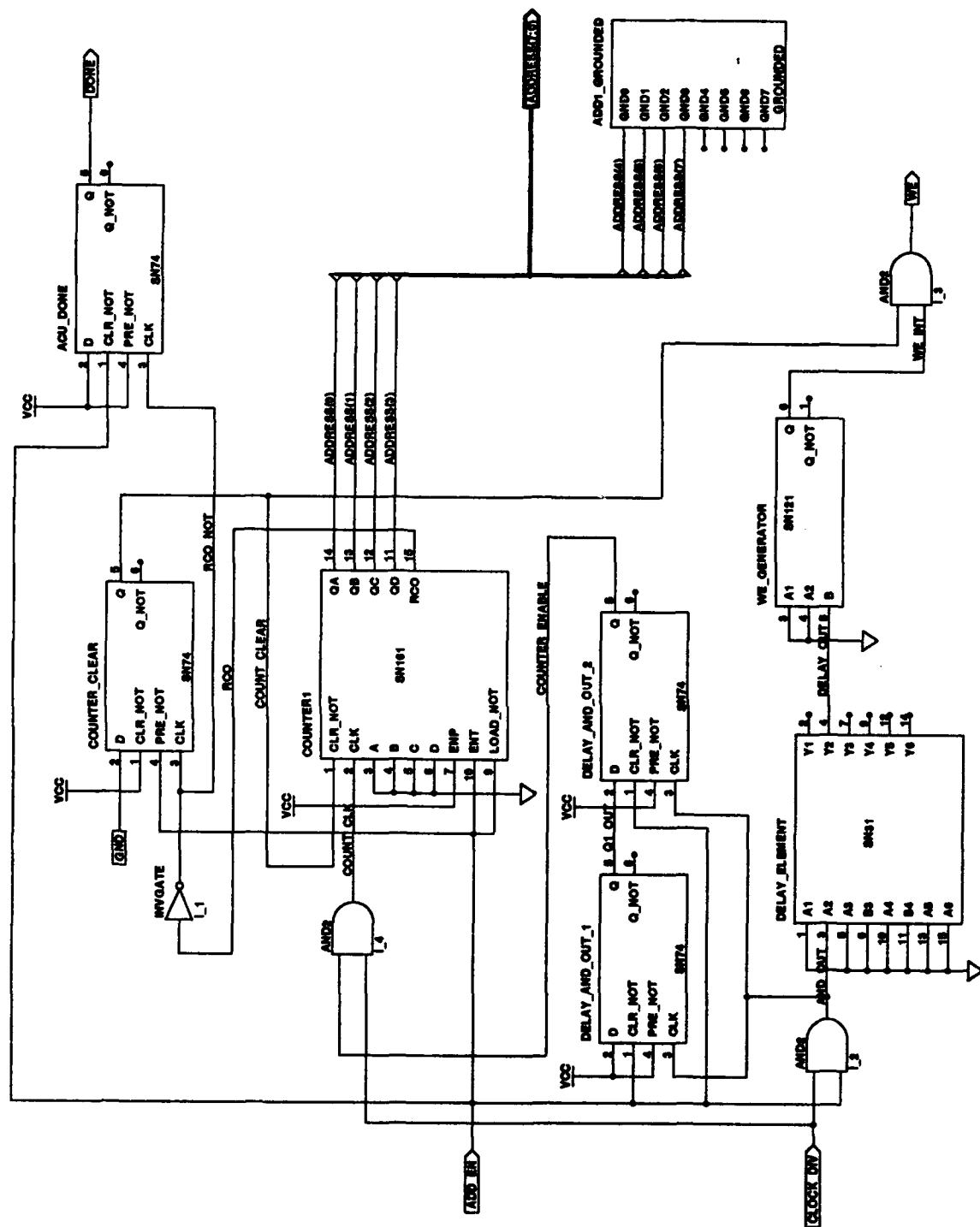


Figure 34. ACU_ADD1 Block Schematic-ACU

Appendix B. *Timing Diagrams for Functional Blocks*

This appendix provides the timing diagrams generated for the major functional blocks of the WFTA system which are discussed in Chapter IV. These timing diagrams show the significant input and output signals of each block and each diagram is discussed in detail in the text of the thesis. These timing diagrams were created from the test benches discussed in Section 4.5, using the trace option in the VHDL simulator provided with the Synopsys software package. The behavior of the input signals was based on the expected signal behavior from the WFTA system. All the values shown are in hexadecimal format.

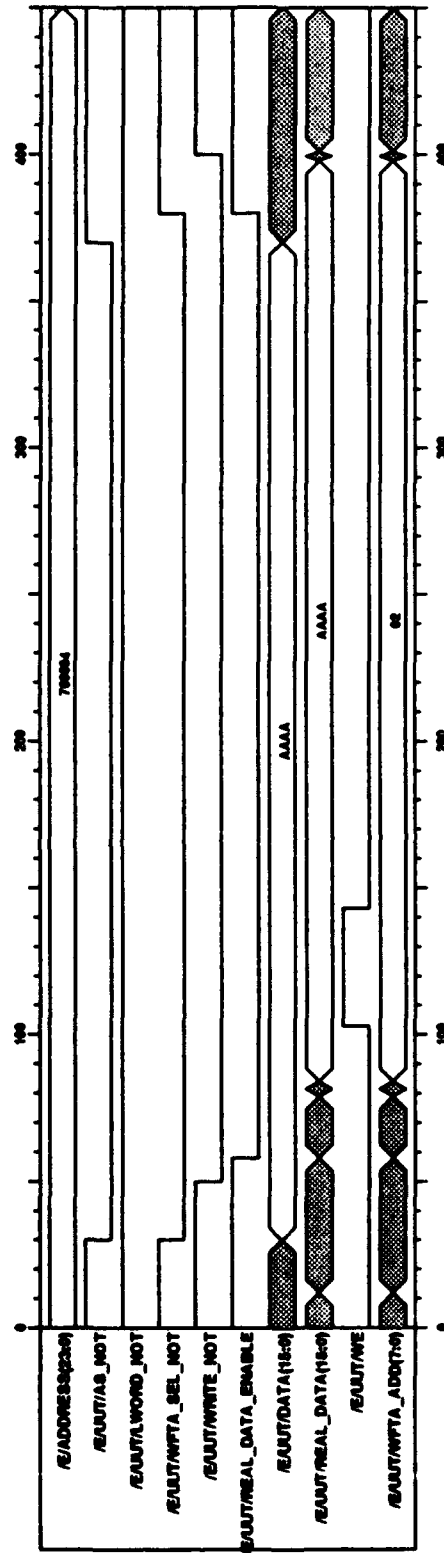
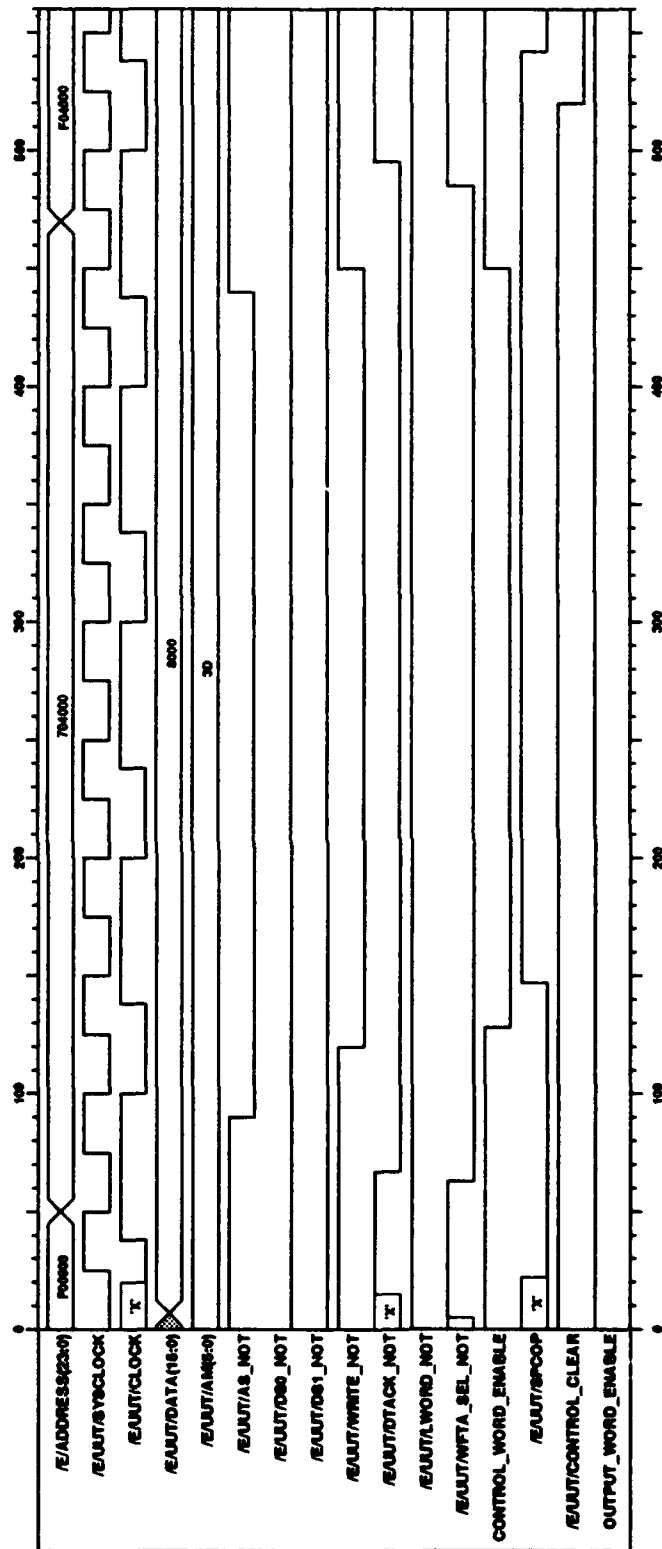


Figure 35. Timing Diagram-Input Section



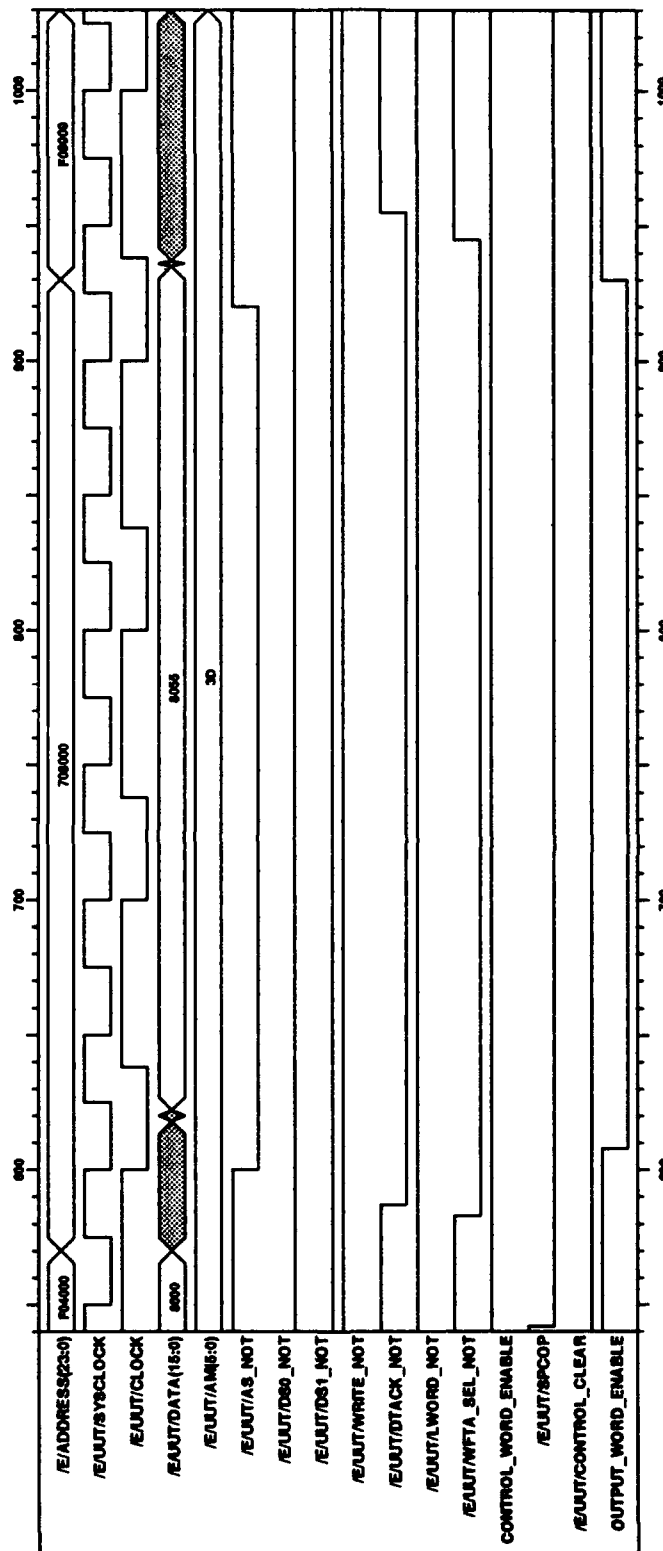


Figure 37. Timing Diagram-Control Section(#2)

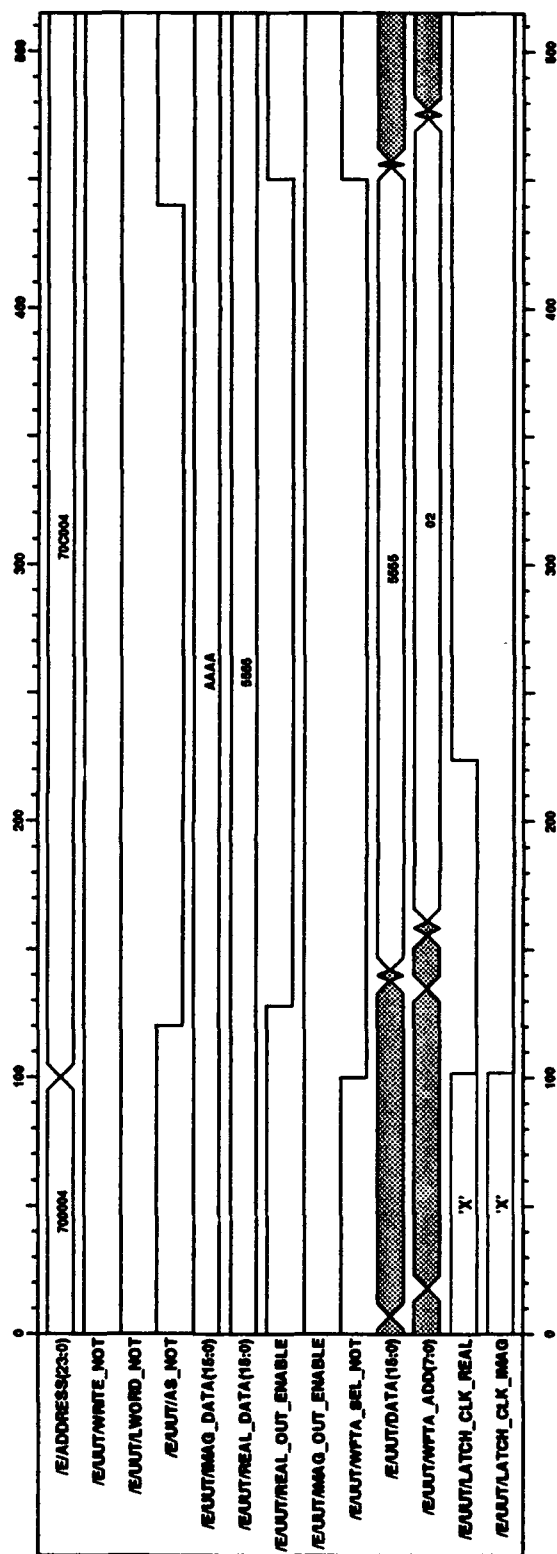


Figure 38. Timing Diagram-Output Section(#1)

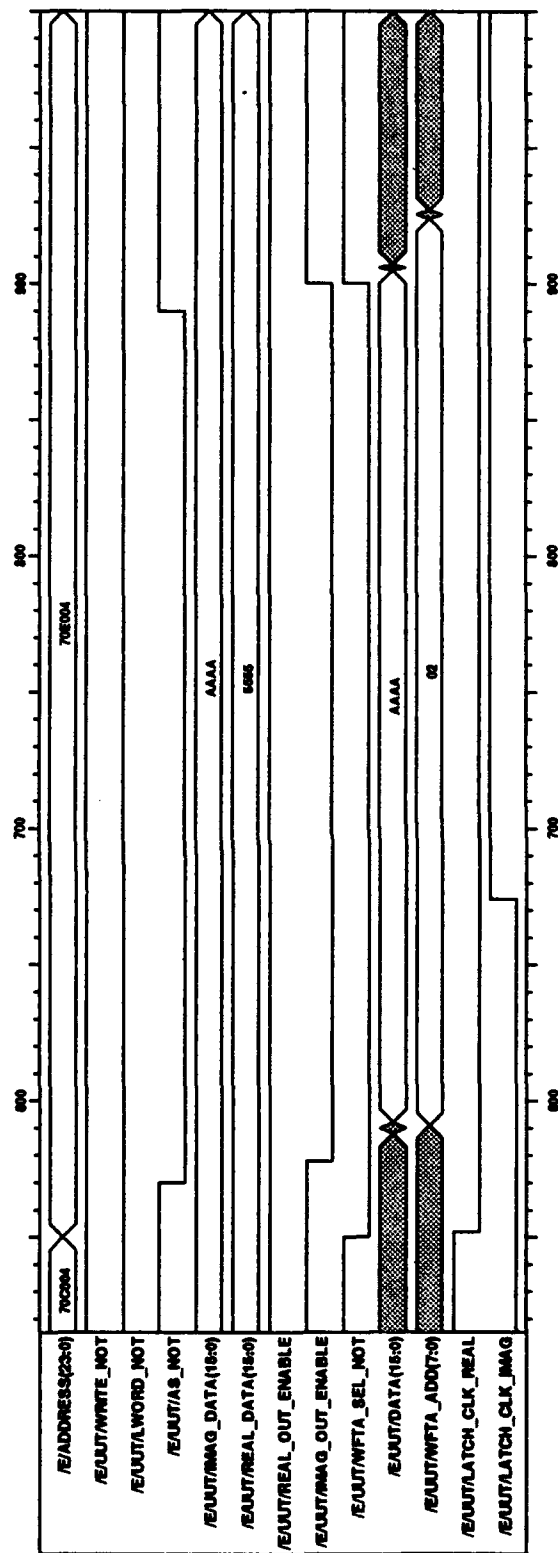


Figure 39. Timing Diagram-Output Section(#2)

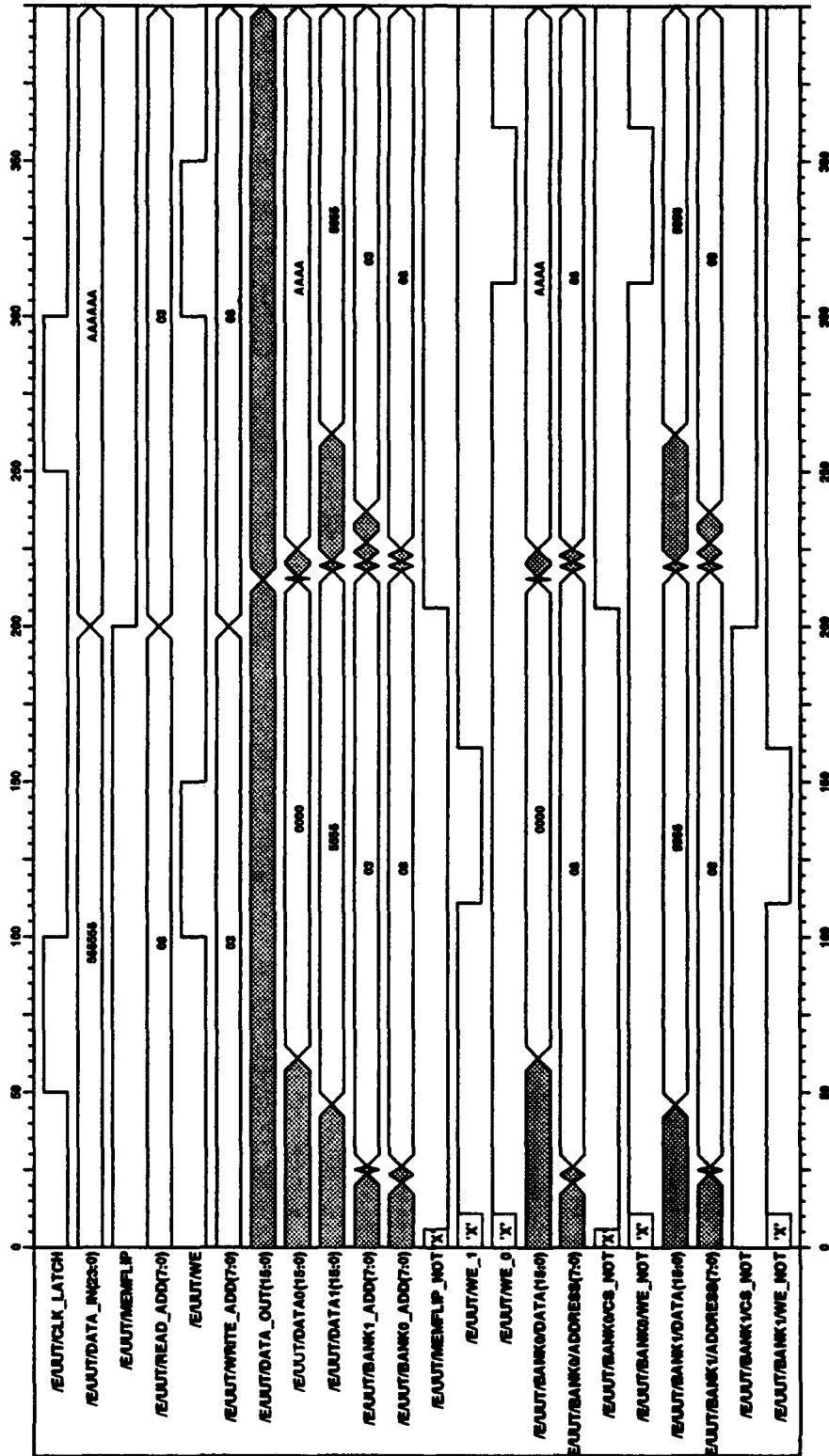


Figure 41. Timing Diagram-Output Memory

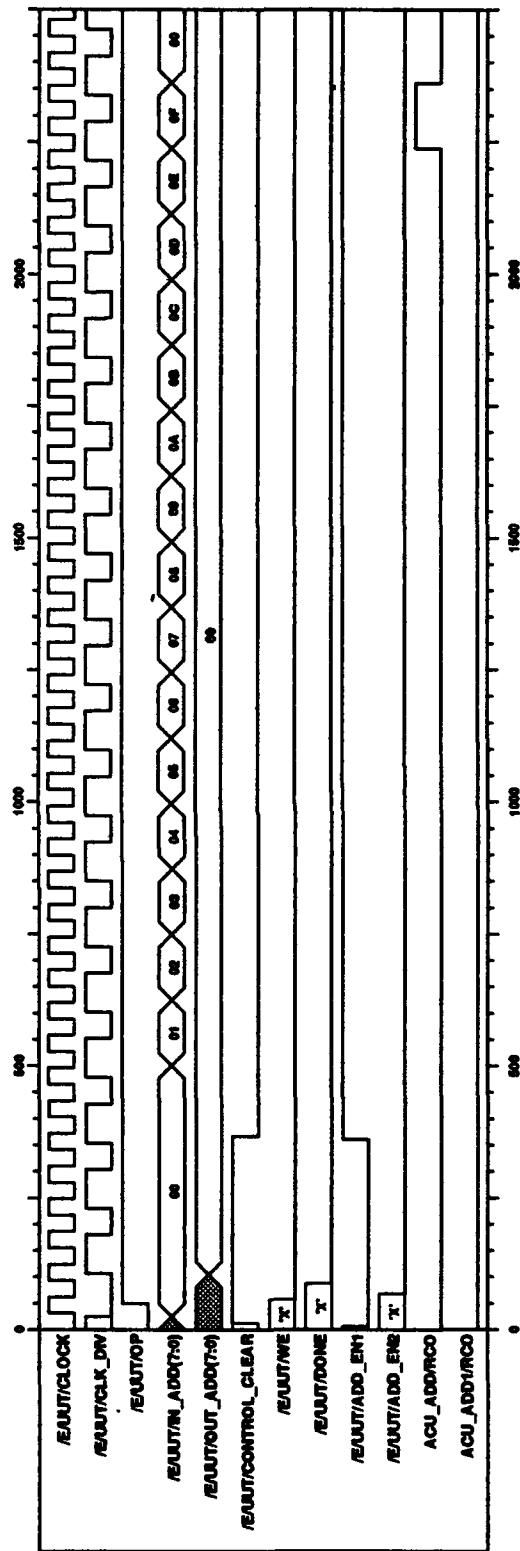


Figure 42. Timing Diagram-ACU(#1)

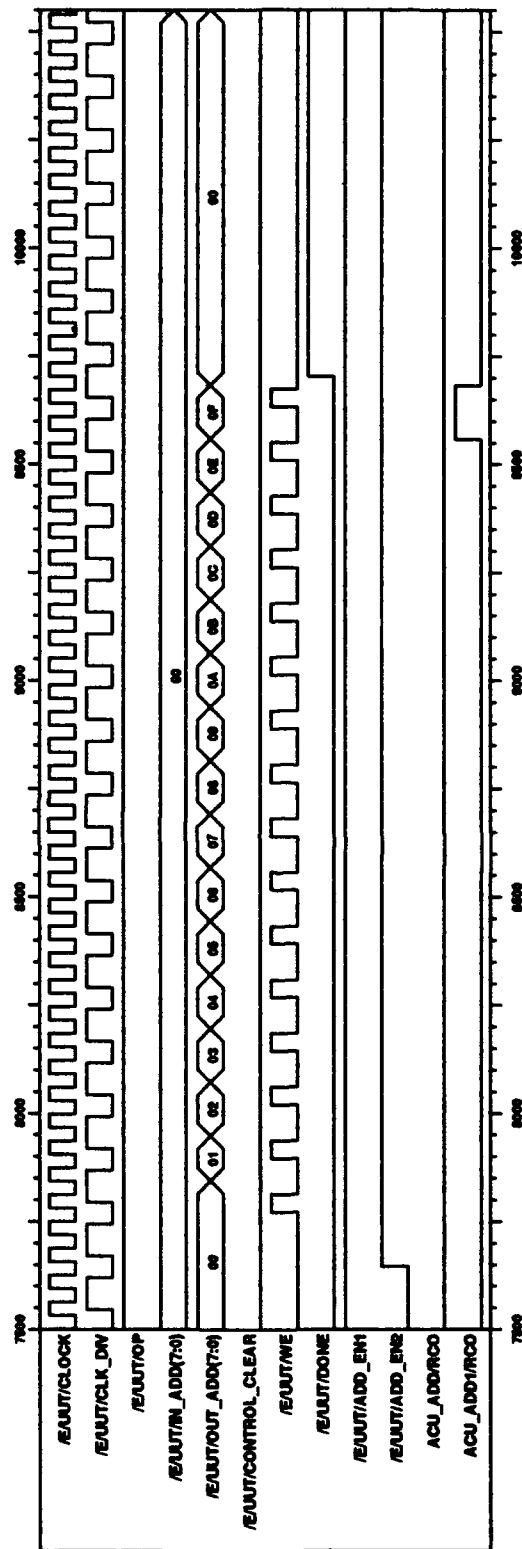


Figure 43. Timing Diagram-ACU(#2)

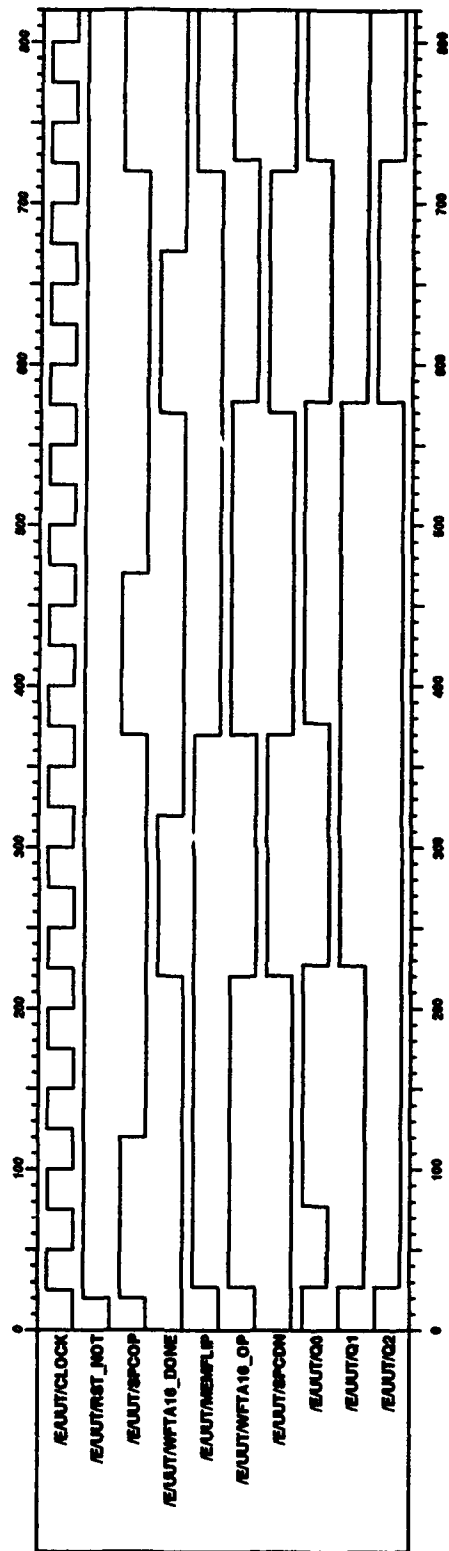


Figure 44. Timing Diagram-MSPC

Table 7. MSPC Timing Table

<i>Time</i>	<i>Inputs</i>			<i>State</i>	<i>Outputs</i>		
	<i>RST NOT</i>	<i>SPCOP</i>	<i>WFTA16 DONE</i>		<i>MEMFLIP</i>	<i>WFTA16 OP</i>	<i>SPCDN</i>
25	1	1	0	OP1	1	1	0
75	1	1	0	OP1	1	1	0
125	1	0	0	OP1	1	1	0
175	1	0	0	OP1	1	1	0
225	1	0	1	DONE1	1	0	1
275	1	0	1	DONE1	1	0	1
325	1	0	0	DONE1	1	0	1
375	1	1	0	OP2	0	1	0
425	1	1	0	OP2	0	1	0
475	1	0	0	OP2	0	1	0
525	1	0	0	OP2	0	1	0
575	1	0	1	DONE2	0	0	1
625	1	0	1	DONE2	0	0	1
675	1	0	0	DONE2	0	0	1
725	1	1	0	OP1	1	1	0
775	1	1	0	OP1	1	1	0

Appendix C. *Test Vectors for 1 Hz Sine Wave*

This appendix provides the test vectors used in verifying the WFTA system design through the VHDL simulation. The signal used was a 1 Hz sine wave because both inputs and outputs were known prior to simulation. All the test vectors have sixteen points of data in a normalized 2's complement format. Table 8 shows the real input test vectors for a 1 Hz sine wave. There are no imaginary input test vectors because the WFTA system designed for this thesis does not accept imaginary input vectors. Table 9 shows the expected and actual real output test vectors (or FFT) for a 1 Hz sine wave. Table 10 shows the expected and actual imaginary output test vectors for a 1 Hz sine wave. The actual test vectors were taken from the output file *fourier_output* after a simulation run.

Table 8. Real Input Test Vectors for a 1 Hz Sine Wave

<i>Point #</i>	<i>Binary</i>	<i>Hexadecimal</i>
1	0000000000000000	0000
2	0011000011111011	30FB
3	0101101010000010	5A82
4	0111011001000001	7641
5	0111111111111111	7FFF
6	0111011001000001	7641
7	0101101010000010	5A82
8	0011000011111011	30FB
9	1000000000000000	8000
10	1100111100000100	CF04
11	1010010101111101	A57D
12	1000100110111110	89BE
13	1000000000000001	8001
14	1000100110111110	89BE
15	1010010101111101	A57D
16	1100111100000100	CF04

Table 9. Expected and Actual Real Output Test Vectors for a 1 Hz Sine Wave

<i>Point #</i>	<i>Expected</i>		<i>Actual</i>	
	<i>Binary</i>	<i>Hexadecimal</i>	<i>Binary</i>	<i>Hexadecimal</i>
1	1111111111111111	FFFF	1111111111111111	FFFF
2	0000000000000000	0000	0000000000000000	0000
3	0000000000000000	0000	0000000000000000	0000
4	0000000000000000	0000	0000000000000000	0000
5	0000000000000000	0000	0000000000000000	0000
6	0000000000000000	0000	0000000000000000	0000
7	0000000000000000	0000	0000000000000000	0000
8	0000000000000000	0000	0000000000000000	0000
9	0000000000000000	0000	0000000000000000	0000
10	0000000000000000	0000	0000000000000000	0000
11	0000000000000000	0000	0000000000000000	0000
12	0000000000000000	0000	0000000000000000	0000
13	0000000000000000	0000	0000000000000000	0000
14	0000000000000000	0000	0000000000000000	0000
15	0000000000000000	0000	0000000000000000	0000
16	0000000000000000	0000	0000000000000000	0000

Table 10. Expected and Actual Imaginary Output Test Vectors for a 1 Hz Sine Wave

<i>Point #</i>	<i>Expected</i>		<i>Actual</i>	
	<i>Binary</i>	<i>Hexadecimal</i>	<i>Binary</i>	<i>Hexadecimal</i>
1	0000000000000000	0000	0000000000000000	0000
2	1100000000000000	C000	1100000000000000	C000
3	0000000000000000	0000	0000000000000000	0000
4	1111111111111111	FFFF	1111111111111111	FFFF
5	0000000000000000	0000	0000000000000000	0000
6	0000000000000000	0000	0000000000000000	0000
7	0000000000000000	0000	0000000000000000	0000
8	1111111111111111	FFFF	1111111111111111	FFFF
9	0000000000000000	0000	0000000000000000	0000
10	0000000000000000	0000	0000000000000000	0000
11	0000000000000000	0000	0000000000000000	0000
12	1111111111111111	FFFF	1111111111111111	FFFF
13	0000000000000000	0000	0000000000000000	0000
14	0000000000000000	0000	0000000000000000	0000
15	0000000000000000	0000	0000000000000000	0000
16	0011111111111111	3FFF	0011111111111111	3FFF

Appendix D. *Timing Diagrams for WFTA System*

This appendix provides the timing diagrams generated during the VHDL simulation of the entire for the entire WFTA system. These timing diagrams were used in the verification of the system design in Chapter IV. All these timing diagrams are taken from a single simulation using the input test vectors in Table 8. In order to better observe the behavior of the signals the simulation was broken down into the seven timing diagrams below, each one showing the significant actions of the WFTA system. All the values shown are in hexadecimal format.

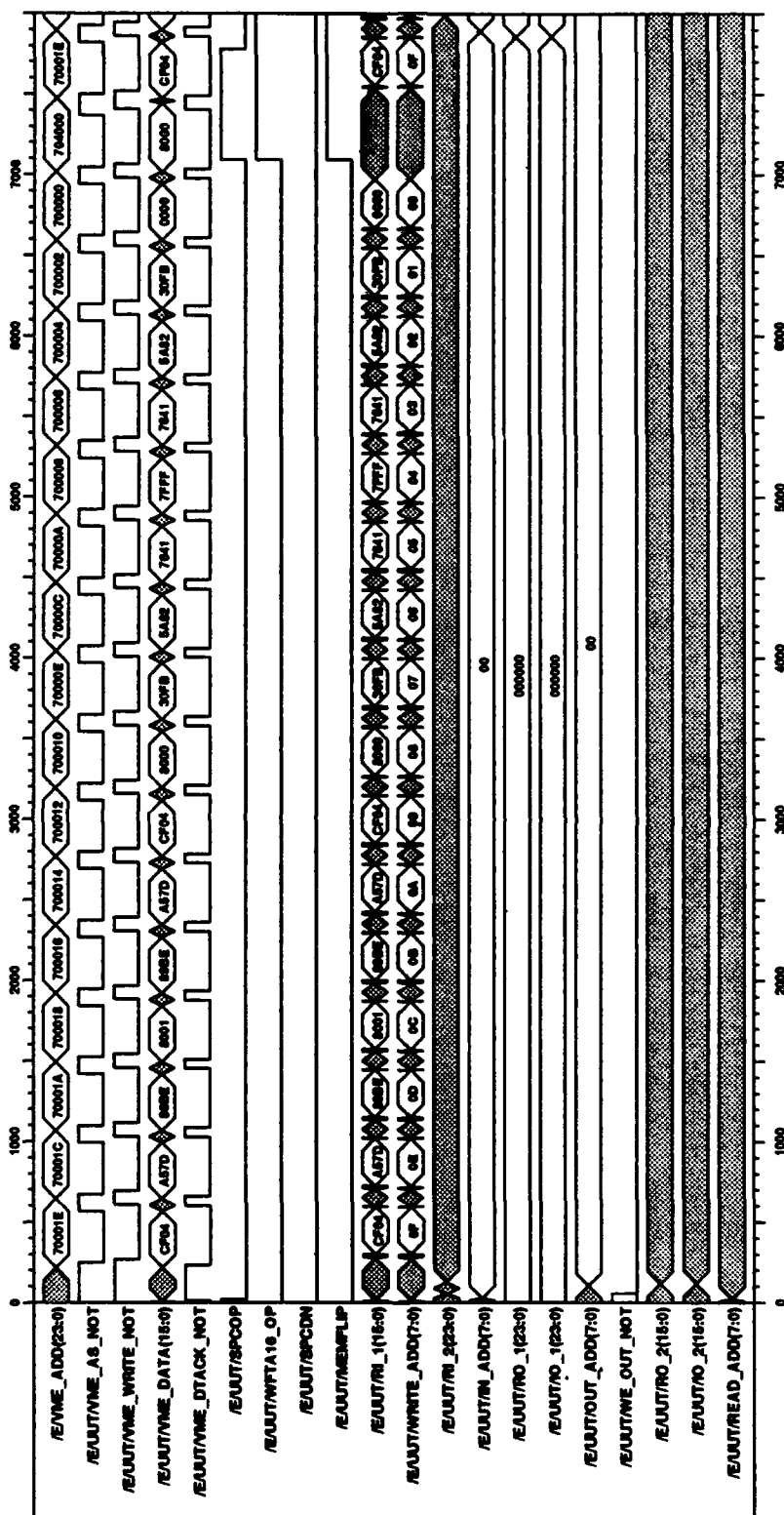


Figure 45. Timing Diagram-WFTA System(#1)

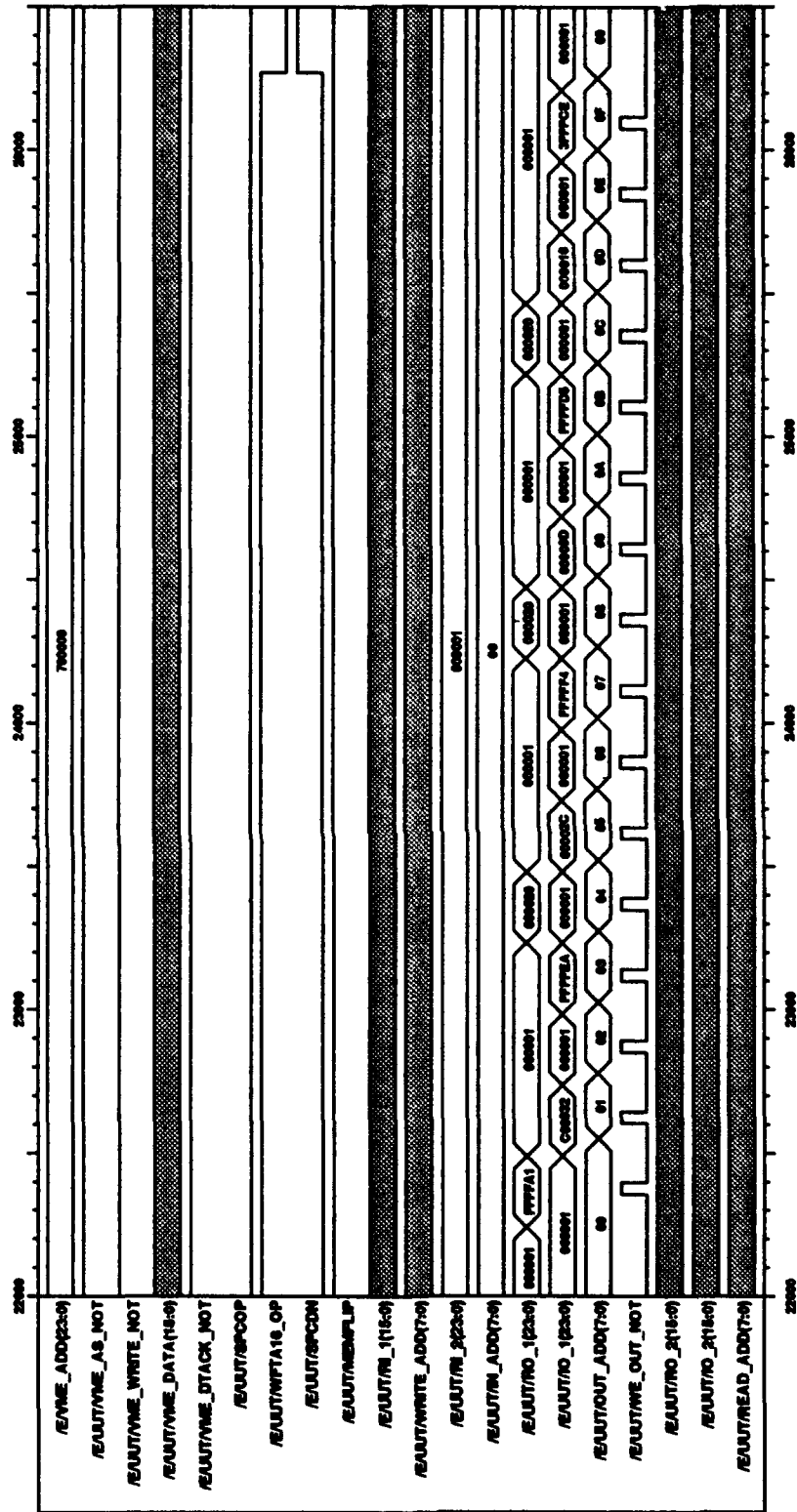


Figure 47. Timing Diagram-WFTA System(#3)

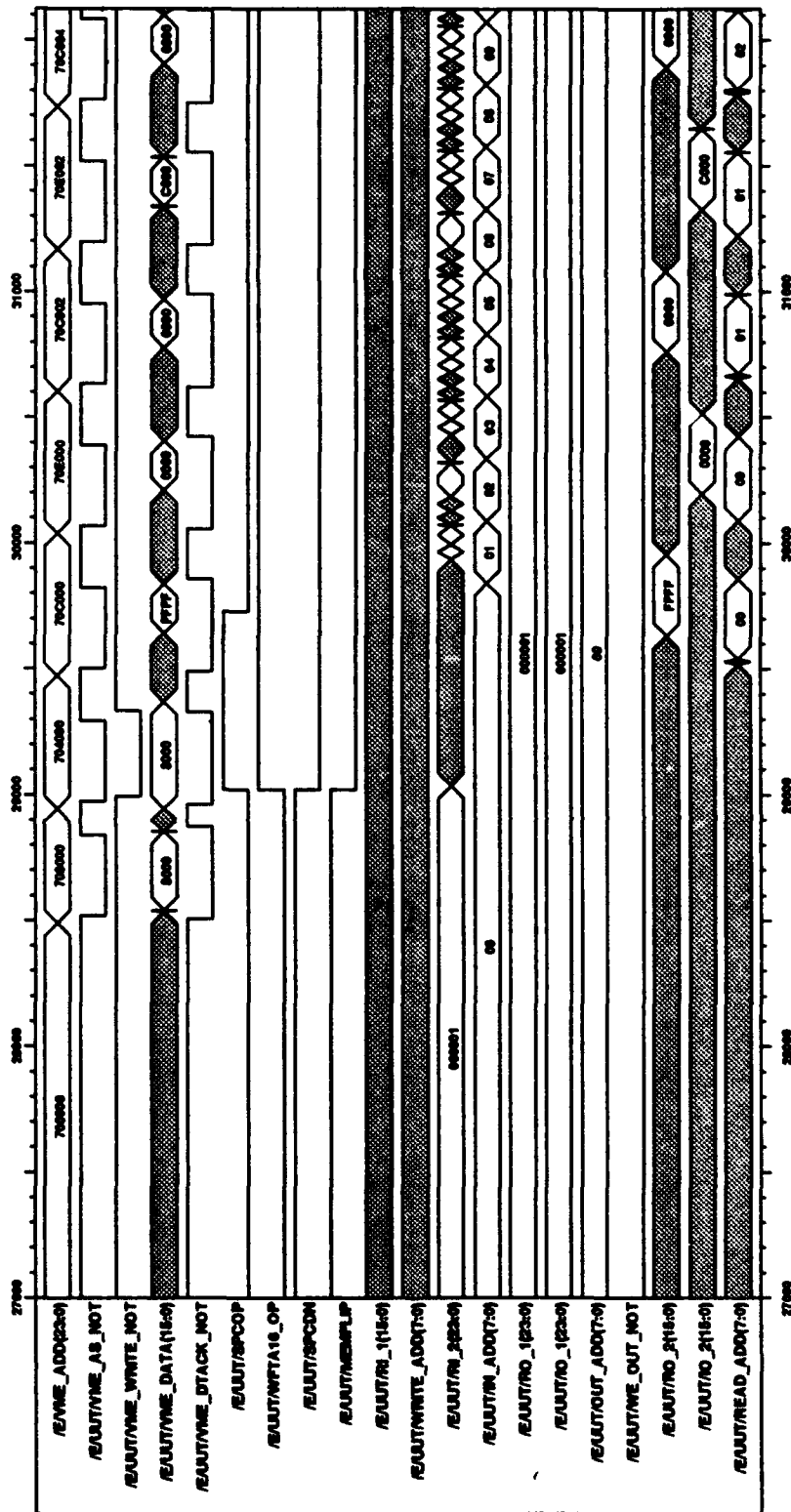


Figure 48. Timing Diagram-WFTA System(#4)

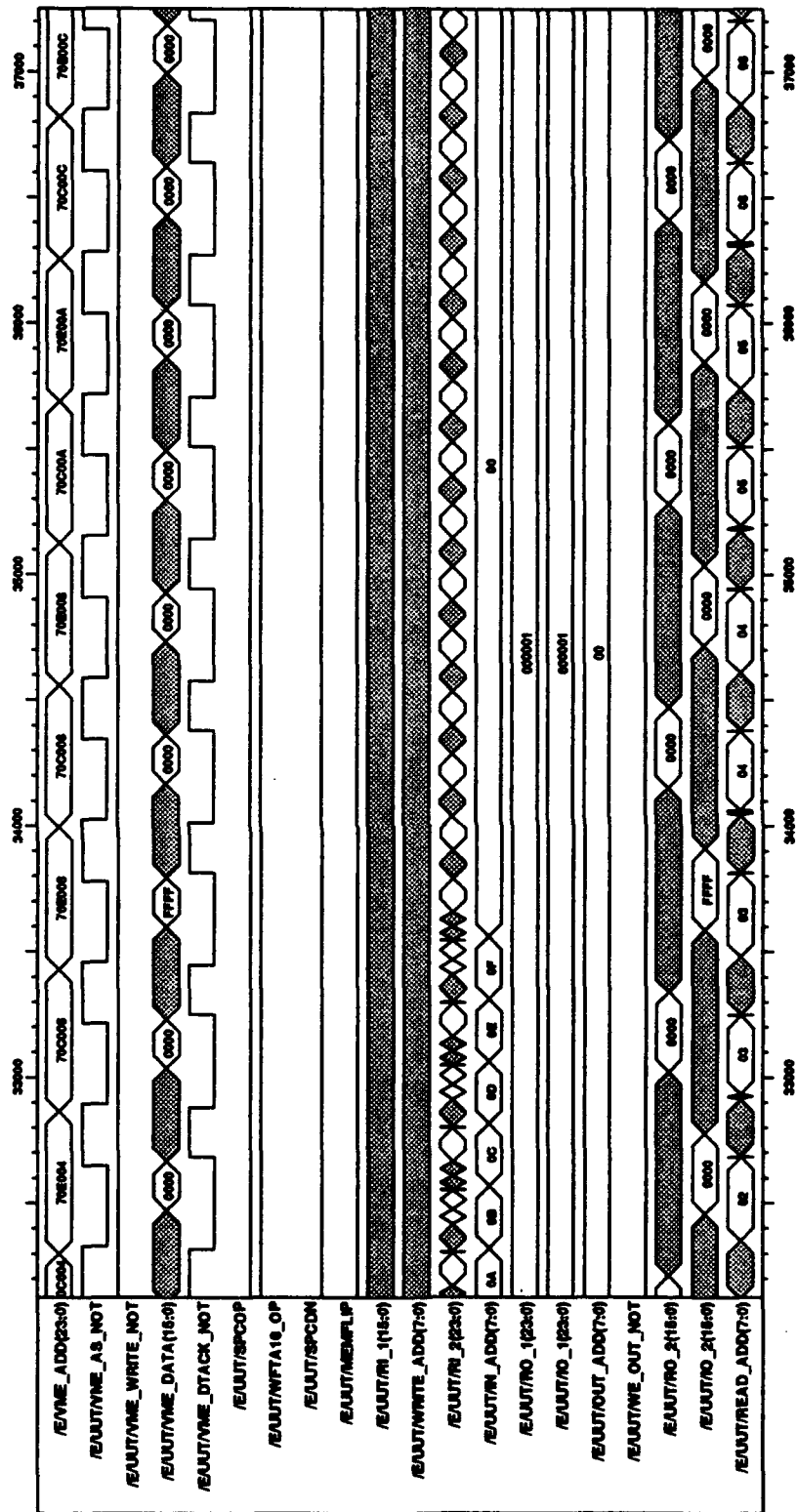


Figure 49. Timing Diagram-WFTA System(#5)

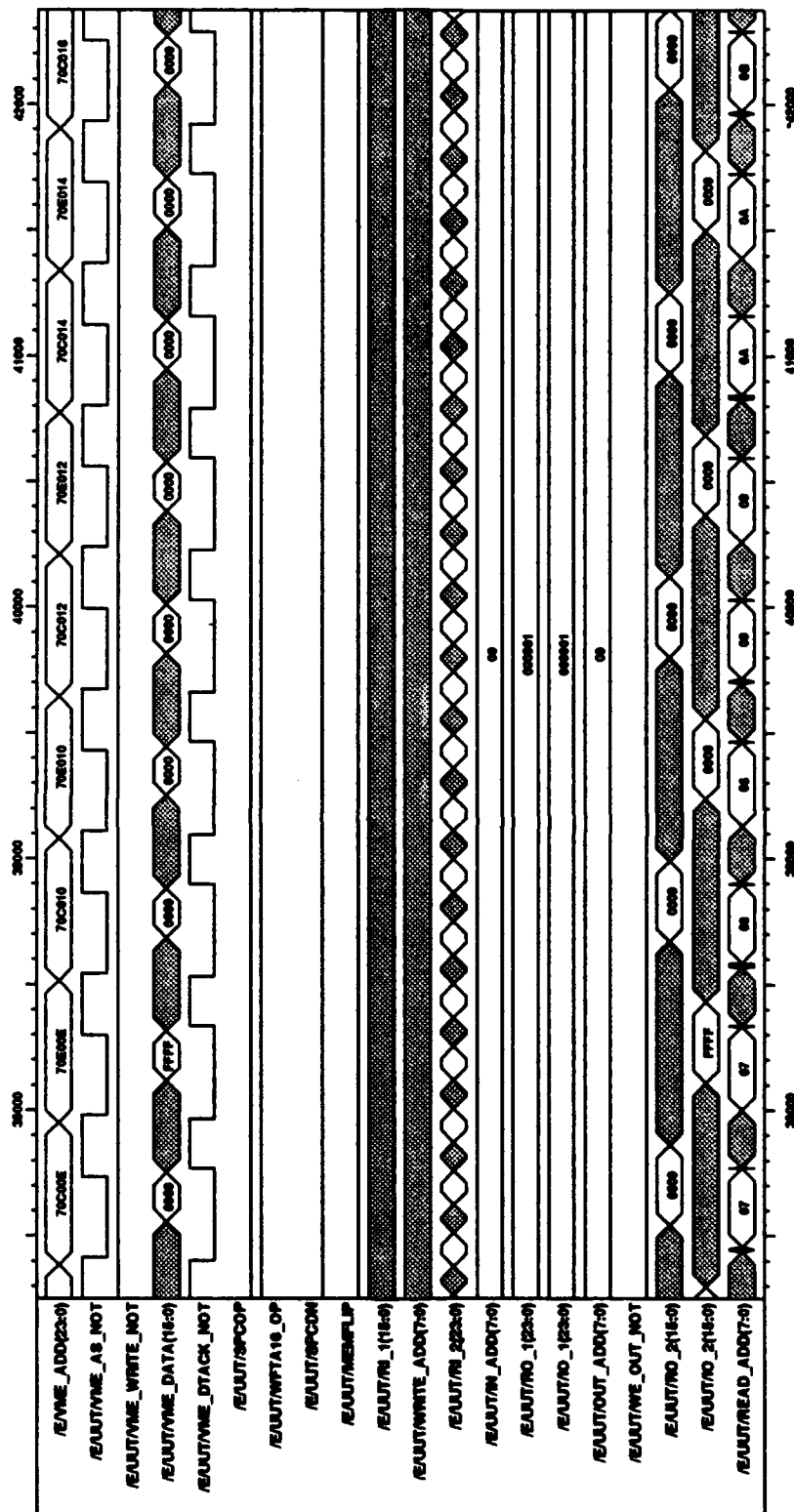


Figure 50. Timing Diagram-WFTA System(#6)

Appendix E. *Major Distributors and Suppliers of Parts*

This appendix provides a list of the local (to AFIT) distributors and suppliers of integrated circuit chips and other parts necessary for the VMEbus research. This list is included in this thesis with the hope that it will decrease the amount of time future researchers must spend locating parts needed for other prototyping theses.

These distributors are nationwide, and catalogs for their products may be obtained from either the digital logic lab staff or from the company itself. Each company has both local and national phone numbers listed whenever possible, as well as any dollar amount for a minimum order. Most of these companies are not tailored to the small order purchase, so parts should be ordered through the school.

- Arrow Electronics Incorporated
(513) 435-5563 (local) 1-800-932-7769 (national)
\$50.00 min order
Licensed TI distributor
- Allied Electronics
1-800-433-5700 (national)
\$25.00 min order
- Hamilton-Adnet Electronics
(513) 439-6721 (local)
\$100.00 min order
- Marshall Industries
(513) 898-4480 (local) 1-800-522-0084 (national)
\$50.00 min order
Licensed TI distributor
- Newark Electronics
(513) 294-8980 (local) 1-800-367-3573 (national)
\$25.00 min order
Licensed TI distributor

One company that specializes in VMEbus boards and interconnects is the Vector Electronic Company. The company might only operate through distributors, like the ones above, but their address is included here to provide future researchers with a name of a manufacturer of the products used in VMEbus design.

- Vector Electronic Company
12460 Gladstone Avenue
Sylmar, California 91342

Appendix F. *Chip Layouts for the VMEbus Boards*

This appendix covers the physical layout of the two VMEbus Eurocards. Figure 52 shows the relative location of the integrated circuits on the VMEbus board containing the VMEbus interface, the input memory, the APU, and the output memory. Table 11 identifies the type of integrated circuit by number. Figure 53 shows the relative location of the integrated circuits on the second VMEbus board, with Table 12 also identifying the integrated circuit by number.

These layouts represent the extent of the partial construction. In Figures 52 and 53, each major component is outlined in the dotted line. The status at this point of the construction is that the input memory was completely constructed, the bus interface partially finished, and the SPC partially finished.

The reasons for separating the WFTA system into two cards and the partitioning of the function blocks is discussed in Section 5.3. Figure 54 shows the mapping of signals on the 50-pin interconnect cable between the two boards. At this stage of the construction, only six signals of the ones discussed in Section 5.3 are mapped to corresponding pins on the cable.

Each of the VME boards were both powered using the +5 Volts DC pins on the VMEbus and the grounded using the GND pins on the VMEbus. These power and ground lines were distributed throughout the boards to insure proper power distribution.

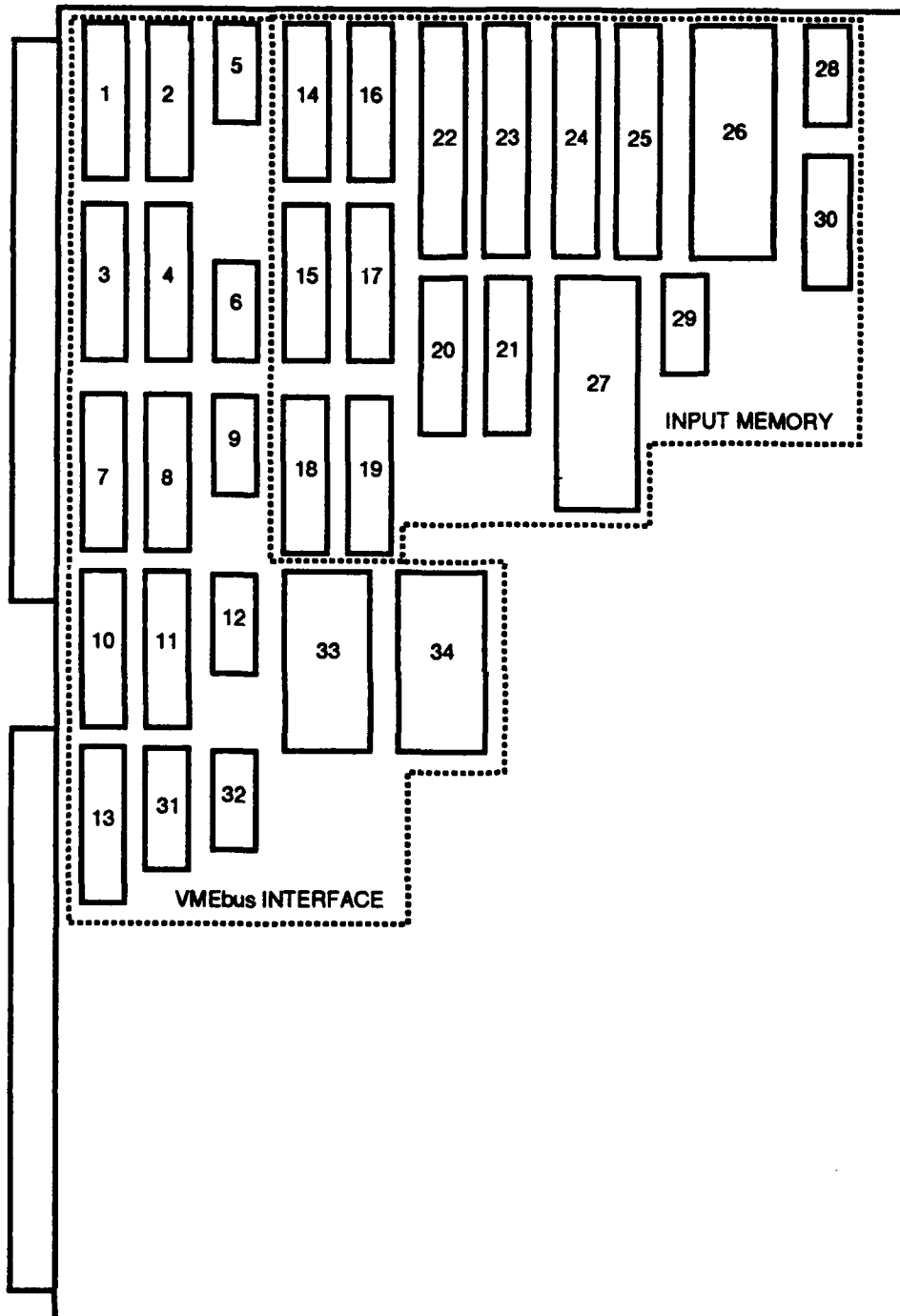


Figure 52. Layout of VME Board # 1

Table 11. Integrated Circuits used on VME Board # 1

<i>Chip #</i>	<i>Type and Name</i>
1	74520 Identity Comparator
2	74374 Octal Latch
3	74374 Octal Latch
4	74374 Octal Latch
5	74121 Monostable Multivibrator
6	7404 Inverter
7	74520 Identity Comparator
8	74520 Identity Comparator
9	7432 OR gate
10	74520 Identity Comparator
11	74520 Identity Comparator
12	7474 Dual D-type Latch
13	74747 Octal Buffer/Line Driver
14	74373 Octal Latch
15	74373 Octal Latch
16	74373 Octal Latch
17	74373 Octal Latch
18	74373 Octal Latch
19	74373 Octal Latch
20	74373 Octal Latch
21	74373 Octal Latch
22	MCM6264 SRAM
23	MCM6264 SRAM
24	MCM6264 SRAM
25	MCM6264 SRAM
26	74604 Multiplexed Latch
27	74604 Multiplexed Latch
28	74180 Parity Generator
29	74180 Parity Generator
30	74135 Exclusive-OR gate
31	74109 Positive Edge-Triggered JK Flip Flop
32	7408 AND gate
33	74116 Dual 4-bit Latch with Clear
34	74116 Dual 4-bit Latch with Clear

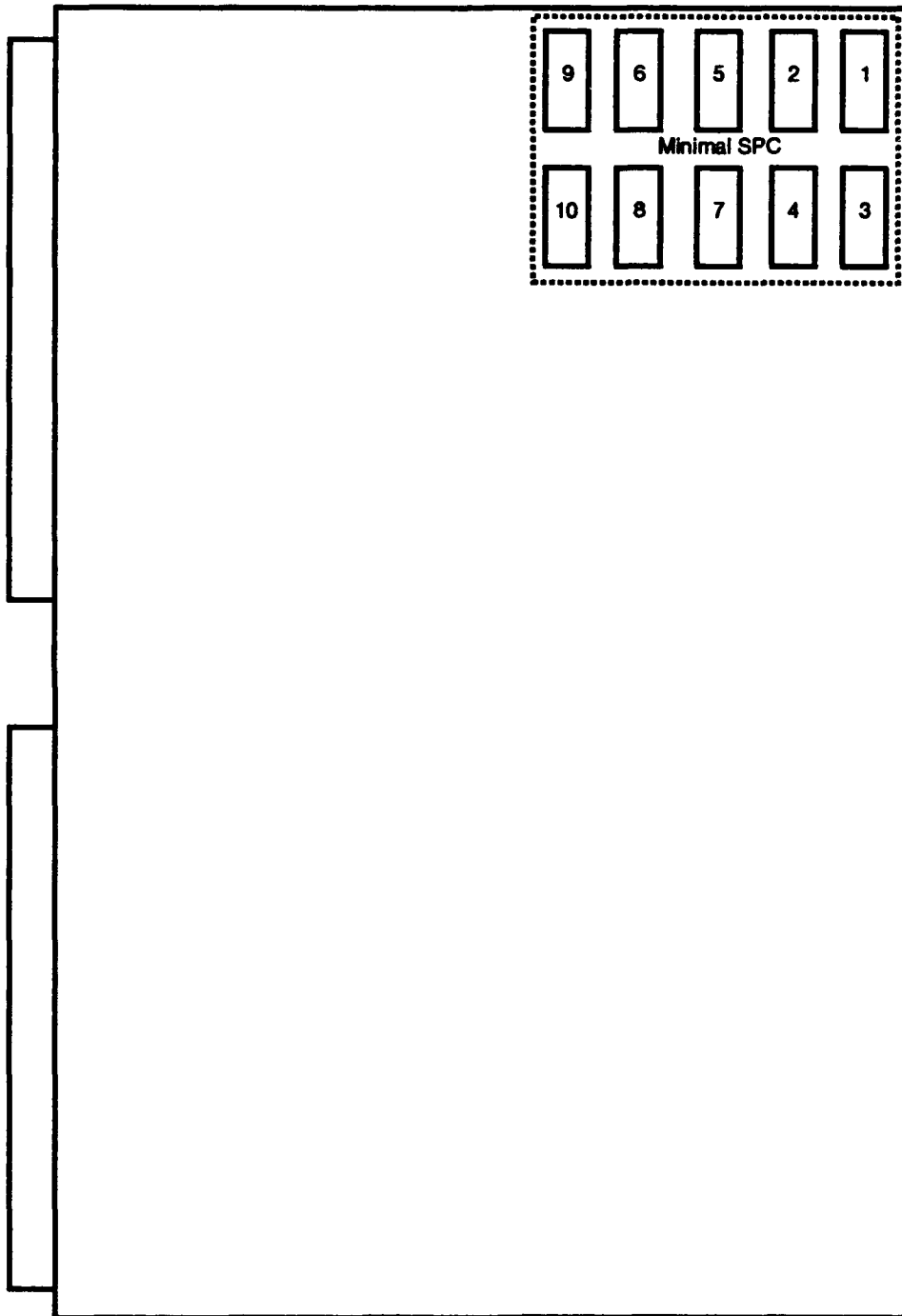


Figure 53. Layout of VME Board # 2

Table 12. Integrated Circuits used on VME Board # 2

<i>Chip #</i>	<i>Type and Name</i>
1	7410 3-Input NAND gate
2	7404 Inverter gate
3	7473 JK Flip Flop
4	7473 JK Flip Flop
5	7410 3-Input NAND gate
6	7402 2-Input NOR gate
7	7400 2-Input NAND gate
8	7400 2-Input NAND gate
9	7400 2-Input NAND gate
10	7400 2-Input NAND gate

	PIN #	
CLOCK	1	26
SPC_OP	2	27
RST_NOT	3	28
MEM_FLIP	4	29
SPC_DN	5	30
WFTA16_OP	6	31
	7	32
	8	33
	9	34
	10	35
	11	36
	12	37
	13	38
	14	39
	15	40
	16	41
	17	42
	18	43
	19	44
	20	45
	21	46
	22	47
	23	48
	24	49
	25	50

Figure 54. Signal Mapping of 50-Pin Interconnect Cable

Appendix G. *Compilation, Download, and Run Procedures for Host Driver Code*

This appendix describes the three procedures developed to compile, download, and run procedures for the host driver code. These procedures are specific to the hardware configuration used during this work. Different hardware setups would require modification to these procedures. These procedures are documented since they are not intuitively obvious and were developed because of system and resource constraints.

This appendix describes the general procedures for compiling, downloading, and running the host driver program. The operator's manual of Appendix J gives the specific commands, to include addresses, used for this thesis.

G.1 Compilation Procedure

The compiler used in this thesis was the Aztec C Compiler created by Manx Software Systems. Its use is documented in the user's manual [38]. This compilation procedure is covered in the text of the user's manual [38], but is confusing enough to make this section necessary. The compiler software must be loaded onto a separate IBM-compatible computer. The different steps are enumerated below with their associated commands.

1. *Create the Source Program.* Using any text editor, create the source code in C and store it in a file.
2. *Compile and Assemble.* In order to compile and assemble the source code, use the Aztec C Compiler command below.

`c68 < filename >`

This command will compile the C code in <filename> into assembly language and then calls the assembler program contained in the Aztec C package in order to create relocatable machine code.

3. *Link*. This relocatable machine code must be linked in order to associate it with a particular arbitrary address in the system RAM. The use of this command is shown below.

```
ln68 +d < address > -o < outputfilename > < filename >
```

The +d option tells the linker what to set the starting address of the program's initialized data. The -o option tells the linker what name to call the output file. Finally, the <filename> here is the name of the file which was compiled before.

4. *Convert to Motorola S-records*. This step converts the memory image generated by the linker into Motorola S-records which will be used to load the RAM memory of the host processor, a Motorola 68010 microprocessor. The command used for this step is shown below.

```
srec68 < outputfilename >
```

The <output filename> here in this command is the same that was used in the linking step.

After compilation, machine code has been generated and is ready to be downloaded into the system RAM of the host processor, along with the real input data points, which is what the next section describes.

G.2 Download Procedure

Already mentioned in Chapter VI is the problem with I/O interface to the host processor. This I/O limitation also precludes a different procedure to enter in the code into the RAM of the host processor card. Using the debug monitor installed in the MVME-120 card, only assembly level commands can be entered one line at a time, making the entering of code tedious and prone to error. However, there is a means of overcoming this obstacle.

After the host driver code has been compiled using the Aztec C Compiler, as described in the compilation procedure discussed earlier, into machine language, the relocatable code can then be linked, converted to S-records, and downloaded to the MVME-120 microprocessor card using Kermit, a file transfer program. The VMEbus chassis has several RS-232 serial ports which can be used to download this compiled code. The one on the actual microprocessor card (which is the default, port 1) is used to communicate to the dumb terminal and cannot be used here. There are two ports in the back of the chassis which can be used to transmit the data. Port number 2 specifies debug monitor port 2 which is MVME-050 serial port 1 located in the back of the chassis and was used for this download process.

The first step the downloading process is to configure the MVME-120 to receive the data. The debug monitor command used is the Load S-records (LO) command. However, before the use of this command, the port needs to set for the baud rate to be used for transferring data. The default is 9600 baud, but it can be set to a slower speed. Setting the data rate to a slower rate will insure the data will not be lost during downloading. The command used for this is the Port Format (PF) command as shown below.

PF2

The number 2 in the command corresponds to the desired port used in the download process. An interactive menu is presented, and the only option that needs to be changed is the baud rate. When the debug monitor asks "Baud rate (1-5) =\$02 ?" the user needs to answer 3 which corresponds to a baud rate of 2400 baud (which will have to be set in the Kermit transfer program). A carriage return can be used to answer the rest of the questions associated with the menu.

Once the baud rate has been set, the Load S-records command can be entered, at which point the MVME-120 will wait for the data transfer. The command is shown below.

LO2 ; X = DU < address >

The number 2 again corresponds to the port number that will be used for loading. The ;x option is used to echo the S-records to the current debug port, or the screen in this case. This option is used when the baud rate is slower than the default. The "= du <address>" part of the command tells the debug monitor where in memory to store the incoming data.

The next step in this procedure is to transmit the data through the RS-232 port from the other computer using the Kermit file transfer program (although any file transfer program can be used). This is a simple procedure, but the reader is cautioned to insure that the data rate is set at the correct rate (2400 baud for this thesis) and the correct port of the computer is set up for the data transfer.

Once completed, the Display Memory (MD) command can be used to verify that data was actually transmitted to the desired location in the RAM. Although Motorola S-records are not easily read and understood, the existence of data at that location in memory is most likely an indication of a successful transfer.

The easiest way to load the raw data points is to use the Memory Modify (M or MM) command and enter them one point at a time. The address used for this must correspond to the one defined in the program. The command used for this was already discussed in Section 5.4 of Chapter V with the only difference being that the ;N option does not need to be used because the host processor can both read and write to the system RAM.

G.3 Run Procedure

After compiling and downloading the host driver code, and entering in the data for an FFT, the program can now be run. The command used for executing the loaded host driver program is the GO (G or GO) command and is shown below. The address used here is the one where the transmitted data was loaded from in the downloading procedure.

GO < address >

Once the program has finished execution, the output data (real and imaginary) will be written to some portion of the RAM of the host processor. In order to view the FFT data, the Display Memory (MD) command can be used to examine the address where this data was written.

Appendix H. *Changes to Pseudocode for Sustained Operations*

This appendix contains the necessary modifications to change the pseudocode of the host driver program from single FFT operation to repeatable and sustained operations. Figure 55 shows the additions. The additional loop is highlighted in capital letters and the second write operation has been added. After the first write operation outside the loop fills the pipeline for the first time, the entire process is repeated until there is no more input data.

```

1.1 for i in 1 to 16;
    read one data point from system memory;
    write one data point to input memory of WFTA;
end for;

1.3 write control word to begin WFTA;
LOOP

1.1 for i in 1 to 16;
    read one data point from system memory;
    write one data point to input memory of WFTA;
end for;

loop
1.4 poll WFTA for completion;
end loop;

1.3 write control word to begin WFTA;

1.2 for i in 1 to 16;
    read one real FFT point from output memory of WFTA;
    write one real FFT point to system memory;
end for;

1.2 for i in 1 to 16;
    read one imaginary FFT point from output memory of WFTA;
    write one imaginary FFT point to system memory;
end for;
END LOOP;

```

Figure 55. Pseudocode for a Sustainable Host Driver Program

Appendix I. *Host Driver Code Listing*

This appendix is a listing of the host driver program developed for this thesis. This code compiles with no errors but has not been tested since it requires that the WFTA system be totally completed.

/*****

File Name : hostcode.c

Title : Host driver program for WFTA system.

Date : 12 Nov 1992

Version : 1

Project : Thesis

Author : CPT James F. Herron

Description : This program was developed to be used with the
WFTA system. The host would run this program in order to
drive the WFTA system.

Language : C

History/Revisions:

*****/

int *real_input_mem, *control_word, *output_word;

int *real_output_mem, *imag_output_mem;

int *read_data, *write_data;

int count;

void main()

{

 *real_input_mem = 0x700000;

 *real_output_mem = 0x70C000;

 *control_word = 0x704000;

 *output_word = 0x708000;

```

*imag_output_mem = 0x70E000;
*read_data = 0x001000;
*write_data = 0x010000;

for (count = 0; count <= 16; count++){
    *(real_input_mem + 2*(count)) = *(read_data + 2*(count));}

*(control_word) = 0x80;

while (*output_word < 128);

*(control_word) = 0x80;

for (count = 0; count <= 16; count++){
    *(write_data + 2*(count)) = *(real_output_mem + 2*(count));}

for (count = 16; count <= 32; count++){
    *(write_data + 2*(count)) = *(imag_output_mem + 2*(count));}

}

```


Appendix J. *Operator's Manual for the 16-point WFTA System*

This appendix is the operator's manual for the 16-point WFTA system developed for this thesis. This appendix is easily detachable from the main thesis for use with the WFTA system. This operator's manual represents a condensation of pieces from several different chapters. As such, the only place in the thesis where it is referenced is in the Section 1.7 of Chapter I. The procedures discussed are specifically tailored for the WFTA system constructed for this thesis. For example, addresses are at specific locations for the WFTA input memory and the WFTA output memory. The structure for this manual is separated into two major sections; the hardware procedures and the software procedures.

J.1 Hardware

The hardware installation and setup procedures are fairly simple and straightforward. The WFTA system consists of two VMEbus cards which must be installed into a VMEbus backplane. The operator only needs to insure that the bus request and grant lines on the VMEbus are jumpered to daisy-chain these lines for the bus arbitrator.

J.1.1 Setup. The hardware configuration is not unique, and many pieces of equipment could be substituted with other devices than were used here. The setup shown in Figure 56 was used for this thesis. The RS-232 connection from the IBM-compatible computer goes to Port 2 on the back of the VMEbus chassis. The other RS-232 connection runs from the front of the MVME-120 microprocessor module to the dumb terminal.

A significant enhancement to this hardware configuration would be for the use of a host processor that uses MS-DOS or other some other common operating system. The compiler could be installed on that host processor eliminating the need for the downloading procedures discussed in the next section.

J.1.2 WFTA Address Change. This thesis assumed a location for the WFTA system in the VMEbus address space of 700000h to 70FFFFh. This address is hardwired into the integrated circuits located in the bus interface. In order to change this location

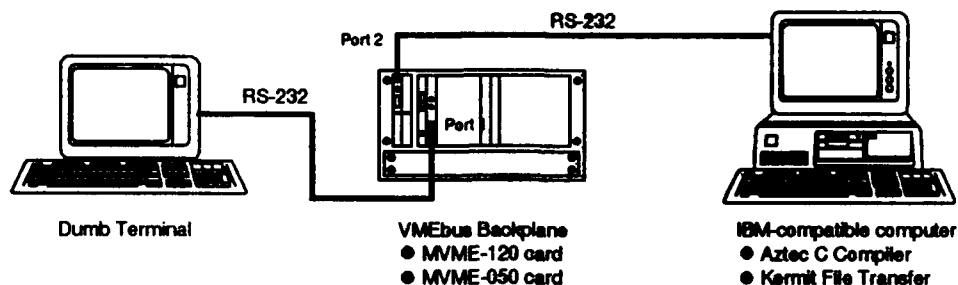


Figure 56. Hardware Setup

in the address space, two chips will need to be re-wired—chips 7 and 8 in Figure 52 of Appendix F.

J.2 Software

The software procedures have been discussed in the text of Chapter VI but are repeated here for convenience of the reader. Another difference here is that the addresses used for this thesis have been added to the commands while the commands used in Chapter VI were more general in nature. This section contains the instructions necessary for the compiling of the host driver source code, downloading this compiled code to the MVME-120 onboard RAM, loading input data into the RAM, running the loaded host driver code, and reading the output data from the RAM. As opposed to the hardware section, these procedures are more involved.

The addresses used below in the instructions are the ones selected for this thesis. Any changes in the address of the compiled program, input data, or output data should be substituted for the addresses shown below.

J.2.1 Host Driver Code and Data. There are two assumptions made at this point of the WFTA operation process. These assumptions are that there is a compiler program (Aztec C for this thesis) and a file transfer program (Kermit for this thesis) are installed in the IBM-compatible computer shown in Figure 56. The instructions listed in this section

are for the application programs mentioned and should be modified for other software that might be used.

J.2.1.1 Compiling the Host Driver Source Code. The compiler used in this thesis was the Aztec C Compiler [38]. The different steps associated with the compilation are enumerated below with their associated Aztec C commands. The procedure assumes that the host driver code has previously been entered using a text editor and stored in a file.

1. *Compile and Assemble.* In order to compile and assemble the source code, use the Aztec C Compiler command that follows.

`c68 < filename >`

This command will compile the C code in <filename> into assembly language and then calls the assembler program contained in the Aztec C software package in order to create relocatable machine code.

2. *Link.* This relocatable machine code must then be linked in order to associate it with a particular arbitrary address in the system RAM. The use of this command is shown below.

`ln68 +d 005000 -o < outputfilename > < filename >`

The +d option tells the linker what to set the starting address (005000h in this thesis) of the program's initialized data. The -o option tells the linker what name to call the output file. Finally, the <filename> here is the name of the file which was compiled before.

3. *Convert to Motorola S-records.* This step converts the memory image generated by the linker into Motorola S-records which will be used to load the RAM memory of the host processor, a Motorola 68010 microprocessor. The command used for this step is shown below.

srec68 < outputfilename >

The <output filename> here in this command is the same that was used in the linking step.

At this point, machine code has been generated and ready to be downloaded into the RAM of the host processor along with the real input data points. The file that needs to be downloaded is the one generated by the srec68 command.

J.2.1.2 Downloading the Compiled Host Driver Program. The first step of the downloading process is to configure the MVME-120 microprocessor card to receive the data. The MVME-120 uses a debug monitor, which consists of limited instruction set defined in the read-only memory (ROM) of the MVME-120. The debug monitor command used for this section is the Load S-records (LO) command. However, before the use of this command, the port needs to set for the baud rate to be used for transferring data. The default is 9600 baud, but it can be set to a slower speed. Setting the data rate to a slower rate will insure the data will not be lost during downloading. The command used for this is the Port Format (PF) command as shown below.

PF2

The number 2 in the command corresponds to the desired port used in the download process. An interactive menu is presented, and the only option that needs to be changed is the baud rate. When the debug monitor asks "Baud rate (1-5) =\$02 ?", answer 3, which corresponds to a baud rate of 2400 baud (which will have to also be set in the Kermit transfer program). A carriage return can be used to answer the rest of the questions associated with the menu.

Once the baud rate has been set, the Load S-records command can be entered, at which point the MVME-120 will wait for the data transfer. The command is shown below.

LO2 ;X = DU 005000

The number 2 again corresponds to the port number that will be used for loading. The ;x option is used to echo the S-records to the current debug port, or the screen, in this case. This option is used when the baud rate is slower than the default. Using this echo option helps insure that the data transfer has actually occurred. The “= du 005000” part of the command tells the debug monitor at what address in RAM to load the incoming data.

The next step in this procedure is to transmit the data through the RS-232 port from the other computer using the Kermit file transfer program (although any file transfer program can be used). This is a simple procedure, but be sure that the baud rate is set at the correct rate (2400 baud for this thesis) and the correct port of the computer is set up for the data transfer.

Once completed, the Display Memory (MD) debug monitor command can be used to verify that data was actually transmitted to the desired location in the RAM. Although Motorola S-records are not easily read and understood, the existence of data at that location in memory is most likely an indication of a successful transfer.

J.2.1.3 Loading the Input Data. The easiest way to load the raw data points is to use the debug monitor Memory Modify (M or MM) command and enter them one point at a time. An example of the command follows. The address 001000h is the arbitrary location used in the host driver program to read the input data.

MM ;W 001000

The ;W option is used to write a 16-bit word. The operator enters in the data in hexadecimal format until reaching 0010010h, at which time a lone carriage return exits the memory modify command.

J.2.2 Running the Host Driver Program. The debug monitor command used for executing the loaded host driver program is the GO (G or GO) command, shown below.

GO 005000

The address 005000h is the arbitrary location selected where the transmitted data from the IBM-compatible computer was loaded in the downloading procedure.

J.2.3 Reading the Output Data. The debug monitor command used to read the FFT data generated by the WFTA system is the Display Memory (MD) command and is shown below.

MD 010000

The address 010000h is the arbitrary location that was used in the host driver program to write the data that was read from the output memory of the WFTA system.

J.3 Problems in Operator's Manual

If the operator experiences any problems with the procedures in this appendix, reference the associated area of the thesis or consult troubleshooting procedures in the associated manuals of the equipment or software.

Appendix K. *VHDL Code and Schematic Listing*

The size of this appendix makes it prohibitive to be included with the main thesis and has been separated into a separate volume. This volume contains all the behavioral and structural VHDL code for the WFTA prototype design discussed in this thesis. Also included in this volume are the VHDL testbench code listing used to test the entities, as well as sample output from these testbenches. Finally, this volume contains the Synopsys generated schematics used in both the VHDL development and construction phase of this thesis. This second volume will be stored in the VLSI laboratory.

References

1. C. Nuthalapati, "Role of High Speed FFT in Radar Signal Processing," *Microwave Journal*, pp. 163-180, October 1987.
2. K. W. Scribner, "Redesign, Simulation, and Development of a High-Speed, 4080-Point Winograd Fast Fourier Transform Processor," Master's thesis, AFIT/GCE/ENG/91D-08, School of Engineering, Air Force Institute of Technology (AU), Wright-Patterson AFB OH, December 1991.
3. William H. Press *et al.*, *Numerical Recipes in C*. Cambridge, Massachusetts: Cambridge University Press, 1988.
4. Mark T. Jong, *Methods of Discrete Signal and System Analysis*. New York, New York: McGraw-Hill Book Company, 1982.
5. William T. Cochran *et al.*, "What is the Fast Fourier Transform?," in *IEEE Transactions on Audio Electroacoustics*, pp. 45-55, IEEE, 1967.
6. Schmucl Winograd, "On Computing the Discrete Fourier Transform," *Mathematics of Computation*, pp. 175-199, January 1978.
7. Institute of Electrical and Electronic Engineers, *IEEE Standard for a Versatile Bus: VMEbus, ANSI/IEEE Standard 1014-1987*, (New York), IEEE, March 1987.
8. K. Taylor, "Architecture and Numerical Accuracy of High-Speed DFT Processing Systems," Master's thesis, AFIT/GE/ENG/85D-47, School of Engineering, Air Force Institute of Technology (AU), Wright-Patterson AFB OH, December 1985.
9. P. W. Coutee, "Arithmetic Cicutry for High Speed VLSI Winograd Fourier Transform Processor," Master's thesis, AFIT/GE/ENG/85D-11, School of Engineering, Air Force Institute of Technology (AU), Wright-Patterson AFB OH, December 1985.
10. P. C. Rossbach, "Control Circuitry for High Speed VLSI Winograd Fourier Transform Processors," Master's thesis, AFIT/GE/ENG/85D-35, School of Engineering, Air Force Institute of Technology (AU), Wright-Patterson AFB OH, December 1985.
11. J. M. Collins, "Simulation and Modeling of a VLSI Winograd Fourier Transform Algorithm," Master's thesis, AFIT/GE/ENG/85D-9, School of Engineering, Air Force Institute of Technology (AU), Wright-Patterson AFB OH, December 1985.
12. C. G. Shephard, "Integration and Design for Testability of a High Speed Winograd Fourier Transform Processor," Master's thesis, AFIT/GE/ENG/86D-46, School of Engineering, Air Force Institute of Technology (AU), Wright-Patterson AFB OH, December 1986.
13. G. D. Hedrick, "Design of Fault Tolerant Prime Factor Array Elements," Master's thesis, AFIT/GE/ENG/86D-45,, Wright-Patterson AFB OH, December 1986.
14. C. H. Cooper, "Modeling and Simulation of the WFTA 16 Processor Using VHSIC Hardware Description Language," Master's thesis, AFIT/GE/ENG/86D-44, School of Engineering, Air Force Institute of Technology (AU), Wright-Patterson AFB OH, December 1986.

15. R. S. Hauser, "Design Implementation of a VLSI Prime Factor Algorithm Processor," Master's thesis, AFIT/GCE/ENG/87D-5, School of Engineering, Air Force Institute of Technology (AU), Wright-Patterson AFB OH, December 1987.
16. S. W. Pavick, "Testing and Data Path Redesign of a High Speed, 16-Point Winograd Fourier Transform Processor," Master's thesis, AFIT/GE/ENG/89D-39, School of Engineering, Air Force Institute of Technology (AU), Wright-Patterson AFB OH, December 1989.
17. R. R. Baker, "Modeling and Simulation of the Winograd Fourier Transform Processor," Master's thesis, AFIT/GE/ENG/90D-02, School of Engineering, Air Force Institute of Technology (AU), Wright-Patterson AFB OH, December 1990.
18. R. E. Sommer, "Microcell Library Development and 15-point Transform Chip Design for a High Speed Winograd Fourier Transform Processor," Master's thesis, AFIT/GE/ENG/90D-57, School of Engineering, Air Force Institute of Technology (AU), Wright-Patterson AFB OH, December 1990.
19. Robert M. Owens, Joseph Ja'Ja', "A VLSI Chip for the Winograd/Prime Factor Algorithm to Compute the Discrete Fourier Transform," in *IEEE Transactions on Acoustics, Speech, and Signal Processing*, pp. 979-989, IEEE, 1986.
20. P. Lavoie, "A High-Speed CMOS Implementation of the Winograd Fourier Transform Algorithm." Submitted to GOMAC, 1992.
21. M. Mehalic, Instructor. Personal interview. Air Force Institute of Technology, Wright-Patterson AFB OH, August 1992.
22. Roger Lipsett *et al.*, *VHDL: Hardware Description and Design*. Boston, Massachusetts: Kluwer Academic Publishers, 1989.
23. Institute of Electrical and Electronic Engineers, *IEEE Standard VHDL Language Reference Manual*, (New York), IEEE, 1987.
24. Synopsys, Inc., *VHDL System Simulator Core Programs Manual, Version 2.2*, Mountain View, CA, October 1991.
25. Synopsys, Inc., *Simulation Graphical Environment User's Guide, Version 2.2*, Mountain View, CA, October 1991.
26. Texas Instruments, *The TTL Data Book Volume Two*, Dallas, Texas, 1985.
27. Texas Instruments, *ALS/AS Logic Data Book*, Dallas, Texas, 1986.
28. Motorola Semiconductors, *Memory Device Data*, Austin, Texas, 1990.
29. Motorola Semiconductors, *MC68010, 16-bit Virtual Memory Microprocessor*, Austin, Texas, August 1983.
30. Synopsys, Inc., *Design Compiler Reference Manual, Version 2.2*, Mountain View, CA, October 1991.
31. C. P. Brothers, PhD candidate. Personal Interview. Air Force Institute of Technology, Wright-Patterson AFB OH, August 1992.
32. Motorola Semiconductors, *MVME945 Chassis User's Manual*, Phoenix, Arizona, February 1988.

33. Motorola Semiconductors, *MVME120, MVME121, MVME122, MVME123 VMEbus Microprocessor Module User's Manual*, Phoenix, Arizona, September 1984.
34. Hewlett Packard, *Operating and Programming Manual Model 1631A/D Logic Analyzer*, Colorado Springs, Colorado, August 1985.
35. Heath Company, *Heathkit Manual for the Video Display Terminal Model H-29*, Benton Harbor, Michigan, 1983.
36. Motorola Semiconductors, *MVME120 Debug Monitor User's Manual*, Phoenix, Arizona, January 1985.
37. R. S. Pressman, *Software Engineering, A Practitioner's Approach*. New York, New York: McGraw-Hill Publishing Company, 1987.
38. Manx Software Systems, Inc., *Aztec C68k/ROM Cross Development System, Version 3.4*, Shrewsbury, New Jersey, November 1987.

Vita

CPT James F. Herron earned a Bachelor of Science in Electrical Engineering in 1986 at the United States Military Academy at West Point. Upon graduation he was commissioned as a second lieutenant in the US Army Signal Corps. After attending the Signal Officer's Basic Course and the Communications-Electronics Staff Officer Course, he was assigned overseas and served with the 141st Signal Battalion, Ansbach, FRG and 34th Signal Battalion, Ludwigburg, FRG in a variety of positions. After returning from overseas he then attended the Signal Officer's Advanced Course, the Echelon Above Corps Course, and the Telecommunications Officer's Operations Course. In 1991 and 1992, CPT Herron attended the Air Force Institute of Technology at Wright-Patterson AFB, where he graduated with a Master of Science in Computer Engineering sequence specializing in computer architecture and very large scale integrated circuit design.

Permanent address: 1849 S. Broadway
Wichita, Kansas 67211

REPORT DOCUMENTATION PAGE

Form Approved
OMB No. 0704-0188

Public reporting burden for this collection of information is estimated to average 1 hour per response, including the time for reviewing instructions, searching existing data sources, gathering and maintaining the data needed, and completing and reviewing the collection of information. Send comments regarding this burden estimate or any other aspect of this collection of information, including suggestions for reducing this burden, to Washington Headquarters Services, Directorate for Information Operations and Reports, 1215 Jefferson Davis Highway, Suite 1204, Arlington, VA 22202-4302, and to the Office of Management and Budget, Paperwork Reduction Project (0704-0188), Washington, DC 20503.

1. AGENCY USE ONLY (Leave blank)		2. REPORT DATE December 1992		3. REPORT TYPE AND DATES COVERED Master's Thesis	
4. TITLE AND SUBTITLE DESIGN AND DEVELOPMENT OF A HIGH-SPEED WINOGRAD FAST FOURIER TRANSFORM PROCESSOR BOARD				5. FUNDING NUMBERS	
6. AUTHOR(S) James F. Herron, CPT, USA					
7. PERFORMING ORGANIZATION NAME(S) AND ADDRESS(ES) Air Force Institute of Technology, WPAFB OH 45433-6583				8. PERFORMING ORGANIZATION REPORT NUMBER AFIT/GCE/ENG/92D-05	
9. SPONSORING/MONITORING AGENCY NAME(S) AND ADDRESS(ES) RL/OCTS Griffiss AFB NY 13441				10. SPONSORING/MONITORING AGENCY REPORT NUMBER	
11. SUPPLEMENTARY NOTES					
12a. DISTRIBUTION/AVAILABILITY STATEMENT Approved for Public Release; Distribution Unlimited				12b. DISTRIBUTION CODE	
13. ABSTRACT (Maximum 200 words) Since 1985, the Air Force Institute of Technology has pursued a project to develop a 4080-point Discrete Fourier Transform processor using the Winograd Fourier Transform Algorithm (WFTA) and Good-Thomas Prime Factoring Algorithm (PFA). In the first attempt to build a working system, this research effort designed and constructed, in part, a modified single processor architecture in order to demonstrate the proof of concept of the WFTA system design. This prototype architecture is simpler in implementation but uses the same principles and procedures as those of the 4080-point WFTA design. The design developed in this thesis was validated using the Very High-Speed Integrated Circuit Hardware Description Language (VHDL) to simulate its operation. A partial construction of the design was built and tested verifying the VHDL results.					
14. SUBJECT TERMS Fast Fourier Transform, Discrete Fourier Transform, Winograd, VHDL, Architecture, Hardware, Prototyping				15. NUMBER OF PAGES 172	
				16. PRICE CODE	
17. SECURITY CLASSIFICATION OF REPORT UNCLASSIFIED	18. SECURITY CLASSIFICATION OF THIS PAGE UNCLASSIFIED	19. SECURITY CLASSIFICATION OF ABSTRACT UNCLASSIFIED	20. LIMITATION OF ABSTRACT UL		

GENERAL INSTRUCTIONS FOR COMPLETING SF 298

The Report Documentation Page (RDP) is used in announcing and cataloging reports. It is important that this information be consistent with the rest of the report, particularly the cover and title page. Instructions for filling in each block of the form follow. It is important to *stay within the lines* to meet optical scanning requirements.

Block 1. Agency Use Only (Leave blank).

Block 2. Report Date. Full publication date including day, month, and year, if available (e.g. 1 Jan 88). Must cite at least the year.

Block 3. Type of Report and Dates Covered. State whether report is interim, final, etc. If applicable, enter inclusive report dates (e.g. 10 Jun 87 - 30 Jun 88).

Block 4. Title and Subtitle. A title is taken from the part of the report that provides the most meaningful and complete information. When a report is prepared in more than one volume, repeat the primary title, add volume number, and include subtitle for the specific volume. On classified documents enter the title classification in parentheses.

Block 5. Funding Numbers. To include contract and grant numbers; may include program element number(s), project number(s), task number(s), and work unit number(s). Use the following labels:

C - Contract	PR - Project
G - Grant	TA - Task
PE - Program Element	WU - Work Unit Accession No.

Block 6. Author(s). Name(s) of person(s) responsible for writing the report, performing the research, or credited with the content of the report. If editor or compiler, this should follow the name(s).

Block 7. Performing Organization Name(s) and Address(es). Self-explanatory.

Block 8. Performing Organization Report Number. Enter the unique alphanumeric report number(s) assigned by the organization performing the report.

Block 9. Sponsoring/Monitoring Agency Name(s) and Address(es). Self-explanatory.

Block 10. Sponsoring/Monitoring Agency Report Number. (If known)

Block 11. Supplementary Notes. Enter information not included elsewhere such as: Prepared in cooperation with...; Trans. of...; To be published in.... When a report is revised, include a statement whether the new report supersedes or supplements the older report.

Block 12a. Distribution/Availability Statement.

Denotes public availability or limitations. Cite any availability to the public. Enter additional limitations or special markings in all capitals (e.g. NOFORN, REL, ITAR).

DOD - See DoDD 5230.24, "Distribution Statements on Technical Documents."

DOE - See authorities.

NASA - See Handbook NHB 2200.2.

NTIS - Leave blank.

Block 12b. Distribution Code.

DOD - Leave blank.

DOE - Enter DOE distribution categories from the Standard Distribution for Unclassified Scientific and Technical Reports.

NASA - Leave blank.

NTIS - Leave blank.

Block 13. Abstract. Include a brief (Maximum 200 words) factual summary of the most significant information contained in the report.

Block 14. Subject Terms. Keywords or phrases identifying major subjects in the report.

Block 15. Number of Pages. Enter the total number of pages.

Block 16. Price Code. Enter appropriate price code (NTIS only).

Blocks 17. - 19. Security Classifications. Self-explanatory. Enter U.S. Security Classification in accordance with U.S. Security Regulations (i.e., UNCLASSIFIED). If form contains classified information, stamp classification on the top and bottom of the page.

Block 20. Limitation of Abstract. This block must be completed to assign a limitation to the abstract. Enter either UL (unlimited) or SAR (same as report). An entry in this block is necessary if the abstract is to be limited. If blank, the abstract is assumed to be unlimited.